THE EFFECT OF FOAM STABILITY IN CO_2-FOAM FLOODING

Miss Kunwadee Teerakijpaiboon

A Thesis Submitted in Partial Fulfillment of the Requirements

for the Degree of Master of Engineering Program in Petroleum Engineering

Department of Mining and Petroleum Engineering

Faculty of Engineering

Chulalongkorn University

Academic Year 2012

ผลกระทบของเสถียรภาพของโฟมในการฉีดอัดโฟมคาร์บอนไดออกไซด์

นางสาวกุลวดี ธีรกิจไพบูลย์

วิทยานิพนธ์นี้เป็นส่วนหนึ่งของการศึกษาตามหลักสูตรปริญญาวิศวกรรมศาสตรมหาบัณฑิต
สาขาวิชาวิศวกรรมปิโตรเลียม ภาควิชาวิศวกรรมเหมืองแร่และปิโตรเลียม
คณะวิศวกรรมศาสตร์ จุฬาลงกรณ์มหาวิทยาลัย
ปีการศึกษา 2555

Thesis Title	THE EFFECT OF FOAM STABILITY IN CO_2-FOAM FLOODING
By	Ms. Kunwadee Teerakijpaiboon
Field of Study	Petroleum Engineering
Thesis Advisor	Falan Srisuriyachai, Ph.D.

Accepted by the Faculty of Engineering, Chulalongkorn University in Partial Fulfillment of the Requirements for the Master's Degree

...……. Dean of the Faculty of Engineering
(Associate Professor Boonsom Lerdhirunwong, Dr.Ing.)

THESIS COMMITTEE

….……Chairman
(Associate Professor Sarithdej Pathanasethpong)

…….Thesis Advisor
(Falan Srisuriyachai, Ph.D.)

…….Examiner
(Assistant Professor Suwat Athichanagorn, Ph.D.)

…….External Examiner
(Witsarut Tungsunthomkhan, Ph.D.)

กุลวดี ธีรกิจไพบูลย์ : ผลกระทบของเสถียรภาพของโฟมในการฉีดอัดโฟมคาร์บอนไดออกไซด์. (THE EFFECT OF FOAM STABILITY IN CO_2-FOAM FLOODING) อ.ที่ปรึกษาวิทยานิพนธ์หลัก: อ.ดร.ฟ้าลั่น ศรีสุริยชัย, 149 หน้า

การฉีดอัดโฟมคาร์บอนไดออกไซด์ถูกนำมาใช้เพื่อ ลดความสามารถในการเคลื่อนที่ของคาร์บอนไดออกไซด์ที่สูงจนทำให้ผลผลิตน้ำมันทั้งหมดลดต่ำลง สารละลายสารลดแรงตึงผิวและแก๊สคาร์บอนไดออกไซด์ถูกฉีดอัดร่วมกันเพื่อสร้างโฟมคาร์บอนไดออกไซด์ โฟมสร้างแนวผิวหน้าของการอัดฉีดที่ราบเรียบมากกว่าการฉีดอัดแก๊สเพียงอย่างเดียว เมื่อโฟมคาร์บอนไดออกไซด์สัมผัสกับน้ำมัน โฟมจะอ่อนแอลงและแตกในที่สุด คาร์บอนไดออกไซด์ที่ถูกห่อหุ้มภายในโฟมจะหลุดออกมาและเกิดการผสมเนื้อเดียวกับน้ำมันในสภาวะที่เหมาะสม

ผลการศึกษาพบว่าการฉีดอัดโฟมคาร์บอนไดออกไซด์ให้ค่าสัดส่วนของน้ำมันที่ผลิตได้มากกว่า 1 ถึง 13 เปอร์เซ็นต์ เมื่อเปรียบเทียบกับการใช้แก๊สคาร์บอนไดออกไซด์เพียงอย่างเดียว ประสิทธิภาพของการฉีดอัดโฟมคาร์บอนไดออกไซด์ขึ้นอยู่กับหลายปัจจัย เสถียรภาพของโฟมเป็นหนึ่งในตัวแปรที่สนใจ แต่จากศึกษาด้วยแบบจำลอง การแปรผันค่าเสถียรภาพของโฟมส่งผลกระทบเพียงเล็กน้อยต่อประสิทธิภาพของการฉีดอัด ดังนั้นเสถียรภาพของโฟม อาจไม่ใช่หนึ่งในตัวแปรที่ต้องพิจารณาเมื่อมีการวางแผนที่จะฉีดอัดโฟมคาร์บอนไดออกไซด์ในบริเวณใดก็ตาม การใช้โฟมคาร์บอนไดออกไซด์จะให้ผลเป็นที่น่าพอใจเมื่อสภาพความเปียกของหินแหล่งกักเก็บอยู่ในช่วงสภาวะความเปียกด้วยน้ำ สำหรับหินแหล่งกักเก็บที่มีสภาวะความเปียกด้วยน้ำมัน การฉีดอัดคาร์บอนไดออกไซด์เพียงอย่างเดียวให้ผลใกล้เคียงหรือดีกว่าเมื่อเทียบกับการฉีดอัดโฟมคาร์บอนไดออกไซด์ ส่วนประกอบของน้ำมันมีผลกระทบต่อการฉีดอัดโฟมคาร์บอนไดออกไซด์เช่นกัน ข้อได้เปรียบของการอัดฉีดโฟมคาร์บอนไดออกไซด์จะยิ่งมากกว่าการฉีดอัดคาร์บอนไดออกไซด์ เมื่อส่วนประกอบของปิโตรเลียมในแหล่งกักเก็บประกอบด้วยสารประกอบไฮโดรคาร์บอนมวลเบาในสัดส่วนที่ต่ำ วิธีที่ดีที่สุดสำหรับการฉีดอัดโฟมคาร์บอนไดออกไซด์คือการฉีดโฟมคาร์บอนไดออกไซด์ทั้งหมดเพียงหนึ่งกลุ่มก้อนและขับดันด้วยน้ำ การแบ่งกลุ่มก้อนของโฟมเป็นกลุ่มย่อย ๆ ไม่ได้ก่อให้เกิดผลลัพธ์ที่น่าพึงพอใจ

ภาควิชา วิศวกรรมเหมืองแร่และปิโตรเลียม ลายมือชื่อนิสิต.....

สาขาวิชา วิศวกรรมปิโตรเลียม ลายมือชื่อ อ. ที่ปรึกษาวิทยานิพนธ์หลัก.....

ปีการศึกษา 2555.....

5471201221: MAJOR PETROLEUM ENGINEERING
KEYWORDS: CO_2-FOAM FLOODING/FOAM STABILITY

KUNWADEE TEERAKIJPAIBOON: THE EFFECT OF FOAM STABILITY IN CO_2-FOAM FLOODING ADVISOR : FALAN SRISURIYACHAI, Ph.D., 149 pp.

CO_2-foam flooding is implemented in order to minimize drawbacks of solely CO_2 flooding by reducing high mobility of CO_2 that could result in impoverishing of ultimate oil recovery. Surfactant solution and CO_2 gas are co-injected simultaneously to generate foam. Foam creates smoother flood front than performing only gas injection. When CO_2-foam contacts with the oil, foam bubbles are weaken and eventually ruptured. Encapsulated CO_2 in those bubbles therefore comes out and be miscible with oil in suitable conditions.

This study shows that CO_2-foam flooding yields higher oil recovery factor in the range of 1 to 13% compared to the use of solely CO_2. Performance of CO_2-foam flooding is dependent on many factors. Foam stability is one of the interest parameters but from the simulation results, varying of foam stability slightly affects to the flooding performance. Hence, foam stability might not be one of the first parameters to consider when foam flooding is planned for any field. CO_2-foam application is favorable when reservoir wettability is in the range water-wet condition. For reservoir rocks that possess oil-wet condition, solely CO_2 flooding shows similar or even better result compared to CO_2-foam flooding. Oil composition also affects CO_2-foam. Benefit from CO_2-foam over CO_2 flooding is greater when the hydrocarbon in reservoir contains low intermediate component. The best strategy for CO_2-foam flooding is injecting a whole one slug of CO_2-foam and chasing by water. Dividing foam slug into smaller slugs does not yield any satisfactory results.

Department: Mining and Petroleum Engineering Student's Signature .....
Field of Study: Petroleum Engineering Advisor's Signature .....
Academic Year: 2012 .....

Acknowledgements

First of all, I would like to thank Dr. Falan Srisuriyachai, my thesis advisor, for providing knowledge in petroleum engineering field, useful advices and constant support throughout the period of this study. This thesis could not be successfully completed without invaluable help of him.

Secondly, I am considerably grateful to thank all of faculty members in the Department of Mining and Petroleum Engineering who have supplied me petroleum engineering knowledge, technical and useful recommendations. I would like to thank all of thesis committee members for their suggestions to fulfill my thesis.

Thirdly, I really appreciate all of CMG technical support team members (Erykah Bityutsky, Amir Moradi, Mark Edmondson and Shawket Ghedan) for bestowing highly advantageous advices and sharing knowledge about the CMG simulation software. Moreover, I would like to thank Dr. Kreangkrai Maneeintr for being licensing coordinator between CMG and the Department of Mining and Petroleum Engineering.

In addition, I would like to express my thankfulness to PTT Exploration and Production Public Company Limited (PTTEP) for providing financial support and the reservoir simulation data.

Finally, I gratefully acknowledge my parents and my friends who always give precious supports and encouragements.

Contents

Page

Page

List of Tables

Page

Page

Page

List of Figures

Page

Page

Page

Page

Page

Page

Page

Page

List of Abbreviations

Atm	Atmospheric pressure
STB	Barrel
STB/D	Barrel per day
cP	Centipoise
C_1	Methane
C_2	Ethane
C_3	Propane
i-C_4	Isobutane
i-C_5	Isopentane
n-C_4	Normal butane
n-C_5	Normal pentane
C_6	Hexane
C_{7+}	Alkane hydrocarbon account from heptanes forward
C_{11}	Undecane
C_{18}	Octadecane
CMC	Critical Micelle Concentration
CO_2	Carbon dioxide
EOR	Enhanced oil recovery
°F	Degree Fahrenheit
FS	Foam stability
GOR	Gas-Oil ratio
IFT	Interfacial tension
IWS	Irreducible water saturation
K	Kinetic reaction rate constant
°K	Degree Kelvin
mD	Millidarcy
MMSTB	Million barrel
MMP	Minimum miscibility pressure
MMSCF	Million standard cubic foot

MMSCF/D	Million standard cubic foot per day
MOC	Method of characteristics
MSCF/D	Thousand standard cubic feet per day
PV	Pore volume
PVT	Pressure-volume-temperature
psi	Pounds per square inch
RF	Resistance Factor
S1	Sirikit oil field
SAG	Surfactant Alternating Gas
SCAL	Special core analysis
SCF	Standard cubic foot
STB	Stock-tank barrel
w/v	Weight per volume
WAG	Water Alternating Gas

Nomenclatures

μ^f	Foam effective viscosity
μ_g^f	Gas viscosity in presence of foam
μ_w	Water viscosity
λ_{rt}	Water and gas total relative mobility
$epsurf$	Exponent for composition contribution to dimensionless foam interpolation calculation
F_1	Surfactant concentration dependent function
F_2	Oil saturation dependent function
F_3	Water saturation dependent function
F_4	Salt mole fraction dependent function
F_5	Capillary number dependent function
F_6	Critical capillary number dependent function
$floil$	Lower oil saturation (volume fraction)
FM	Dimensionless interpolation factor for relative permeability to gas in the presence of foam
$fmmob$	Reference mobility reduction factor
$fmsurf$	Critical concentration of surfactant which normally is the injected fluid concentration
f_w	Water fractional flow function
k_{rg}	Relative permeability to gas
k_{rg}^f	Relative permeability to gas in presence of foam
k_{rg}^{nf}	Relative permeability to gas in the absence of foam
k_{ro}	Relative permeability to oil (Oil/Water function)
k_{rog}	Relative permeability to oil (Gas/Liquid function)
k_{rw}	Relative permeability to water
P_c^*	Limiting capillary pressure
$t_{1/2}$	Foam stability (foam's half-life)
S_l	Liquid saturation
S_{orw}	Residual oil saturation (to water)

S_w	Water saturation
S_{wc}	Connate water saturation
S_{wcr}	Critical water saturation
S_{wi}	Initial water saturation (connate water saturation)
S_{wmin}	Minimum water saturation (irreducible water saturation)
S_{wmax}	Maximum water saturation
S_o^*	Critical oil saturation
$S_w^*.$	Limiting water saturation
W_s	Concentration of surfactant in the grid block
Z	Compressibility factor

CHAPTER I

INTRODUCTION

1.1 Background

Enhanced Oil Recovery (EOR) becomes the most well-known technique to increase the amount of producible oil by means of injecting substances which are not present in the reservoir in order to improve displacement and sweep efficiencies. Carbon dioxide (CO_2) flooding is one of the most widely used and the most well-known EOR techniques because CO_2 can perform both miscible and immiscible conditions in a wide range of hydrocarbon properties to improve oil recovery. However, displacement by CO_2 still has an unavoidable disadvantage; CO_2 viscosity is much lower than that of crude oil. This results in high mobility ratio and consecutively leaves oil by-passed behind. Viscous fingering and gravity override effects are commonly the results from the unfavorable mobility ratio, leading to an early breakthrough of injected CO_2. This in total is considerably an undesirable situation.

In order to minimize drawbacks of CO_2 flooding, foam is generated to reduce the mobility of gas phase and hence, improve the sweep efficiency by decreasing the mobility ratio. Foam has been used as controlling and blocking agent to prevent rapid gas invasion in high permeability streaks. The oil recovery mechanism obtained by foam flooding is the combination between surfactant and CO_2 characteristics which are: 1) lowering the interfacial tension (IFT) to a proper value that oil can be liberated and consecutively stabilized as small droplets in aqueous phase and; 2) CO_2 can be miscible with oil, reducing oil viscosity and hence, making oil ready to flow.

The efficiency of foam flooding depends on many factors such as oil properties, formation lithology, foam qualities etc. One of the most important parameters is foam stability. Foam stability is defined as half-life of foam or time required for half of the foam volume to decay or collapse. In foam flooding, foam stability should be controlled at an appropriated value because when foam gets in contact with the oil, foam disintegrates and turns into CO_2 gaseous and surfactant

liquid forms. If the foam stability is too low, the foam bubble will break down easily in a short period of time. The result will not be much different from implementation of solely gas flooding. On the other hand, if the foam stability is too high, CO_2 which is encapsulated in the foam bubble will not be able to contact oil, resulting in an unfavorable condition for miscibility and therefore, low oil recovery is obtained. Hence, investigation of the optimal foam stability for foam flooding will partly lead to success in EOR project.

In this study, the reservoir simulator STARS® commercialized by Computer Modeling Group Ltd. (CMG) will be used as investigation tool. A homogeneous reservoir model will be constructed with proper petrophysical range for CO_2 flooding. A volatile oil represents the oil phase in this study since this reservoir fluid type principally can create miscibility from high pressure gas drive mechanism. Appropriate values of foam stability are applied for foam slug with a constructed model. Oil recovery is detected when the preset pore volume of injectant is reached. Lithology of rock is the first parameter in sensitivity analysis. A range of wettability from moderately water-wet to strongly water-wet is chosen in this study. Different in wetting condition implies the different in mineralogy and lithology of rock. Wetting condition of reservoir rock is expressed in term of relative permeability curve. The percentage of intermediate in volatile oil is also considered in this study. As CO_2 is known as a potential vaporizer, the amount of intermediate plays a major role in high pressure gas drive process and hence, partly control the miscibility. Last, the foam slug size is chosen for operational parameter study. The total foam slug is equal in all cases but foam slugs are divided into many slugs and injected alternately with chasing water in case where slug size is smaller. At the end of the study, oil recovery from CO_2-foam flooding will be illustrated together with foam stability and parameter studies. The results and conclusions will give a preliminary idea of several concerned parameters prior to the CO_2-foam implementation, helping us to ensure the feasibility of the method.

1.2 Objectives

1. To study the effects of the wettability of rock formation, the intermediate percentages of hydrocarbon in volatile oil, and the foam slug size in CO_2-foam flooding process.
2. To evaluate effects of foam stability in CO_2-foam flooding process.

1.3 Outline of Methodology

1. Create a homogeneous reservoir model.
2. Simulate CO_2 flooding base case.
3. Perform CO_2-foam flooding on the same reservoir mode of CO_2 flooding base case. Five foam stability values are selected, which are 20, 40, 80, 160 and 320 days.
4. Study the effect of wetting condition of reservoir rock. The study is performed on formation wettability varied from original value in a direction to more oil-wet condition. The wetting condition is varied to moderately water-wet, neutral-wet, moderately oil-wet, and strongly oil-wet conditions.
5. Study the effect of intermediate percentages of hydrocarbon in volatile oil which is adjusted by increasing and decreasing percentage of intermediate compounds approximately 10% and 20% compared to base case.
6. Study the effect of slug size by dividing 0.4 pore volume into two slugs of 0.2 pore volume and three slugs of 0.133 pore volume, each slug is alternated by chasing water.
7. All simulation results are compared among cases of each study parameter to determine effectiveness of foam flooding.
8. Compare, analyze and summarize the most suitable foam stability in each circumstance which yields the highest oil recovery.

1.4 Outline of thesis

This thesis is divided into six parts as mentioned below.

Chapter I introduces background of CO_2-foam flooding application, objectives and methodology of this study.

Chapter II describes previous studies, researches related to CO_2-foamflooding, effects of several parameters on CO_2-foam flooding behavior and CO_2-foam performances. Those parameters include foam stability, formation wettability, oil composition and slug size of CO_2-foam.

Chapter III summarizes significant theories of CO_2-foam flooding, foam stability and foam mechanism such as foam generation, foam-oil interaction and foam degradation. Moreover, foam model that is used for simulation study is referred in this chapter as well.

Chapter IV explains features of reservoir simulation model including reservoir dimension, rock and fluid properties, PVT data and well information.

Chapter V discusses results obtained from reservoir simulation of CO_2-foam flooding for each parameter and compares all cases with CO_2 flooding.

Chapter VI concludes findings from the study and provides several recommendations for further study.

CHAPTER II

LITERATURE REVIEW

This chapter describes the some previous studies and works which associates to CO_2-foam-flooding.

2.1 Application of foam flooding

Foam is defined as a dispersion of gas in liquid, stabilized by the assistance of surfactant. Foam was firstly studied for mobility control by Bond and Holbrook [1] in 1958. However, some other researchers also paid good attentions on foam flooding studies where those results have shown that a stable flood front would be developed by injection of foam. Foam characteristics are very favorable for the flooding application with a concept that gas spreads in surfactant solution, forming a foam formation. Foam generally has lower mobility compared to surfactant solution and gas which are its parental materials. Consequently, foam is more preferable for oil displacement compared to solely gas injection and it also can prevent the channeling and gravity segregation effects. A gas phase of foam can be any type of gas. The most commonly used gas is CO_2 because it is a potential vaporizer for intermediate-enriched hydrocarbon component, resulting in multi-contact miscibility with reservoir oil and hence, creating fluid with improved flow properties at its miscibility condition. Furthermore, the Minimum Miscibility Pressure (MMP) or pressure at which certain crude oil starts to be miscible with injected CO_2 is relatively low compared to other gases providing similar oil recovery mechanism. Accordingly, oil displacement can be accomplished at relatively shallow depth. Moreover, CO_2 flooding can perform immiscible action through pressurizing formation fluids and can be soluble in the crude oil. Oil is then easily produced since it is less viscous and swell.

Wang [2] performed laboratory experiments to study oil displacement mechanism by CO_2-foam. He conducted a test on core sample with a glassy flow-observation tube. The result showed that when foam is in contact with oil, foam front is stable in a short period and then foam bubbles are broken drastically, turning into

gas and liquid forms. Afterwards, the independent flows of gas, liquid and large foam bubbles are noticed. Moreover, he experimented on foam stability by observing the effects of pressure and temperature on foam stability. The outcomes appeared that foam is more stable when pressure is raised but temperature shows a contrary result. The surfactant concentration also has an influence on the foam quantity and quality, i.e., the increase of concentration raises both foam quantity and quality until the concentration reached a certain value. In this study, a surfactant concentration of 0.5% (w/v), is the point at which foam quantity and quality attains their maximum. Wang also indicated that the excessive surfactant concentration creates an extremely rigid foam bubble which obstructs the oil movement and brings about the lower recovery. He also compared the performance between foam displacement in secondary and tertiary displacement. The results showed that the recoveries from secondary and tertiary are quite similar. Hence, his conclusion was that oil recovery from CO_2-foam displacement does not seriously depend on the initial oil saturation.

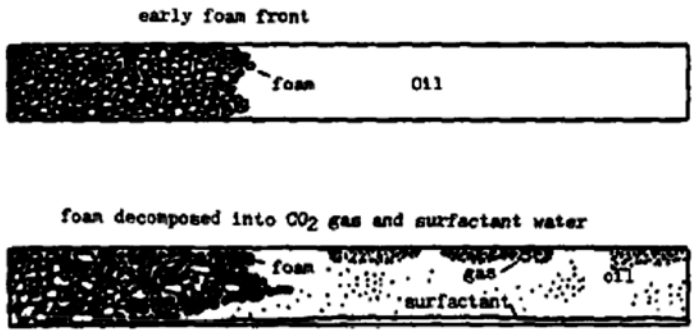

Figure 2.1 Photographic views of foam disintegration (after Wang [2])

Zhang et al. [3] described the blocking effect of foam in the formation. The blocking characteristic of foam relies on foam Resistance Factor (RF) defined as a ratio of normalized pressure drop over total flow rate. The higher foam resistance factor is correspondent to the better foam blocking effect. In this study, it is indicated that reservoir with high permeability has more foam resistant factor value compared to the one with lower permeability. According to the fact that high permeability formation has larger average pore sizes than the lower ones, thus the foam flowing velocity in a big pore throat is lower than in smaller ones. As the flowing behavior of

foam is shear thinning, the viscosity is considered to be an inverse function of velocity. For this reason, in high permeable formation it yields the higher apparent viscosity than the low permeable zone which contributes to the larger foam resistance. In addition, they found that the deviation of fluid flowing performance from the high permeability to low and medium permeability depends on the resistance factor of foam according to a powerful blocking characteristic of foam in the high permeability formation, causing the displacing fluid to move more into the medium and low permeability formations instead of going only through the high permeability zone.

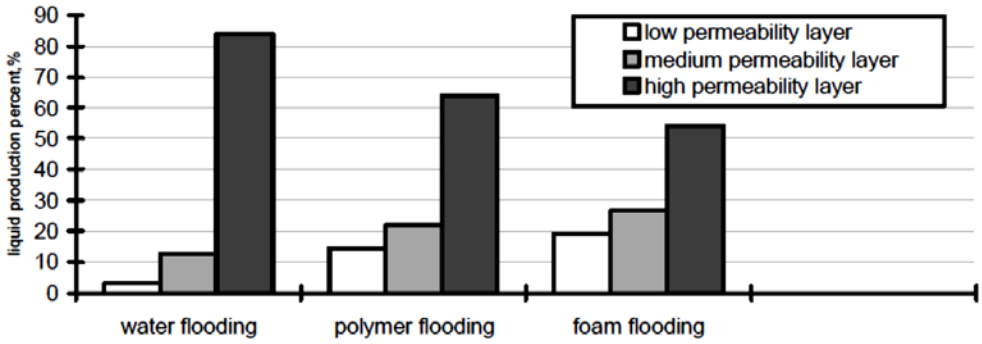

Figure 2.2 Production profiles of water flooding, polymer flooding and foam flooding (after Zhang [3])

2.2 Effects of parameters on foam behavior

Liu et al. [4] studied the effects of pressure, temperature and surfactant concentration on CO_2-foam stability by performing experiments varying each parameter. The foam and CO_2 layer thickness were measured. The results showed that at a low surfactant concentration, foam stability declines when the temperature rises up, but at a higher concentration until a certain concentration value, foam is stable throughout the experiment. According to the effect of pressure, the increment of pressure causes the reduction of foam stability at a low concentration of surfactant but at a higher concentration, foam stability is no more affected by pressure. For the consideration of surfactant concentration, they concluded that the CO_2-foam is not obviously responsive to surfactant. They noticed that foam does not collapse until the

concentration is much lower than the Critical Micelle Concentration (CMC) value. At this concentration, the foam stability is extremely poor. Although foam is not stable all the time because foam is colloidal dissolution, when foam collapses, it may maintain surfactant-stabilized, so bubbles and films may exist for months in the appropriate condition.

Ashoori and Rossen [5] examined the impact of the formation relative permeability on the foam mobility in Surfactant Alternating Gas (SAG); an injection method alternating gas and surfactant slugs into a reservoir. This method is suitable for a field that has limitation of the injection pressure, whereas foam will be dry and disintegrate rapidly around the injection well, so this method provides a high injectivity. They used the fractional-flow theory to analyze the relationship between relative mobility and water saturation and also considered effects of relative permeability function. From the results, it can be explained that in SAG process, the foam mobility decreases when the relative permeability function is going to the direction of non-linear. The reason is that the more non-linear of relative permeability function implies the more water-wet in a formation and water-wet formation is favorable for foam flooding. They also made a conclusion that the reduction of mobility is higher when the critical water saturation is close to the connate water saturation because the reduction of critical water saturation which is the saturation where foam completely collapses, resulting in an increase of foam stability.

Schramn and Mannhardt [6] compared foam sensitivity by performing foam flooding on the water-wet rock and oil-wet rock. They used Berea sandstone or glass micro-visual cells to represent the water-wet surface and treated them with chemical solution Quilon in order to convert their wettability to an oil-wet surface. They conducted micro-visual and core flooding experiments. The results showed that the wettability is influential in the efficiency of foam by which the foam efficiency decreases when the water-wetting decreased. At the residual oil saturation, foam has a tendency to be least efficient and sensitive. Moreover, they found that surfactant may be absorbed by the solid surfaces and rock wettability may be reversed to a more water-wet direction.

This phenomenon of wettability alteration was explained by Sanchez and Hazlett [7] who studied the foam flow in the oil-wet porous medium. They concluded

that when the oil-wet surface absorbs the surfactant surrounding the foam bubbles, the relative permeability to liquid curve shifted apparently to a more water-wet condition. In addition, they found that the oil-wet surface absorbs great amount of surfactant, leading to a substantial reduction of interfacial tension and declining of contact angle. This study also indicated that foam flooding can essentially reduce the gas mobility. However, this reduction of gas mobility does not show big different in both water-wet and oil-wet rock at certain surfactant concentration.

Suffridge et al. [8] conducted the laboratory experiment to investigate the foam behavior from the effects of hydrocarbons. The experiment was performed on Berea cores. Normally, foam collapses when it is in contact with oil. The investigators compared the effect of the molecular weight of alkane in oils. In this experiment, C_{11} and C_{18} hydrocarbon represented oils. Determination of foam stability was accomplished by measuring the foam-generated gas flow rate. The more gas required the more disastrous effect of oil on foam. The result showed that the gas requirement for foam generation in C_{11} oil is higher than in C_{18} oil. They concluded that the lower molecular weight of alkane tends to be more detrimental to foam stability. In order to confirm their conclusion, they performed other experiments by varying the molecular weight of alkane and measuring the permeability of gas. The reduction of gas permeability results in the reduction of mobility. The result showed that in the existence of C_{18} oil, the foam has more ability to reduce the gas permeability than the foam that is generated in the presence of C_{11} oil. They discussed that C_{18} oil may create small amount of oil-in-water emulsions, yielding additional foam.

Moreover, Schramm and Novosad [9] confirmed assumption that light oil destabilizes foam stability more severe than heavy oil. They explained that light oil has ability to penetrate into the interface between gas and surfactant, leading foam to be weakened and eventually ruptured.

Based on the studies above, the investigators emphasized the characteristics of CO_2-foam flooding where individual study was conducted in the laboratory experiment. All of these ultimate results have proven the benefits of CO_2-foam method to be used in the improving oil recovery.

CHAPTER III

THEORY AND CONCEPT

The significant theories of the CO_2-foam flooding, the mechanism of foam and the foam model used for simulation are described in this chapter.

3.1 CO_2-foam flooding

In in-situ condition, CO_2 is generally dense and has a good characteristic of displacing fluid for oil recovery mechanism. CO_2 has an ability to create miscibility with a wide range of hydrocarbons, varying from ethane to heavy oil. But the miscibility can be partially performed when carbon atom in hydrocarbon substance is greater than 14. Another advantage of high density CO_2 is that it is less soluble in water compared to the gaseous state. Hence, loss of CO_2 in formation water is minimized, leading to a more effective miscibility of CO_2 with reservoir oil [10].

Nevertheless, CO_2 flooding still has several unavoidable drawbacks due to its much lower viscosity compared to oil. Consequently, this results in improper mobility ratio during the displacement mechanism. The mobility ratio is defined as the mobility of displacing phase to the mobility of displaced phase. The high mobility ratio causes the unfavorable condition for fluid displacement mechanism such as channeling or gravity segregation, resulting in an early breakthrough.

Foam was introduced in EOR in order to control the mobility of gas phase and to improve sweep efficiency. Physically, foam is a dispersion of gas stabilized by the presence of surfactant in liquid solution as illustrated in Figure 3.1.

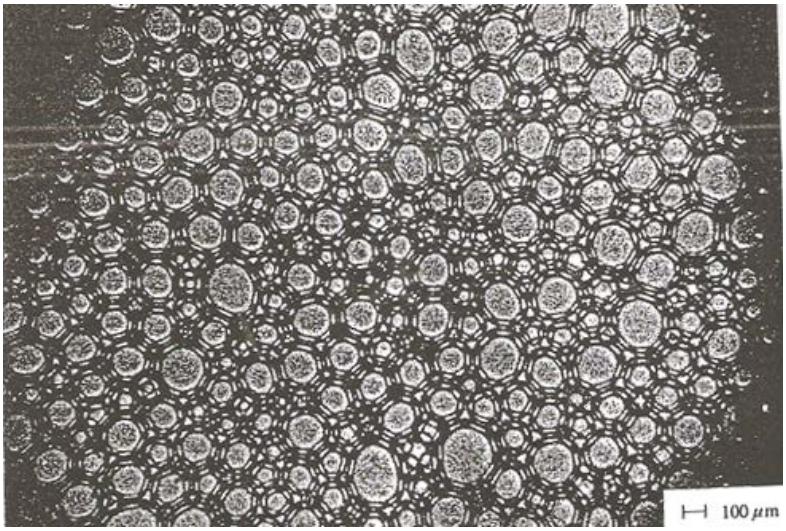

Figure 3.1 Foam bubbles flattened 0.107-mm thick (after Schramm [10].

Foam is generated from gas and small amount of surfactant together with provided mechanical energy in order to build up the turbulence between phases. The volume of gas is much higher than liquid one; generally gas is in the range of 80-98% of total volume of foam [11]. The gas bubbles stay closely packed to each other due to the high amount of gas; they cannot move freely on account of the encapsulation of gas in liquid bubbles called lamellae.

Because foam has higher viscosity than surfactant solution and gas which are parental substances, foam is therefore very beneficial in EOR application. It also has ability to resist the flow; hence, the displacement is significantly effective. Moreover, foam is also suitable for controlling the gas mobility and blocking fractures or high permeability zones. More fluid moves to the lower permeability formation since foam tends to form in high permeability zones first. Therefore it yields a more stabilized flood front when applied in reservoir contains vertical heterogeneity. In summary, the goals of foam operations in reservoir are described as followed:

1. To restrain the flow of undesired fluids into the borehole, for example, coned water and gas,
2. To limit the loss of injectant into the high permeability zones or thief zone and
3. To reduce the mobility of displacing phase.

Mainly, foam is generated at in-situ condition by injecting surfactant into the formation first and followed by gas. The in-situ foam also enhances the trapped gas saturation in reservoir which in turn, leads to the higher pressure gradient and results in lower gas mobility.

3.2 Foam mechanisms

3.2.1 Foam generation mechanisms

There are three fundamental foam generation mechanisms which are snap-off, lamella division, and leave behind. Each foam generation mechanism is described in the following section.

1. Snap-off

Snap-off is a primary mechanism of foam generation. It occurs when the capillary pressure at pore throat declines as gas flows through that throat. Then gas snaps off as bubble. This mechanism is represented schematically in Figure 3.2.

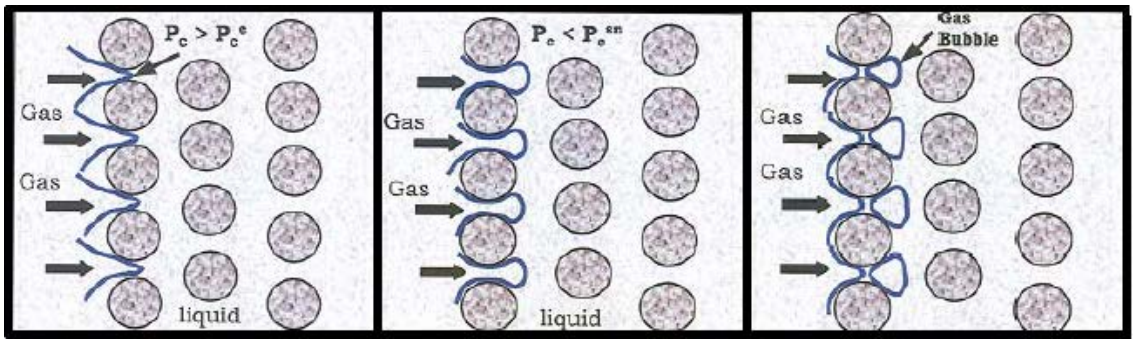

Figure 3.2 Snap-off mechanism (after Dholkawara [12]).

2. Lamella division

Foam lamellas flow against branch junctions and are divided into many channels. Thus, pre-existence of foam flowing is necessary for the lamella division mechanism. The mechanism schematic is shown in the Figure 3.3.

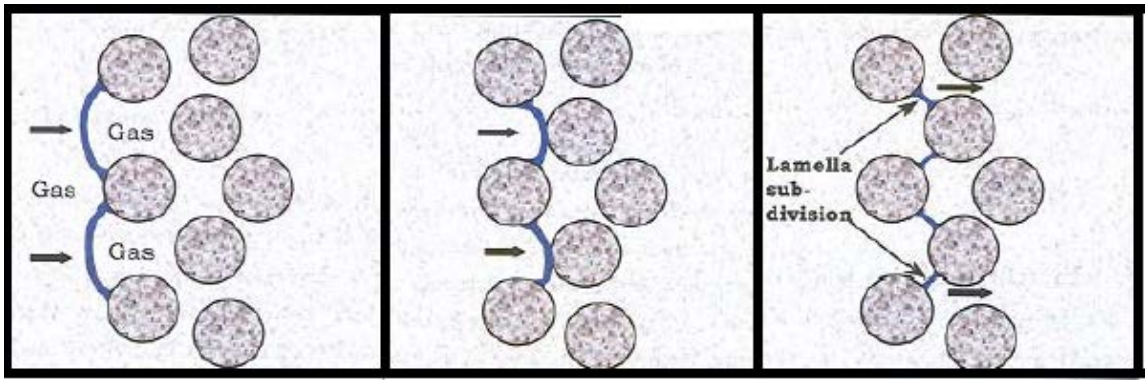

Figure 3.3 Lamella division mechanism (after Dholkawara [12]).

3. Leave-behind

The leave-behind mechanism emerges within two adjacent wetted media. While the non-wetting gas flows through porous medium, the lamellae may be left behind between adjoining media. Figure 3.4 shows the schematic of leave-behind mechanism.

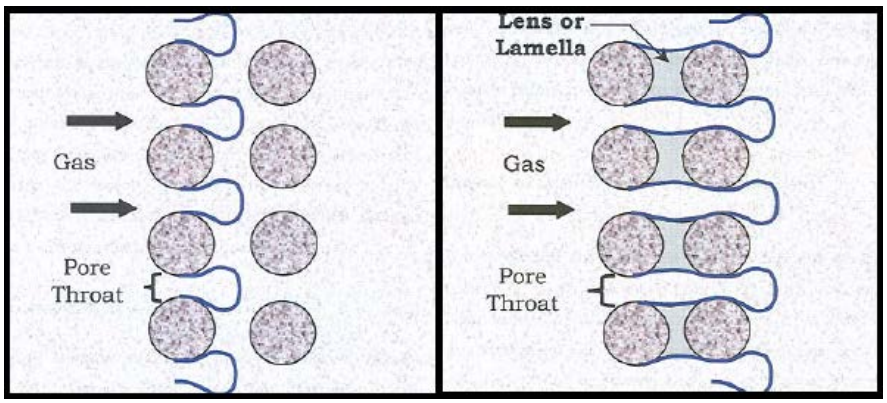

Figure 3.4 Leave-behind mechanism (after Dholkawara [12]).

3.2.2 Foam-oil interaction

The emulsification of oil in the reservoir can destabilize the foam bubble. Hence, foam stability deceases rapidly when foam gets contact with oil. The oil-foam

interaction, therefore highly effects on the efficiency of foam flooding in EOR application.

The interaction mechanisms between foam and oil are quite complex. The foam stability decreases by oil accelerating the foam film thinning. The configuration of oil in contact with foams is shown in Figure 3.5.

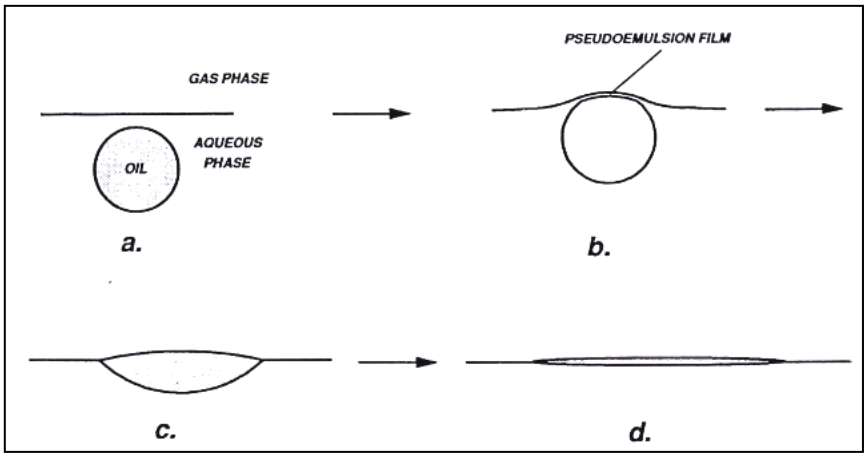

Figure 3.5 Configuration of oil at the gas and liquid interface (after Schramm [10]).

From Figure 3.5a, oil droplet is initially not in contact with foam bubble yet and hence, there is no interaction with foam. The oil droplet starts to interact with foam surface in Figure 3.5b. The oil droplet is deformed into a pseudoemulsion film, occurring between the interfaces. In Figure 3.5c, the pseudoemulsion film breaks and oil goes onto the surface, turning into lens shape. Eventually, a spread oil layer or film is formed from the lens on the solution surface as shown in Figure 3.5d.

The foam stability directly depends on the stability of the previously explained pseudoemulsion. If the pseudoemulsion film is firmly formed, it will prevent the coalescence of foam bubbles by providing the barrier force. On the other hand, if the pseudoemulsion film is vulnerable, only small barrier force is generated and oil droplet behaves like a foam deformer, breaking this film easily and spreading over the surface of bubble.

3.2.3 Foam degradation

In the defoaming process, oil droplet breaks the pseudoemulsion film. After the pseudoemulsion ruptures, oil forms in lens shape and spread over at the interface as shown in Figure 3.5c and 3.5d. The spreading of oil plays an important role in the foam breaking. If oil spread both sides of the film, the foam stability will barely decrease by the reason of balanced tensions in both sides. Unfortunately, oil can spread only on one side of foam bubbles since foam has a closed structure, making foam to have contact with oil only from the exterior surface. The different tension between both sides of the foam contributes to the extremely reduction of foam stability. Eventually, foam bubbles rupture.

Capillary pressure is a significant parameter for determining the foam rupture. The "limiting capillary pressure" P_c^* is defined as the capillary pressure at which single foam cannot maintain its stability. As limiting capillary pressure for rupture is reached, foam bubbles coalesce and become larger bubbles with a consequence of thinning bubble film. Eventually, foam bubbles collapse after several coalescences. Because the limiting pressure is dependent on water saturation in porous media, the water saturation at which the critical capillary pressure for rupture occurs is called "limiting water saturation"S_w^*. In the situation that water is insufficient, foam can be dry out and finally collapse [13].

Destabilization of foam lamellae increases with the rising of oil saturation. The oil saturation at which foam starts collapsing called "critical oil saturation"S_o^*. Above that point of oil saturation, foam degradation rate is accelerated and foam viscosity is obviously decreased by the higher oil saturation. Below the critical oil saturation, foam is weakened and dried out with a directly proportional rate to the oil saturation. Aveyard et al. [14] explained that droplet of oil can diminish foam stability by entering into the interface between gas and surfactant. Oil spreads as multi-molecular films and debilitates foam stability. Foams are weakened and eventually ruptured. Furthermore, Schramm and Novosad [9] discovered that highly viscous oil can delay emulsification reaction between oil and foam, resulting in higher foam stability compared to less viscous oil.

3.3 Foam stability

The foam stability is an ability of foam bubble to resist foam collapse which may be caused from coalescence of foam, pressure reduction, heating, and bubble rupture. The stability of foam can be determined from foam half-life, a period of time required to decrease foam volume to half of its initial volume. The kinetic reaction rate of foam degradation process [15] is described as the equation below:

$$K = \frac{\ln(2)}{t_{1/2}} \tag{3.1}$$

where K = Kinetic reaction rate constant,

$t_{1/2}$ = foam stability (foam's half-life).

The foam stability is a function of oil saturation, time and capillary pressure. The stability of foam is often declined by the oil saturation; thereby foam is destabilized rapidly when formation contains high oil saturation. The higher foam stability can be achieved at higher pressure, lower temperature, and higher concentration of surfactant. Chemically, foam stability can be enhanced by adding some additives such as gellants and cross-linkers compounds which increase the surface viscosity of foam [16].

3.4 Foam models

3.4.1 Method of Characteristics

Method of characteristics (MOC) [5], [17] or fractional-flow theory [18] is used to analyze and explain foam mechanism and foam simulation model. MOC describes the foam displacement mechanism with an assumption that oil in foam displacement processes is immobile oil at the residual oil saturation. The relationship of fractional-flow curve in this method is obtained from the steady-state experiment in the laboratory:

$$f_w(S_w) = \frac{k_{rw}(S_w)/\mu_w}{\left(\frac{k_{rw}(S_w)}{\mu_w}\right) + \left(\frac{k_{rg}^f(S_w)}{\mu_g^f}\right)} \tag{3.2}$$

where f_w = water fractional flow function,

k_{rw} = relative permeability to water,

μ_w = water viscosity,

k_{rg}^f = relative permeability to gas in presence of foam,

μ_g^f = gas viscosity in presence of foam.

In reality, the component of gas mobility consisting of the effective gas relative permeability and effective gas viscosity are complicated to differentiate. But for the simplicity and convenience, most of the models typically determine these two properties independently. When immobile oil or insoluble oil is existed in the foam process system, the mobility of gas and water are diverse. These contribute to changing of the water fractional-flow curve, whereas the oil saturation is not changed.

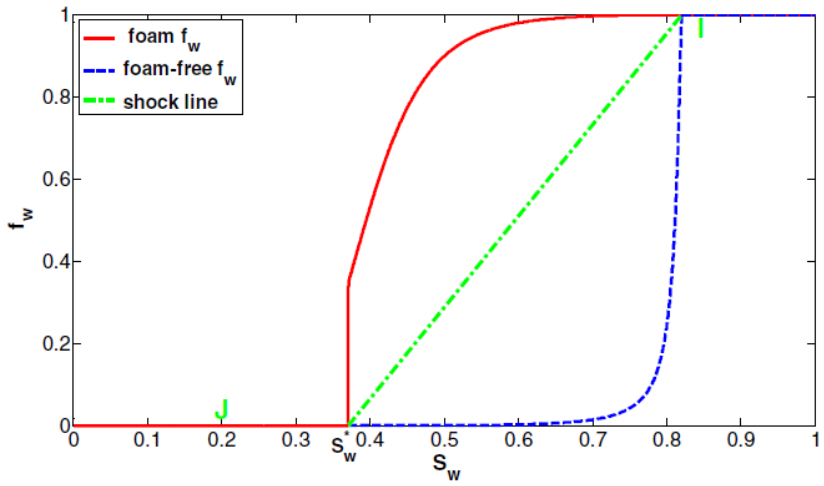

Figure 3.6 Fractional-flow curves in foam process. (after Ashoori and Rossen [5]).

Figure 3.6 shows the fractional-flow curve of foam process both in the presence and absence of foam. It can be observed that the fractional-flow is shifted

upwards in case of foam flood and that is the result of gas mobility reduction. At the limited water saturation (S_w^*), foam breakdowns sharply and this situation leads to a drastic increment of mobility of gas and water fractional flow function value comes close to zero.

The total relative mobility of water and gas could be derived from the basic equation of $f_w(S_w)$which is represented as following:

$$\lambda_{rt}(f_w, S_w) = \frac{k_{rw}(S_w)/\mu_w}{f_w} \tag{3.3}$$

where λ_{rt} = water and gas total relative mobility.

The effective velocity of foam which is considered as a single-phase fluid, defined equivalently to be reciprocal of the total relative mobility:

$$\mu^f \equiv \frac{1}{\lambda_{rt}} = \frac{f_w/\mu_w}{k_{rw}(S_w)} \tag{3.4}$$

where μ^f = foam effective viscosity.

Ground on the foam model of a simulator STARS[19][20], it assumes that gas mobility is changed because of the alteration of the relative permeability to gas only; the relative permeabilities to water and oil are not influenced by the presence of foam. A relationship between relative permeability to gas with foam and without foam as follows:

$$k_{rg}^f = k_{rg}^{nf} \times FM \tag{3.5}$$

$$FM = \frac{1}{1 + fmmob \times F_1 \times F_2 \times F_3 \times F_4 \times F_5 \times F_6} \tag{3.6}$$

where k_{rg}^f = relative permeability to gas in the presence of foam,

k_{rg}^{nf} = relative permeability to gas in the absence of foam,

FM = dimensionless interpolation factor for relative permeability to gas in the presence of foam,

$fmmob$ = reference mobility reduction factor,

F_1 = surfactant concentration dependent function,

F_2 = oil saturation dependent function,

F_3 = water saturation dependent function

F_4 = salt mole fraction dependent function,

F_5 = capillary number dependent function,

F_6 = critical capillary number dependent function,

According to equation 3.6, the effects of surfactant concentration, oil saturation are involved only in this study. The dependent functions of water saturation, gas velocity, capillary number and critical capillary number are set to be the default value which is 1. The following paragraphs describe each concerned term included in FM.

Surfactant concentration dependent function ($\boldsymbol{F_1}$)

$$F_1 = \begin{cases} \left(\frac{W_s}{fmsurf}\right)^{epsurf} & for\ W_s \le fmsurf \\ 1 & for\ W_s > fmsurf \end{cases} \quad (3.7)$$

where W_s = concentration of surfactant in the grid block,

$fmsurf$ = critical concentration of surfactant which normally is The injected fluid concentration,

$epsurf$ = exponent for composition contribution to dimensionless foam interpolation calculation.

Oil saturation dependent function($\boldsymbol{F_2}$)

$$F_2 = \begin{cases} \left(\frac{fmoil - S_o}{fmoil - floil}\right)^{epoil} & floil \le S_o \le fmoil \\ 0 & fmoil \le S_o \le (1 - S_{wr}) \end{cases} \quad (3.8)$$

where $fmoil$ = critical oil saturation (volume fraction),

$floil$ = lower oil saturation (volume fraction).

3.4.2 Foam reactions

In order to create foam in the simulator, the reactions of each process are required. The foam processes concerned in this study are the foam generation and foam degradation which are described as the chemical reactions [21] as shown below.

$$Water + Surfactant + CO_2 \rightarrow Lamella + CO_2 \quad (3.9)$$

$$Lamella + CO_2 \rightarrow Foam\_Gas + Lamella \quad (3.10)$$

$$Foam\_Gas + Oil \rightarrow CO_2 + oil \quad (3.11)$$

In foam model, foam consists of two main components which are Foam_gas and Lamella. The aqueous component of foam is represented by Lamella and the gas component is represented by Foam_Gas. In this case, foam is designed to inject as a liquid, therefore the water-oil relative permeability curve controls the flowing of foam.

CHAPTER IV

RESERVOIR SIMULATION

The simulator STARS will be utilized as a tool to evaluate the performance of CO_2-foam flooding application in this study. This chapter explains about important information that used to construct the reservoir model in each section of the simulator. The general properties of the reservoir are acquired from PTT Exploration and Production Public Company Limited (PTTEP) who provided the Sirikit oil field information for this project.

4.1 Reservoir section

The studied reservoir model is created as Cartesian grid and represents homogeneous reservoir. The simulated reservoir properties are based on information of the Sirikit oil field such as the permeability, porosity, reservoir pressure, oil compositions etc. The summary of the reservoir properties are shown in Table 4.1

Table 4.1 General reservoir model properties acquired from Sirikit oil field.

Property	Value
Top reservoir depth, feet	6,000
Grid block number	30 × 15 × 20
Grid size, feet	100 × 100 × 10
Thickness, feet	200
Porosity	0.25
Initial water saturation	0.28
Horizontal permeability, mD	220
Vertical permeability, mD	22

4.2 Pressure-Volume-Temperature (PVT) properties section

The oil composition of Sirikit oil field was analyzed to determine the phase behavior and to create the properties of components by using **Winprop**, a CMG's equation of state multiphase equilibrium property package which is able to identify fluid properties, lump the components and simulate the multiple contact miscibility processes etc. The equation of state used in this study is based on Peng-Robinson equation (1978)[19]. The oil composition from Sirikit oil field are shown in Table 4.2.

Table 4.2 Hydrocarbon composition of the reservoir fluid from Sirikit oil field.

Component	**Mole fraction**
Carbon dioxide (CO_2)	0.0091
Nitrogen (N_2)	0.0006
Methane (C_1)	0.3383
Ethane (C_2)	0.0904
Propane (C_3)	0.0799
Isobutane (i-C_4)	0.0197
Normal butane (n-C_4)	0.0469
Isopentane (i-C_5)	0.036
Normal pentane (n-C_5)	0.0178
Hexane (C_6)	0.0501
Heptane plus (C_{7+})	0.3112

It is noted that the properties of hepthane plus (C_{7+}) is an average value. From the additional analysis, the specific gravity of this part of hydrocarbon is 0.8615, whereas the average molecular weight is 267.

Winprop was used to determine the MMP from the information provided in oil composition, reservoir temperature and reservoir pressure. These properties are considered as elements that control the magnitude of MMP. The calculated MMP

from previously mentioned properties is about 2,800 psi. Moreover, the component lumping function of Winprop is used to reduce number of component by grouping components together. The new group of oil composition is shown below in the Table 4.3. The properties of each oil composition are shown in the Table 4.4a and 4.4b and the binary interaction coefficients of this system are displayed in Table 4.5.

Table 4.3 Hydrocarbon composition after lumping process by Winprop.

Component	**Mole fraction**
Carbon dioxide (CO_2)	0.0091
Nitrogen (N_2)	0.0006
Methane (C_1)	0.3383
Ethane-Hexane ($C_2 - C_6$)	0.3408
Heptane plus (C_{7+})	0.3112

Table 4.4a Physical properties of each component.

Component	**Critical pressure (atm)**	**Critical temp. (^oK)**	**Acentric factor**	**Molecular weight**	**Vol. shift**
CO_2	72.800	304.200	0.22500	44.010	0.00000
N_2	33.500	126.200	0.04000	28.013	0.00000
C_1	45.400	190.600	0.00800	16.043	0.00000
$C_2 - C_6$	39.608	405.021	0.17589	53.706	0.00000
C_{7+}	13.760	799.287	0.76974	267.000	0.21869

Table 4.4b Physical properties of each component (continued).

Component	**Critical z-factor**	**Critical volume (l/mol)**	**Specific gravity**	**Boiling points (^oK)**
CO_2	0.27360	0.09400	0.81800	194.700
N_2	0.29050	0.08950	0.80900	77.400
C_1	0.28760	0.09900	0.30000	111.700
$C_2 – C_6$	0.27479	0.23241	0.54276	307.740
C_{7+}	0.23378	1.06021	0.86150	623.340

Table 4.5 Binary interaction coefficient of each component.

Component	**CO_2**	**N_2**	**C_1**	**$C_2 – C_6$**	**C_{7+}**
CO_2	0.000000	-0.020000	0.103000	0.133323	0.000000
N_2	-0.020000	0.000000	0.031000	0.083679	0.000000
C_1	0.103000	0.031000	0.000000	0.000000	0.000000
$C_2 – C_6$	0.133323	0.083679	0.000000	0.000000	0.000000
C_{7+}	0.000000	0.000000	0.000000	0.000000	0.000000

4.3 Special Core Analysis (SCAL) section

In this study, Stone's second model [19] is applied to create relative permeability of three-phase system. Table 4.6 shows the parameters that are used in the relative permeability correlation. The values of water–oil and liquid-gas relative permeability are shown in the Tables 4.7 and 4.8, respectively. The illustrations of relative permeability of both cases are displayed in Figures 4.1 and 4.2., respectively.

Table 4.6 Parameters applied in relative permeability generation.

Keyword	Description	Value
SWCON	connate Water	0.28
SWCRIT	critical Water	0.28
SOIRW	irreducible Oil for Water-Oil Table	0.24
SORW	residual Oil for Water-Oil Table	0.24
SOIRG	irreducible Oil for Gas-Liquid Table	0.05
SORG	residual Oil for Gas-Liquid Table	0.10
SGCON	connate Gas	0.00
SGCRIT	critical Gas	0.15
KROCW	k_{ro} at connate Water	0.41
KRWIRO	k_{rw} at irreducible Oil	0.13
KRGCL	k_{rg} at connate Liquid	0.6
	exponent for calculating k_{rw} from KRWIRO	3
	exponent for calculating k_{row} from KROCW	3
	exponent for calculating k_{rog} from KROGCG	3
	exponent for calculating k_{rg} from KRGCL	3

Table 4.7 Relative permeabilities to oil and water as functions of water saturation.

Water saturation (S_w)	**Relative perm. to water (k_{rw})**	**Relative perm. to oil (k_{ro})**
0.28	0.28	0.0000
0.31	0.31	0.0000
0.34	0.34	0.0003
0.37	0.37	0.0009
0.40	0.4	0.0020
0.43	0.43	0.0040
0.46	0.46	0.0069
0.49	0.49	0.0109
0.52	0.52	0.0163
0.55	0.55	0.0231
0.58	0.58	0.0317
0.61	0.61	0.0422
0.64	0.64	0.0548
0.67	0.67	0.0697
0.70	0.7	0.0871
0.73	0.73	0.1071
0.76	0.76	0.1300

Table 4.8 Relative permeabilities to gas and liquid as functions of liquid saturation.

Liquid saturation (S_l)	**Relative perm. to gas (k_{rg})**	**Relative perm. to liquid (k_{rog})**
0.33	0.6000	0.0000
0.36	0.5176	0.0000
0.38	0.4430	0.0000
0.41	0.3650	0.0000
0.44	0.2968	0.0003
0.47	0.2376	0.0012
0.50	0.1869	0.0028
0.53	0.1440	0.0055
0.56	0.1082	0.0094
0.59	0.0789	0.0150
0.62	0.0554	0.0223
0.64	0.0371	0.0318
0.67	0.0234	0.0436
0.70	0.0135	0.0580
0.73	0.0069	0.0754
0.76	0.0029	0.0958
0.79	0.0009	0.1197
0.82	0.0001	0.1472
0.85	0.0000	0.1786
0.93	0.0000	0.2785
1.00	0.0000	0.4100

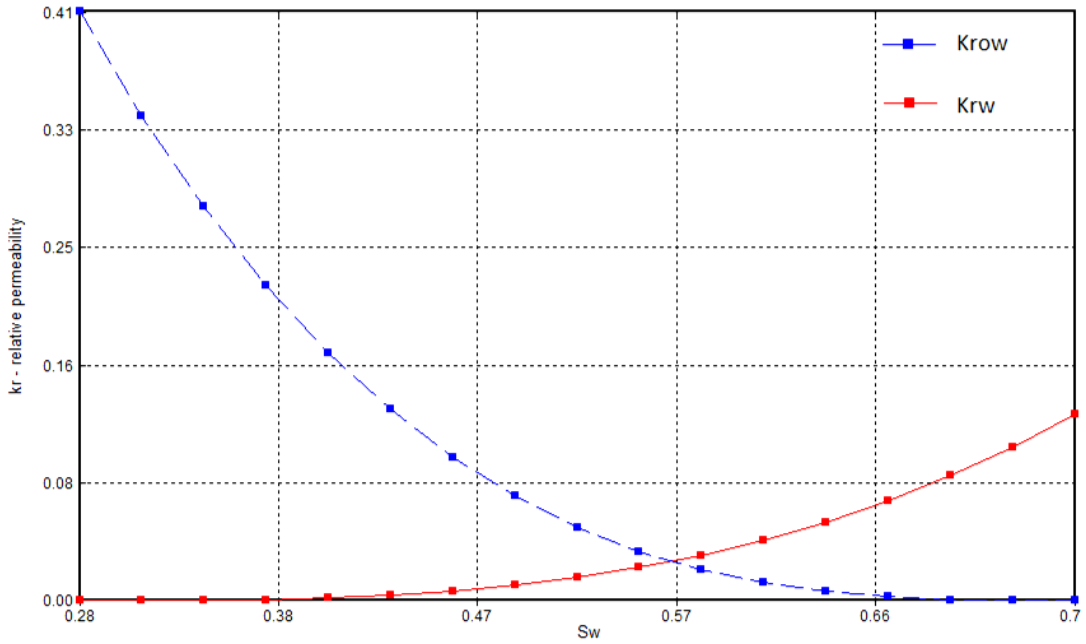

Figure 4.1 Relative permeabilities to oil and water as functions of water saturation.

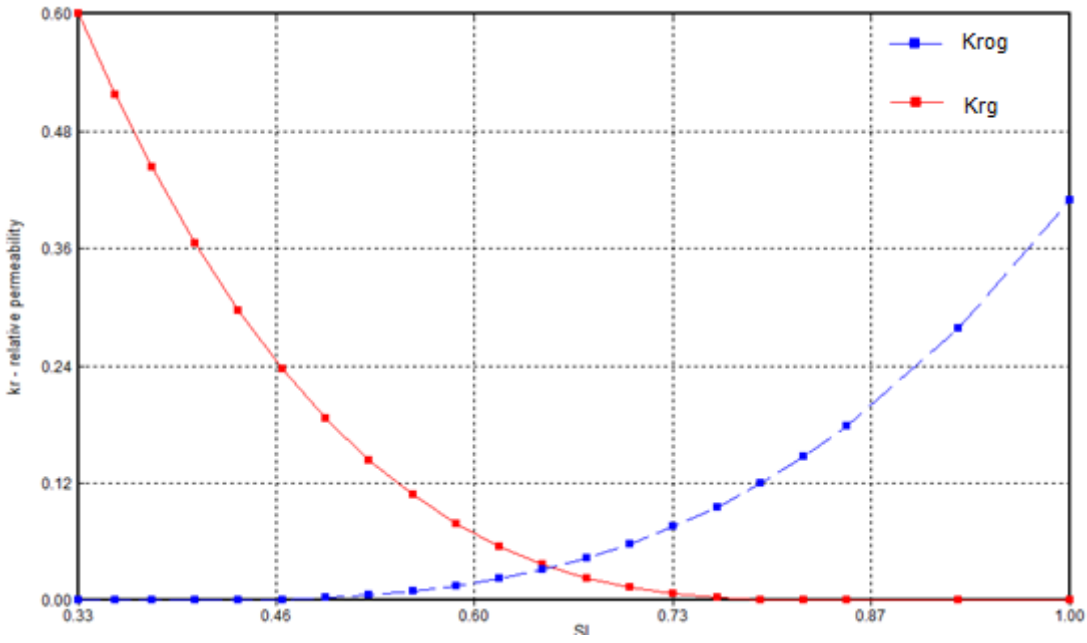

Figure 4.2 Relative permeabilities to gas and liquid as functions of liquid saturation.

4.4 Wells and recurrent section

The production well is located at the edge of the reservoir, while the injection well is at the edge on another side of the model. Both wells have the same in size of wellbore diameter of 3-3/8 inches and are fully perforated. The top view, side view, and 3-dimensional view of reservoir model, are illustrated in Figures 4.3 to 4.5, respectively.

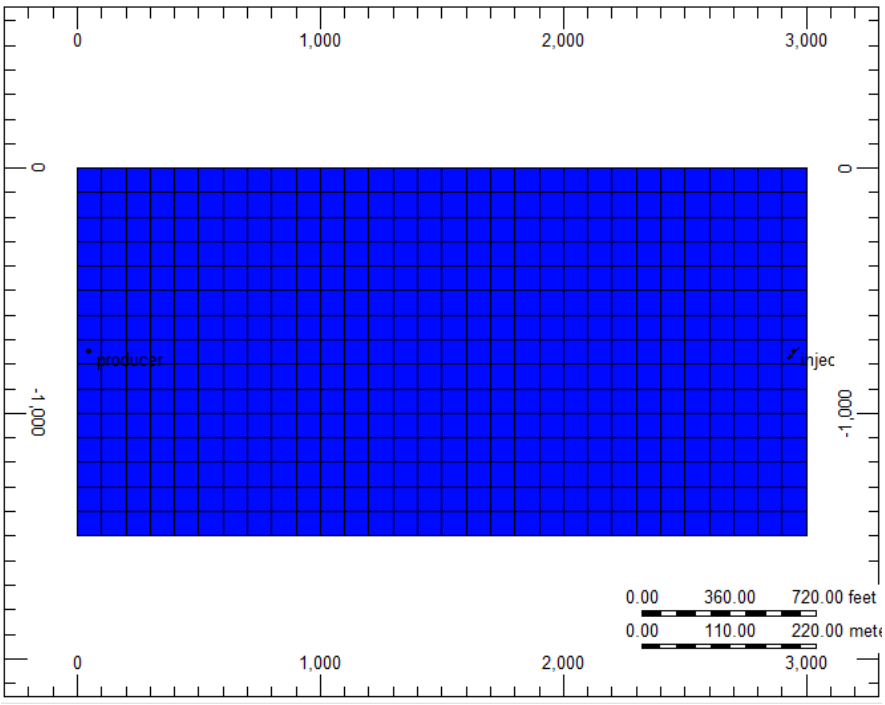

Figure 4.3 Top view of the reservoir model.

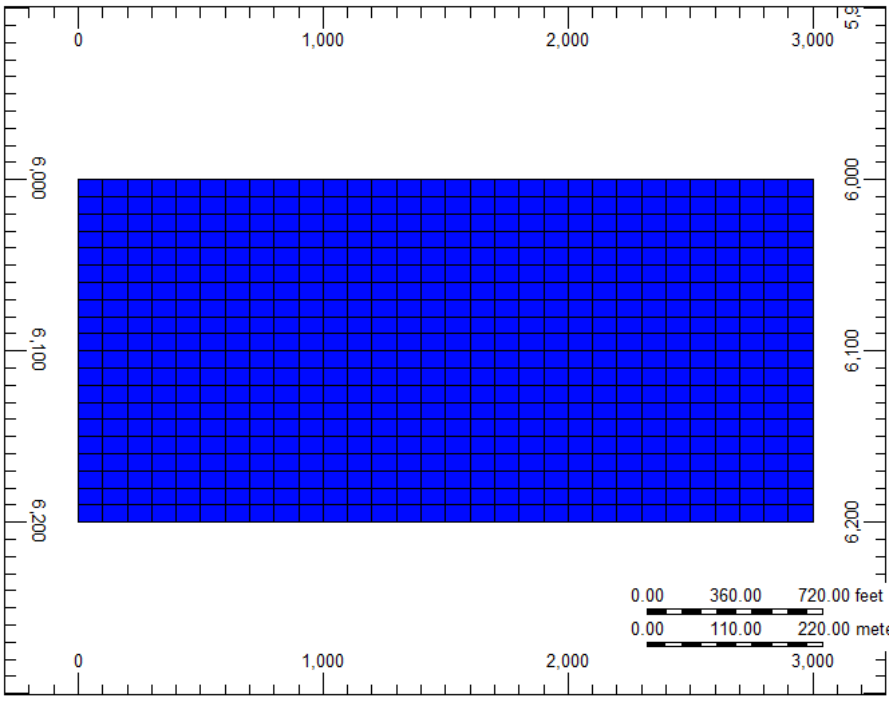

Figure 4.4 Side view of the reservoir model.

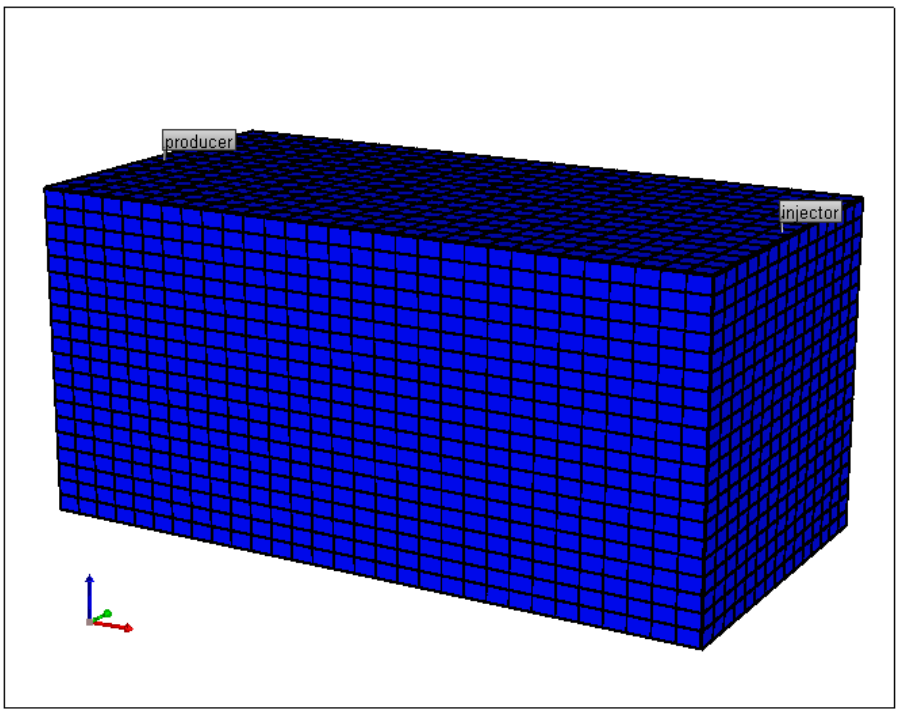

Figure 4.5 Three-dimensional illustration of the reservoir model.

The production constraints and economic limits are shown in Table 4.9.

Table 4.9 Constraints of the production well and injection well.

Constraint	value
Production well	
Maximum oil rate**,** STB/D	2,000
Maximum water rate, STB/D	2,000
Maximum gas rate, MMSCF/D	10
Minimum bottomhole pressure, psi	800
Cut-off oil production rate, STB/D	100
Water cut, %	95
Injection well	
Maximum bottom hole pressure, psi	4,100
Injection pressure, psi	3,000

4.5 Methodology

1. Construct a homogeneous reservoir model.
2. Run a base case model for foam flooding. In this stage, CO_2 flooding is used as injectant since CO_2-foam is principally expected to yield miscibility from injected CO_2. The wettability condition of rock surface and oil properties are obtained from the S1 (Sirikit Oil Field) LaanKrabue district, province of Kampaengpetch. The CO_2 injection is performed at the first day of production with slug size of 0.4 hydrocarbon pore volume. Water is injected after CO_2 to chase previously injected slug until the production constraints is achieved and the oil production is terminated. After the simulation run, production rate (oil, gas, and water), cumulative production recovery factor, bottomhole pressure are collected when the total amount of water reach 0.4 pore volume. Results are used for comparison with foam flood project. The 3D runs of oil recovery,

fluid density, and fluid gravity are also included to identify existence of miscibility.

3. Perform foam flooding on the same reservoir model constructed in step 2, replacing CO_2 by CO_2-foam. Five difference foam stability values are chosen in this step, which are 20, 40, 80, 160 and 320 days. In this step of work, existence of foam is tracked through water mole fraction of foam gas which can be seen on 3D illustration.
4. Study the effect of wetting condition of reservoir rock by keeping the foam injection scheme as same as step 3. Initially, the wetting condition of reservoir rock obtained from S1 oil field is considered strongly water-wet. The study is performed on wetting conditions that are altered from the original value in a direction to more oil-wet condition. This is to perform sensitivity analysis of the relative permeability on the effectiveness of foam flooding as the SCAL data may not represent the actual wetting condition of the reservoir rock at in-situ condition. The wetting condition is altered to moderately water-wet, neutral-wet, moderately oil-wet, and strongly oil-wet conditions. The difference of wetting conditions can be controlled from changing irreducible water saturation (IWS), residual oil saturation (ROS), and relative permeability to water k_{rw} at residual oil saturation.
5. Extend the investigation on composition of oil in order to examine the effect of intermediate component on ultimate oil recovery. The percentage of intermediate is varied from oil composition obtained from S1 oil field by increasing percentage of intermediate compounds approximately 10% and 20% compared to the base case. When the intermediate content is increased, part of heavy compounds (C_{7+}) is decreased proportionally. Other two additional cases of lower percentage intermediate approximately 10% and 20% are also investigated.
6. Study the effect of slug size by dividing 0.4 pore volume into two slugs of 0.2 pore volume and three slugs of 0.133 pore volume. Each slug is alternated with chasing water slugs. The total foam volume must be equal in all case and also the ratio between foam and alternating water slug is kept constant. The investigation is performed similarly to the step 4.

7. Several parameters such as production rate (oil, gas, and water), cumulative recovery factor, bottomhole pressure are compared among cases of each study parameter (intermediate component, surface wettability, and foam slug size) to determine effective of foam flooding.
8. Analyze, make the comparisons and summarize the most suitable foam stability in each circumstance which yields the best production strategy and the highest oil recovery.

CHAPTER V

SIMULATION RESULTS AND DISCUSSION

After the reservoir model is constructed, the foam models are simulated by using the reservoir data obtained from PTTEP. The varied five foam stabilities are applied in these foam models. Alteration of the oil compositions, rock wettability, and foam slug size are performed in the following as the studied parameters. In this study, the CO_2 flooding is selected as reference used for comparison with each case. Simulation results are recorded throughout the production period. Analysis and discussion of reservoir simulation results are described in this chapter.

5.1. CO_2 flooding

Regarding the CO_2 flooding application, production well is located at the middle of the leftmost edge of the reservoir at the coordinate (1,8), while the injection well is located at the opposite edge at the coordinate (30,8). The maximum oil rate at production well is set at 2,000 STB/D. Fluid injection schedule at injector can be divided in two periods. First, CO_2 is injected for 0.4 hydrocarbon pore volume, afterwards water is injected after CO_2 slug to chase all slugs until cumulative amount of water reach 0.4 pore volume. The simulation results are measured at the time where cumulative water is 0.4 pore volume. The injection rate of CO_2 is one of the important concerns. The optimization of CO_2 injection rate is performed to investigate the suitable value for the whole study.

5.1.1. Optimization of CO_2 injection rate

An approximation of optimal injection rate is determined by using the voidage function in the simulator. In this case, gas voidage replacement ratio is set to be unity. From Figure 5.1, it shows that suitable CO_2 injection rate is about 11.5 MMSCF/D. This rate can keep the bottomhole pressure from exceeding the fracture pressure limitation of 4,100 psi.

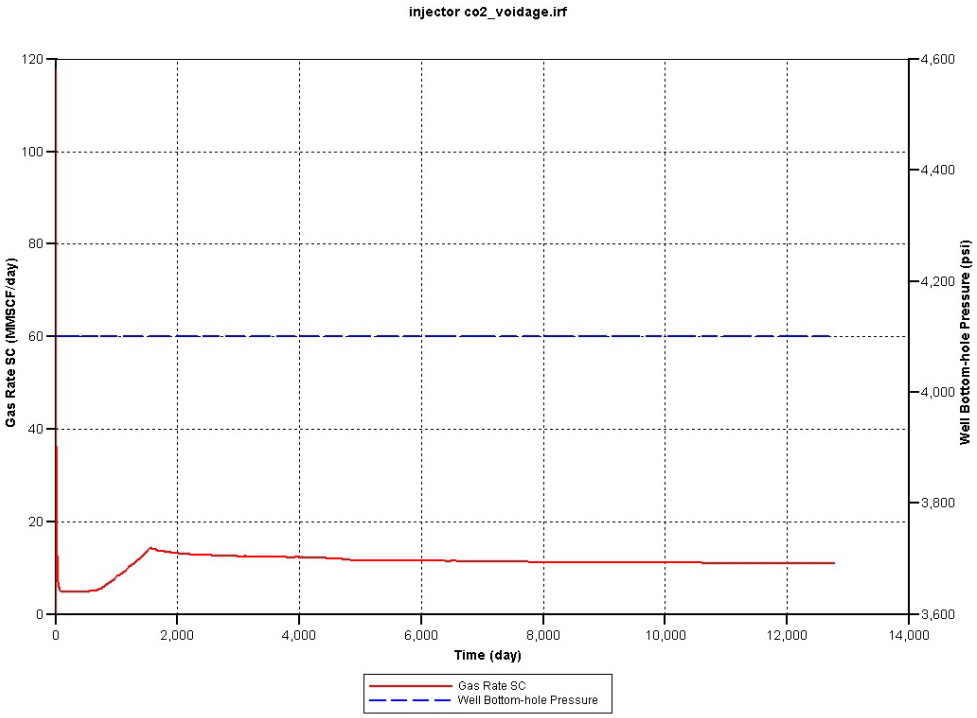

Figure 5.1 The CO_2 injection rates and bottomhole pressures when voidage ratio is unity.

However, CO_2 is not the only injected fluid throughout the production period, water is required for injection to chase previously injected CO_2 gas. CO_2 injection rate obtained from voidage method may be varied. Therefore, the CO_2 flooding is performed by simulating with the variation of injection rate from 9.5-13.5 MMSCF/D in order to achieve an optimal CO_2 injection rate. Results from variation of injection rate are compared at the date which total injected water reaches 0.4 pore volume. The cumulative oil, water, and gas at the production well, and also oil recovery factor are summarized in the Table 5.1 and Figures 5.2 to 5.5. Although the results are not much different, the suitable injection rate in this study is found at 9.5 MMSCF/D. At this rate, CO_2 injection yields the highest oil recovery factor compared to other higher injection rates. Moreover, this lowest injection rate is selected because of power energy required for surface facilities is the smallest one.

Table 5.1 Cumulative oil production, water production, gas production and oil recovery factor of CO_2 injection rate optimization cases.

CO_2 injection rate (MMSCF/D)	**9.5**	**11.5**	**13.5**
Time for injected water to reach 0.4 PV, day	6,350	6,100	5,960
Cumulative oil production (MMSTB)	7.91	7.89	7.91
Cumulative water production, (MMSTB)	0.98	0.8	0.66
Cumulative gas production (MMSCF)	30,520	30,520	30,420
Oil recovery factor, %	42.62	42.5	42.55

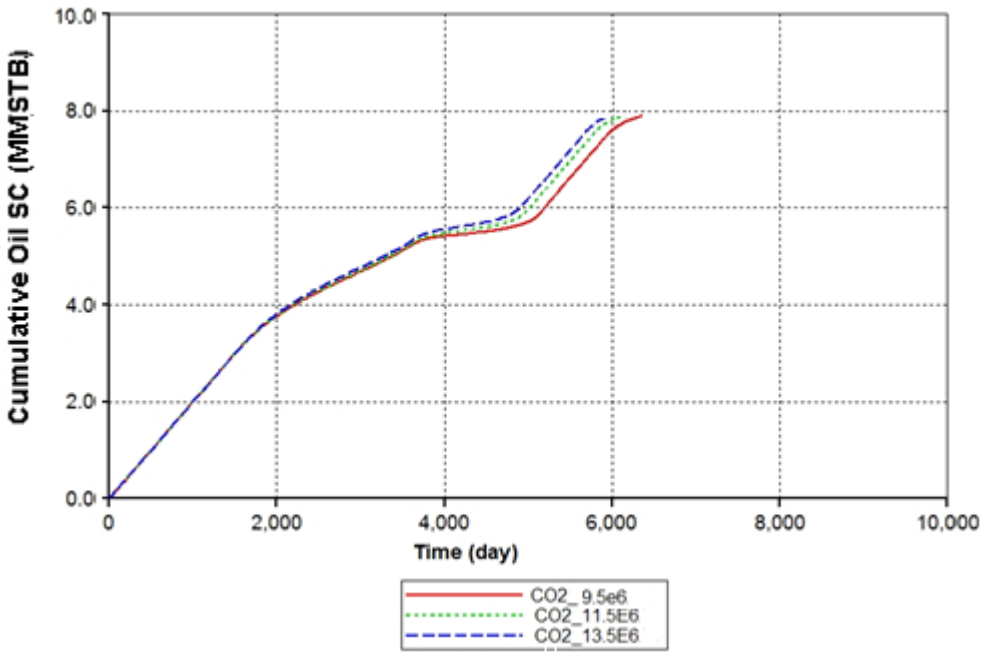

Figure 5.2 Cumulative oil productions of CO_2 injection rate optimization.

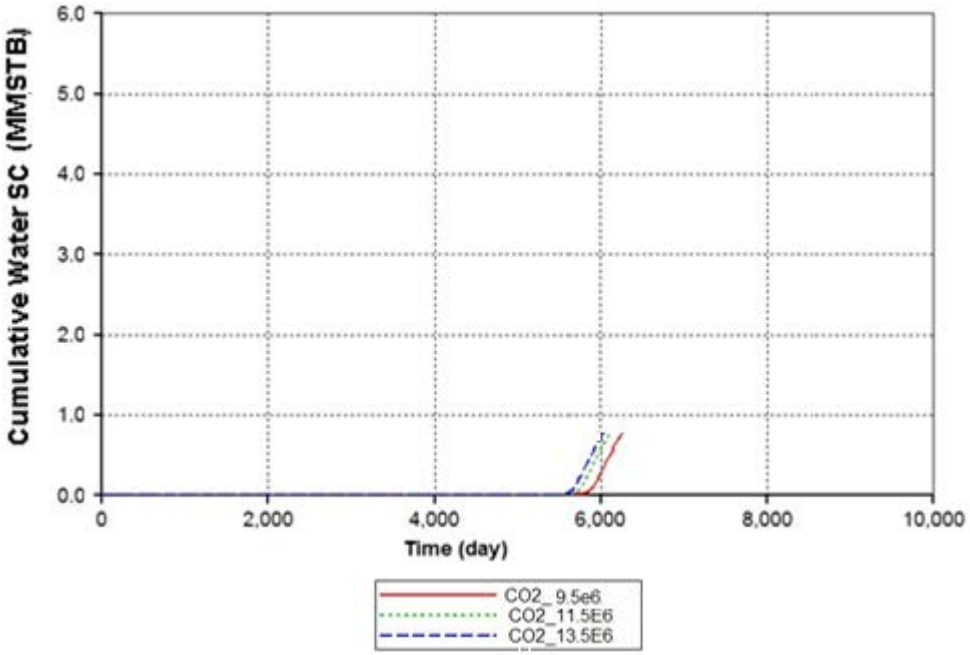

Figure 5.3 Cumulative water productions of CO_2 injection rate optimization.

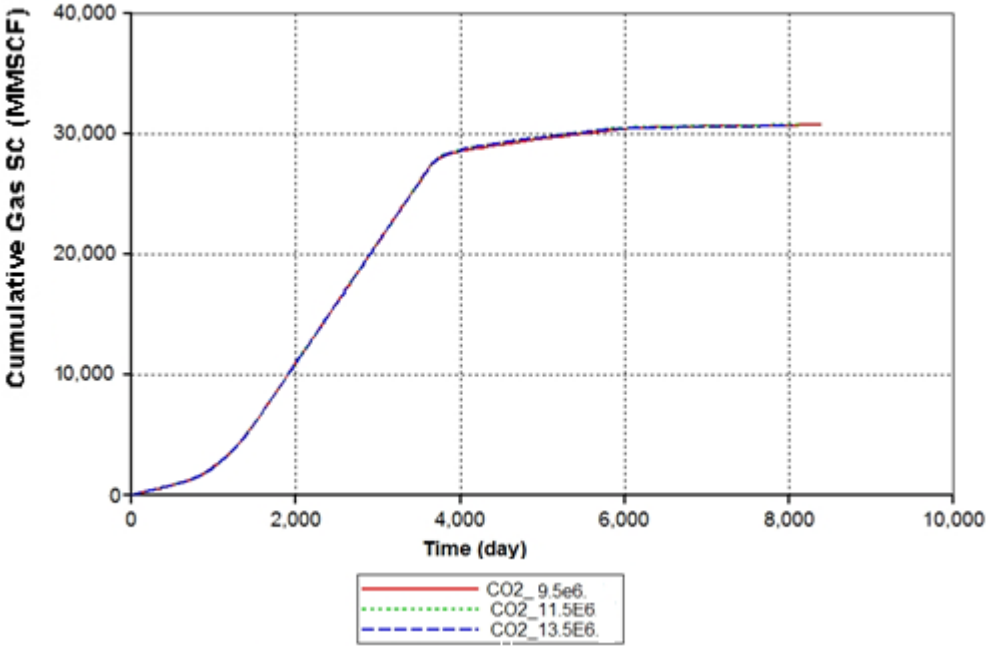

Figure 5.4 Cumulative gas productions of CO_2 injection rate optimization.

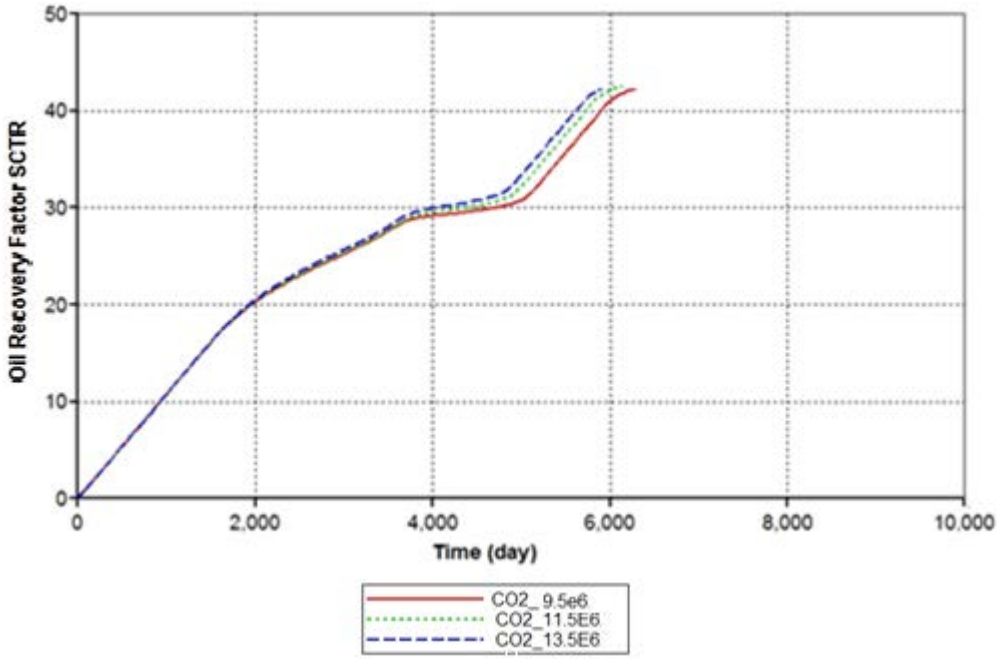

Figure 5.5 Oil recovery factors of CO_2 injection rate optimization.

5.1.2. Finalized CO_2 flooding base case

For CO_2 flooding base case, the injection rate of CO_2 is initially set at 9.5 MMSCF/D but this preset injection rate cannot be constantly achieved due to the bottomhole pressure that could reach the fracture pressure of 4,100 psi when injectivity of CO_2 is too low (at the initial of gas injection). Therefore, the rate is adjusted automatically and hence, the bottomhole pressure does not exceed the maximum pressure that could lead to undesired fractures. The injection pressure is fixed at 3,000 psi in order to ensure that miscibility of CO_2 can be achieved throughout the process. The miscibility is observed by the changes of oil mass density and gas mass density as illustrated in Figure 5.6 and Figure 5.7. When CO_2 is in contact with oil, CO_2 vaporize the intermediate part of oil, leaving heavy composition in oil behind. The left oil that cannot be vaporized from contact with CO_2 is getting higher in density compared to the initial oil density as shown in the red zone in Figure 5.6. However, this oil could be vaporized and displaced by CO_2 afterwards. The blue

zone which is adjacent to the wellbore represents formation with no oil left and pores are all occupied by CO_2.

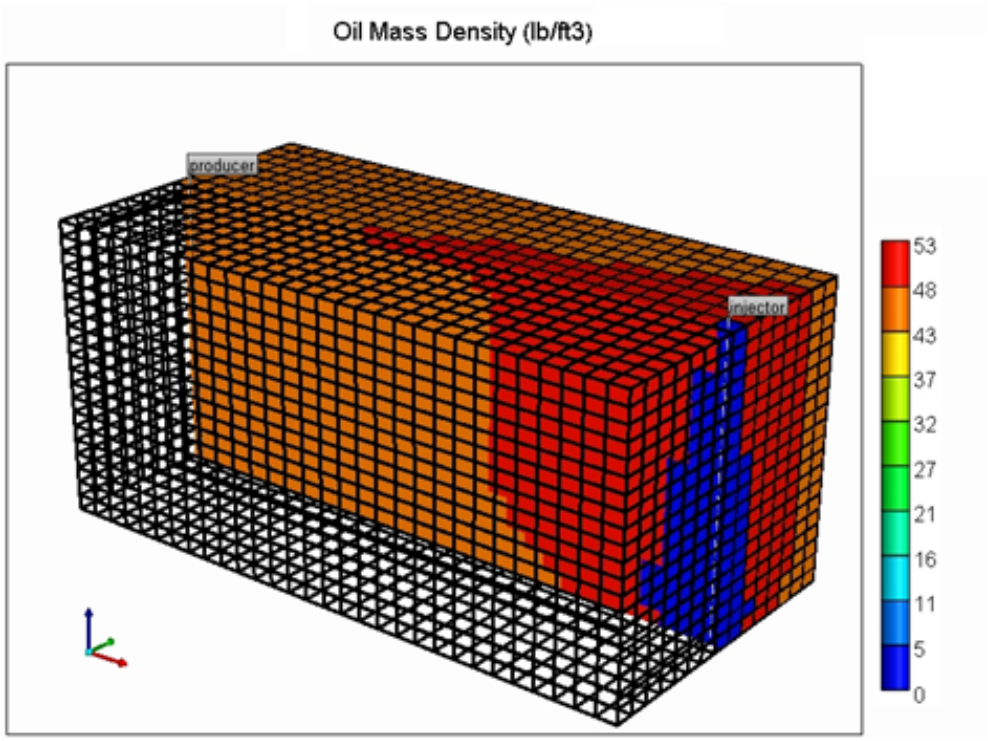

Figure 5.6 Miscibility effect on oil mass density.

The vaporized oil is considered equivalently as gas phase. From Figure 5.7, gases which have lower mass density compared to CO_2 such as methane move faster than others as seen in green color. The red color zone is the zone where CO_2 occupies pore space and the yellow zone is the mixing zone between CO_2 and vaporized gas. From these two figures the definite miscible front is located at the boundary between red and orange color in Figure 5.6.

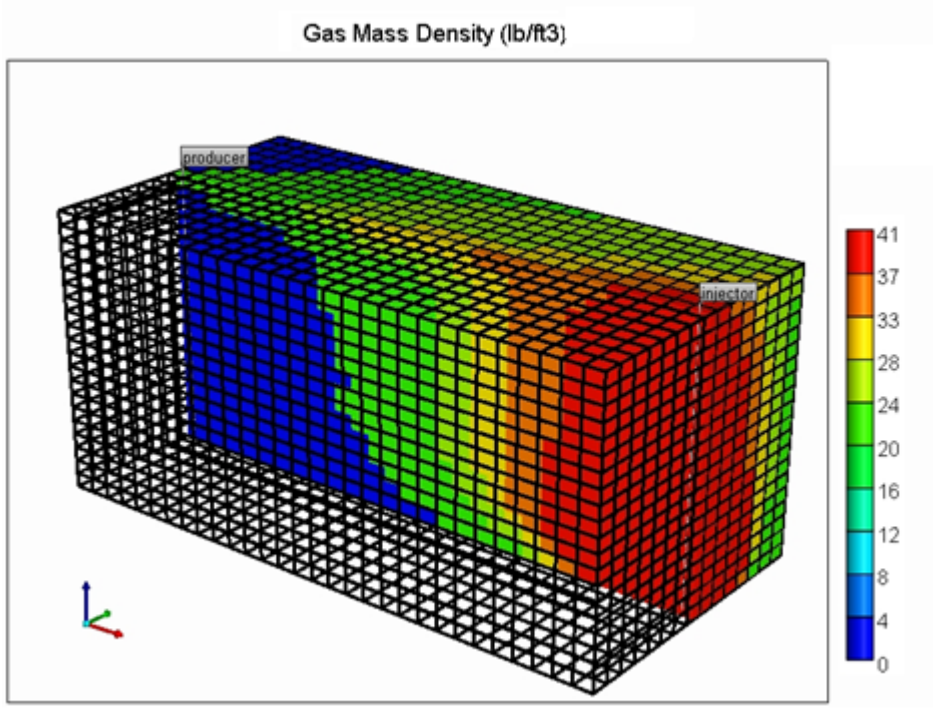

Figure 5.7 Miscibility effect on gas mass density.

The produced oil is constantly maintained at the rate of 2,000 STB/D for 1,525 days, after that the rate declines as a result of gas breakthrough at the production well as shown in Figure 5.8. Reduction of oil production rate is due to CO_2 breakthrough; gas production rate rapidly increases in at 570 days of production period. Gas rate increases abruptly until it reaches the maximum gas rate of production well which is 10 MMSCF/D. However, gas production rate is controlled at this value as mentioned in production limitation and hence, the rate does not exceed this throughout the production period. The first slightly increment of oil rate starts at 2,950 days or approximately two years after injecting of chasing water. This incident is a result from an increase of relative permeability of water. Hence, influence of gas on oil flowing is minimized. High rate of oil production is maintained for a while before a drastic decline because bottmehole pressure reaches the minimum point as shown in Figure 5.9. The production well is controlled by bottomhole pressure instead and hence the production rates fall. The second increment of oil rate starts at around 4,300 days. This incremental recovery comes from oil that moves in front of the

chasing water sweeping oil from the bottom zone. This arrival of oil is in coincidence with high water production rate that is water breakthrough period. Oil rate rises up for while and then declines again because water is a dominant phase in flowing. Water rate escalates rapidly, and remains constant at the maximum rate throughout the production period.

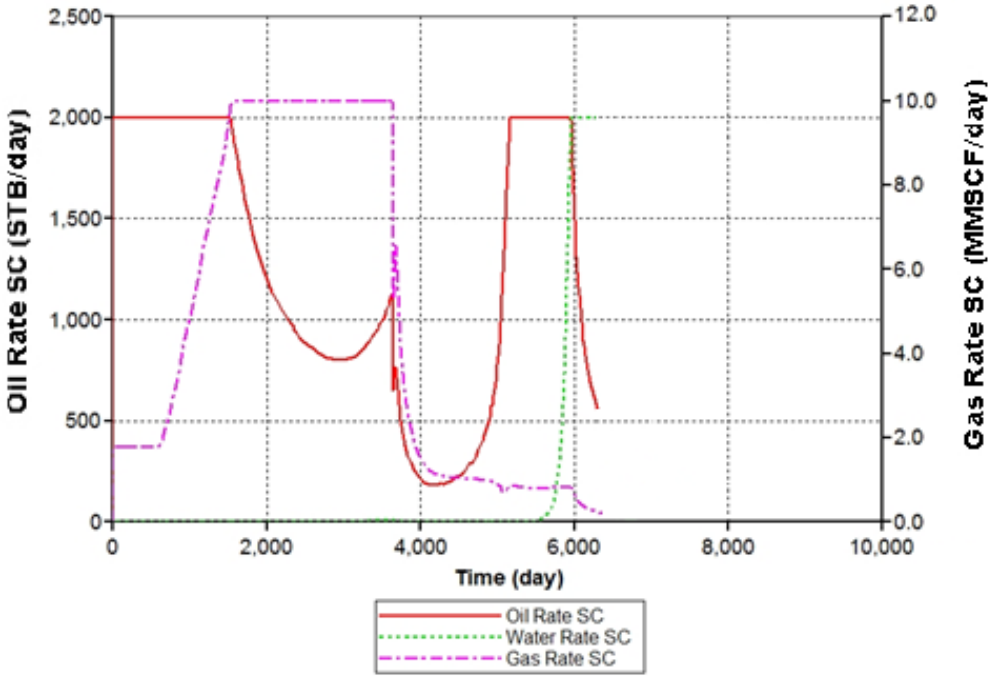

Figure 5.8 Oil, water and gas production rates of CO_2 flooding base case.

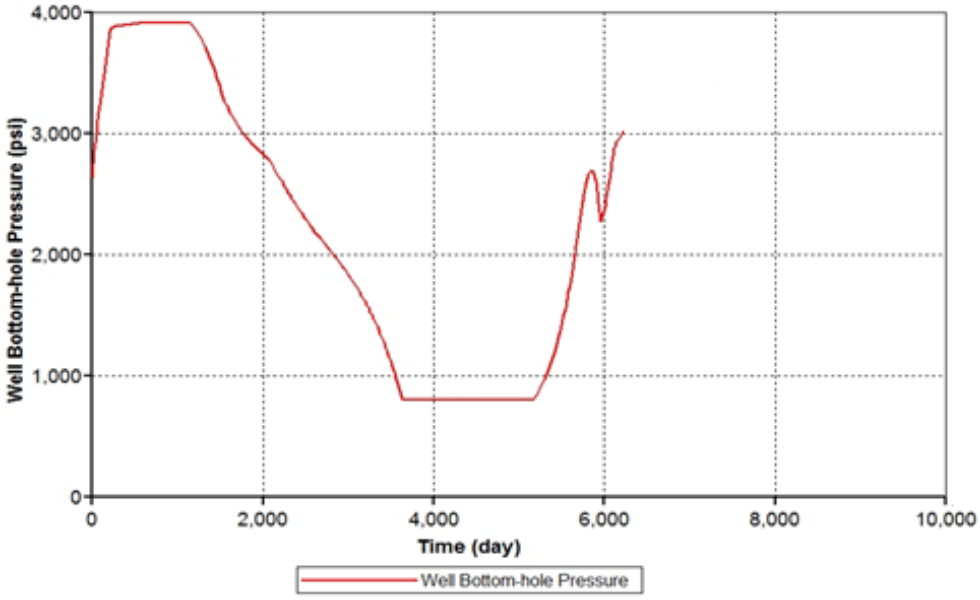

Figure 5.9 Bottomhole pressure at the production well of CO_2 flooding base case.

Considering injection well, Figure 5.10 shows that gas rate is injected at 9.5 MMSCF/D for approximately 200 days and this makes the bottomhole pressure of injection well approaching to the fracture pressure. Therefore, injection rate is reduced automatically below the limit to prevent the undesired fracture. The bottomhole pressure of the injection well is presented in Figure 5.11. After CO_2 is completely injected at 2,070 days which is equivalent to cumulative gas of 0.4 hydrocarbon pore volume (16,700 MMSCF), water is injected with the injection rate 4,000 STB/D to displace previously injected CO_2 slug until the end of production.

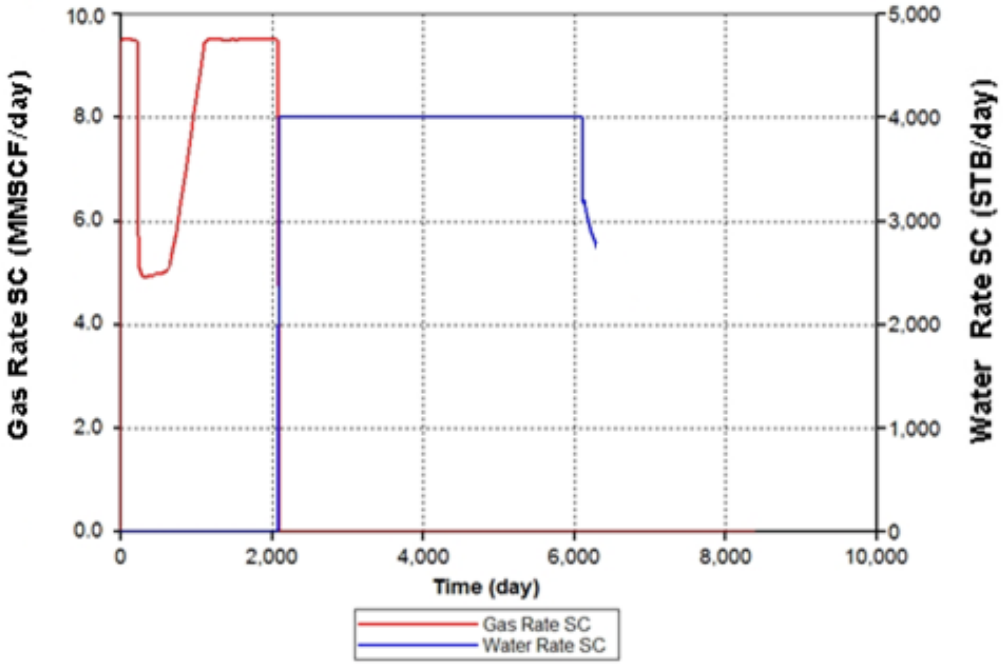

Figure 5.10 Gas and water injection rates at injection well of CO_2 flooding base case as functions of time.

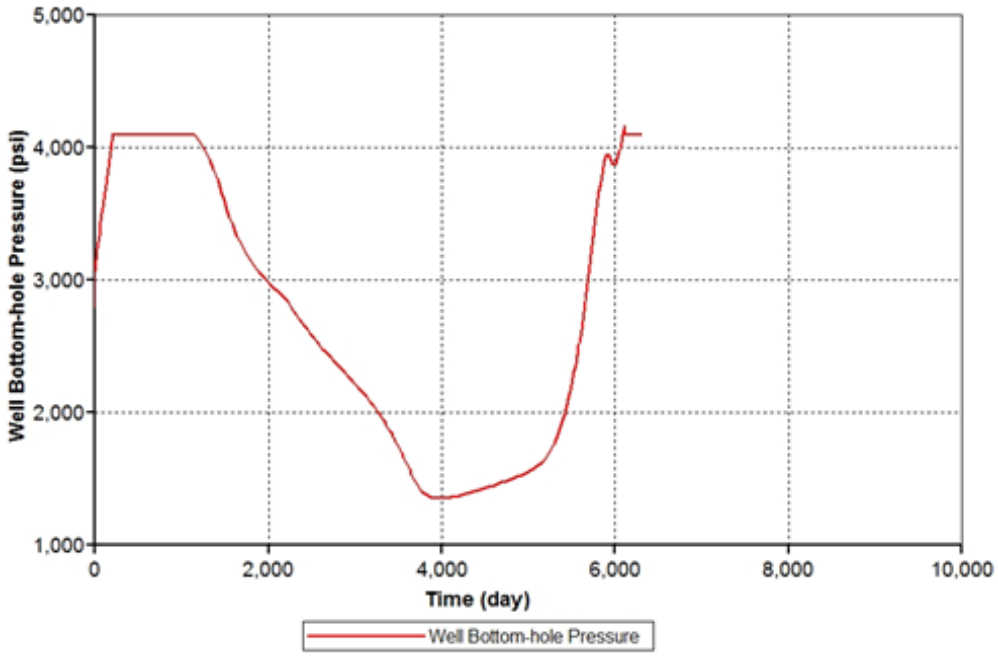

Figure 5.11 Well bottomhole pressures at injection well of CO_2 flooding base case as a function of time.

Cumulative amounts of produced oil, gas and water measured at the day the cumulative injected water reach 0.4 pore volume which are illustrated in Figure 5.12 which total amount of oil, gas and water are 7.91 MMSTB, 30,520 MMSCF and 0.98 MMSTB, respectively. The ultimate oil recovery factor is about 42.62%. Changes of the oil recovery factor with time are shown in Figure 5.13.

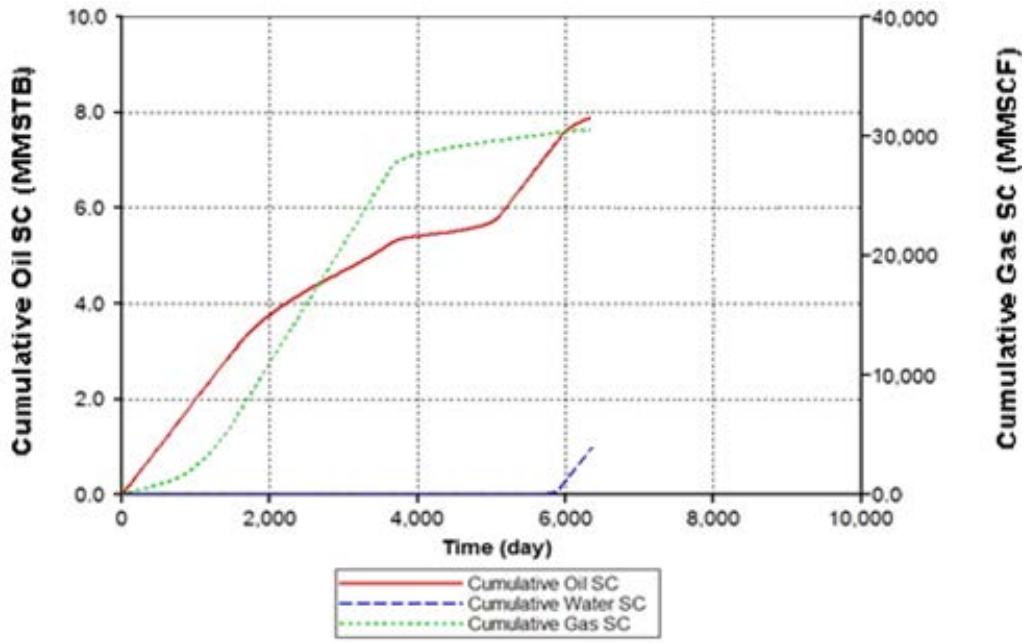

Figure 5.12 Cumulative oil, water and gas production of CO_2 flooding base case.

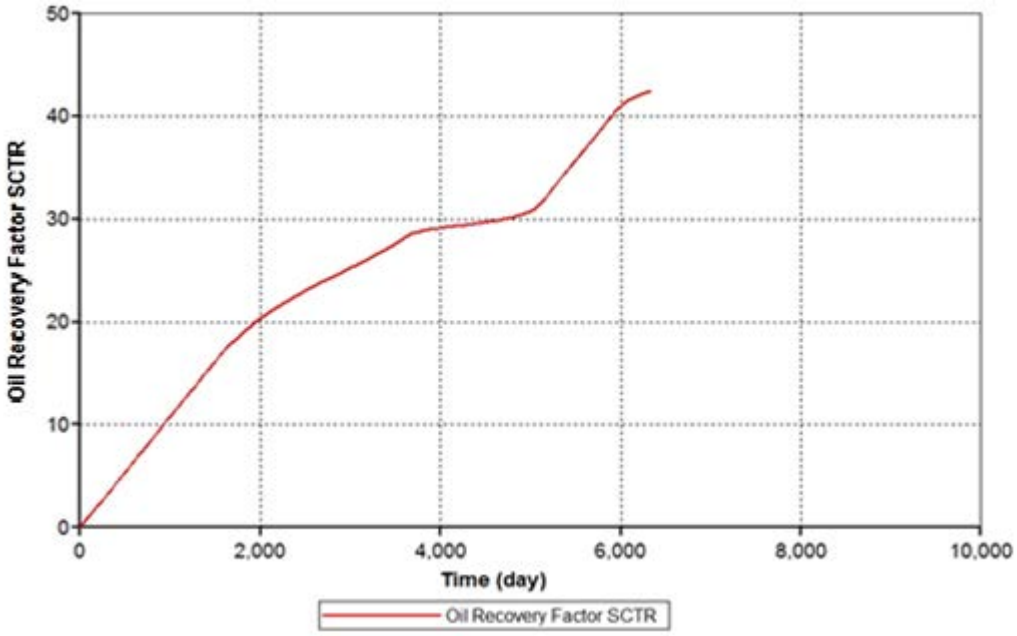

Figure 5.13 Oil recovery factors of CO_2 flooding base case.

5.2. CO_2-foam flooding

The performance of CO_2-foam flooding is discussed in this section by analyzing the simulation results. Basic reservoir construction and production constraints are similar to those of CO_2 flooding. Due to complexity that two phases of fluid cannot be injected in the same well the simulation program, CO_2 and water are injected in separated imaginary wells but they are both in the same location at coordinate (30, 8). The foam application is performed from the first day of production until the amount of CO_2 reaches 0.4 hydrocarbon pore volume. Then, water injection is executed subsequently. The simulation results are measured at the time where cumulative water reaches 0.4 pore volume. In order to obtain the best performance of foam flooding, the optimization should be performed. In this case, the injection rates of injected fluids and the perforation intervals of wells are considered.

5.2.1. Optimization of injection rates

Injection rate of CO_2 and surfactant solution is very important because it leads to the suitable foam quality (or formability). High gas rate and low liquid rate causes high foam quality, creating light foam that causes the effect of gravity segregation. On the contrary, high liquid rate and low gas rate results in an early breakthrough of water. The summation of CO_2 injection rate and the liquid rate in foam application is approximately equal to the CO_2 injection rate in CO_2 flooding. There are four cases of the fluid injection rate chosen are shown as follows:

Case 1: CO_2 rate 7.77 MMSCF/D and liquid rate 1,200 STB/D

Case 2: CO_2 rate 8.78 MMSCF/D and liquid rate 500 STB/D

Case 3: CO_2 rate 9.14 MMSCF/D and liquid rate 250 STB/D

Case 4: CO_2 rate 9.36MMSCF/D and liquid rate 100 STB/D

The cumulative oil, gas, and water and recovery factors are measured at the day that 0.4 pore volume of chasing water is reached and are summarized in Table 5.2 and illustrated graphically in Figures 5.14 to 5.17.

Table 5.2 Cumulative oil production, water production, gas production and oil recovery factor of fluid injection rate optimization cases.

Details	Case 1	Case 2	Case 3	Case 4
Surface gas rate (MMSCF/D)	7.77	8.78	9.14	9.36
Surface water rate (STB/D)	1,200	500	250	100
Time for injected water to reach 0.4 PV, day	10,169	10,010	9,554	8,366
Cumulative oil production (MMSTB)	9.93	10.00	9.76	9.11
Cumulative water production, (MMSTB)	11.73	11.37	10.65	8.72
Cumulative gas production (MMSCF)	15,530	20,070	20,670	22,440
Oil recovery factor, %	55.41	55.84	54.51	50.90

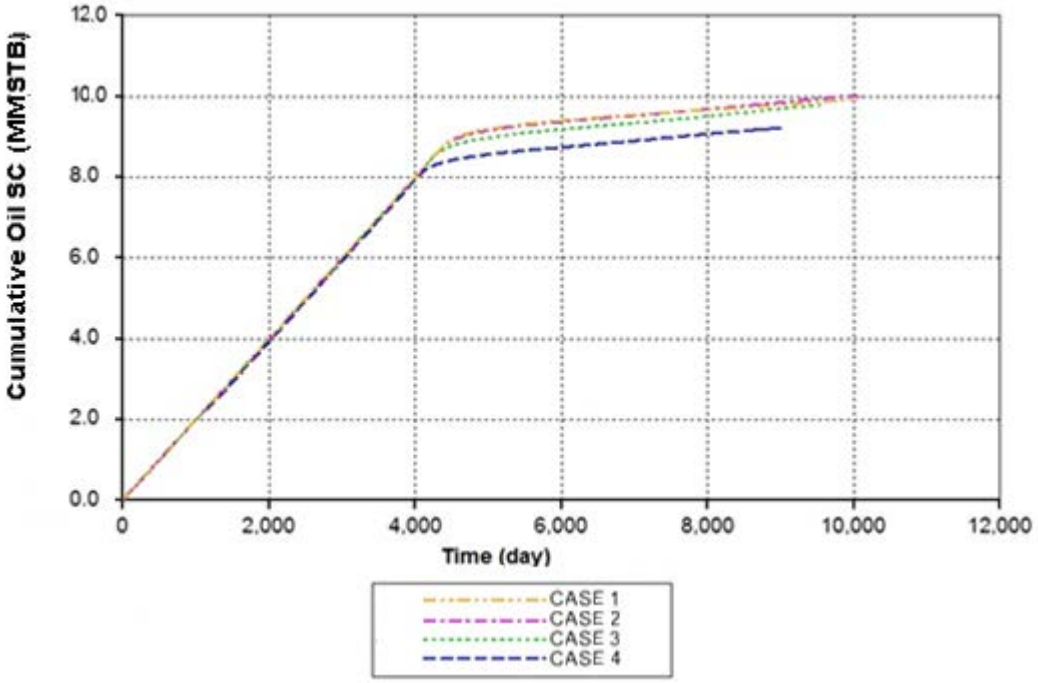

Figure 5.14 Cumulative oil productions of fluid injection rate optimization.

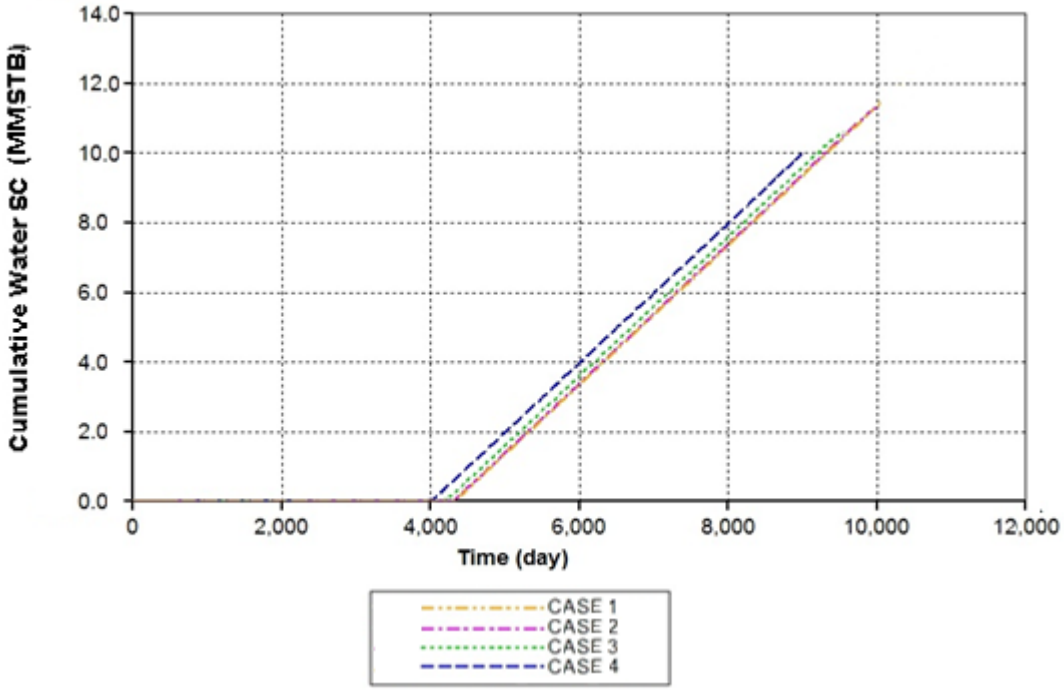

Figure 5.15 Cumulative water productions of fluid injection rate optimization.

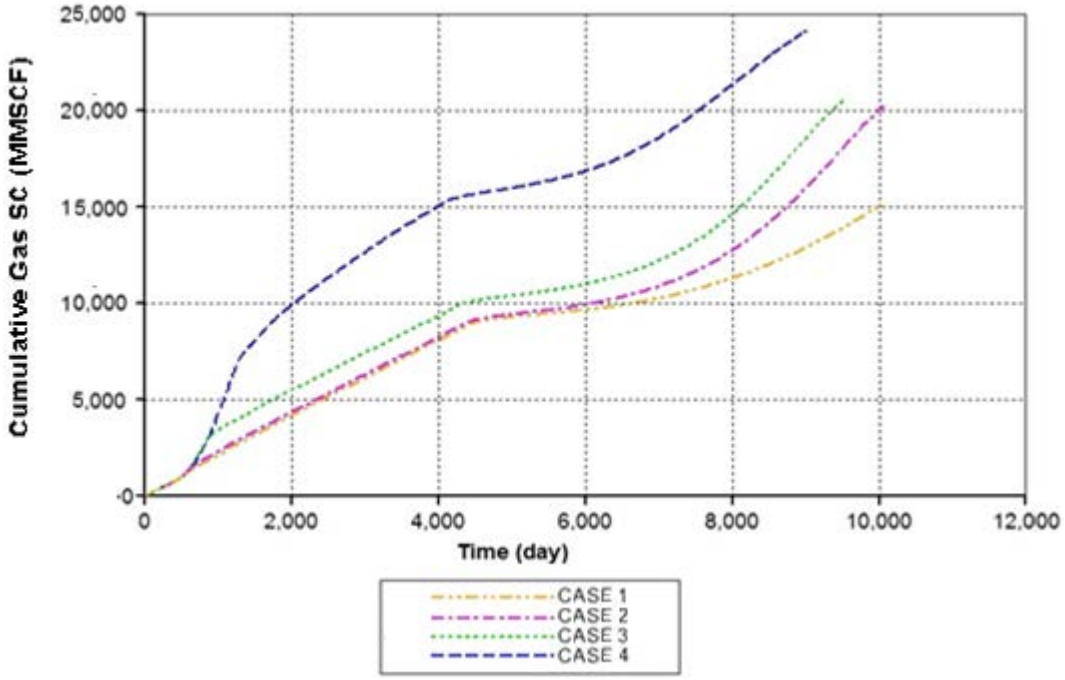

Figure 5.16 Cumulative gas productions of fluid injection rate optimization.

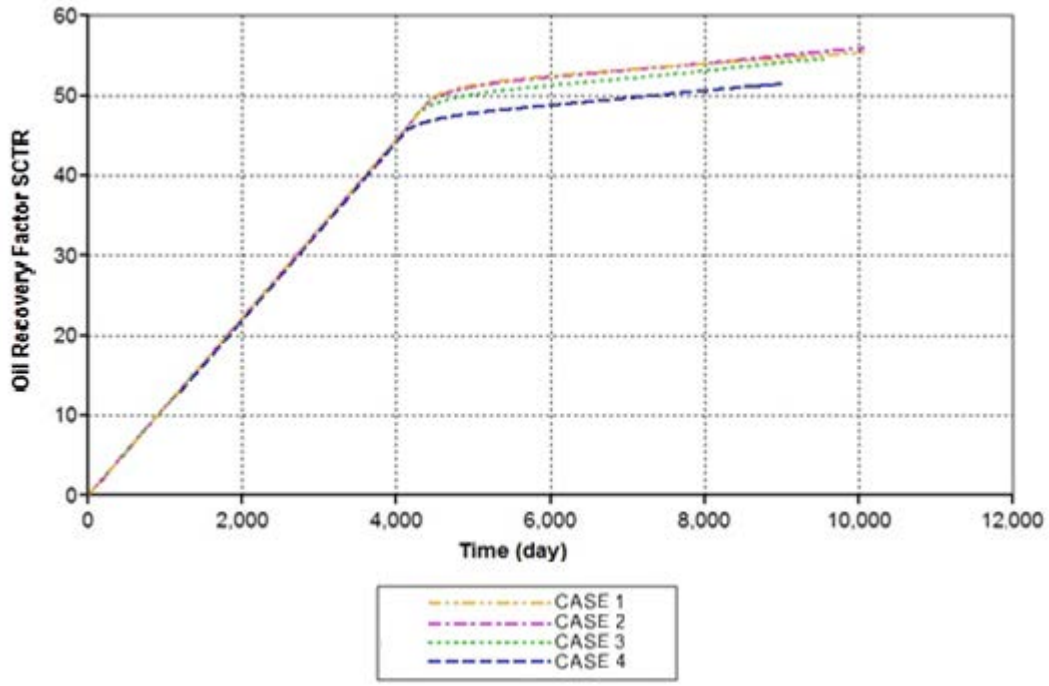

Figure 5.17 Oil recovery factors of fluid injection rate optimization.

From Table 5.2 and Figures 5.14 to 5.17, case 2 of which the CO_2 injection rate 8.78 MMSCF/D and liquid injection rate 500 STB/D is the optimized case where optimal rate is fixed for foam flooding throughout in this study because these rates yield the highest cumulative oil production and the highest oil recovery factor.

5.2.2. Finalized CO_2-foam flooding

After the optimal injection rates of CO_2 and water are identified, foam flooding application is executed. Foam stabilities are varied from 20 days, 40 days, 80 days, 160 days, and 320 days in order to study their effect on foam flooding performance. For all foam simulations in this study, surfactant concentration is kept constant at 0.5% (w/v). CO_2 gas is injected at the rate 8.87 MMSCF/D, whereas surfactant solution is injected at 500 STB/D. The gas rate is constant for short period and then it is adjusted automatically due to the preset well bottomhole pressure is reached, while surfactant solution rate is kept constant at 500 STB/D. This is due to the previously present phase of surfactant solution which is aqueous phase (represented by connate water), resulting in higher injectivity compared to CO_2. Figures 5.18 and 5.19 illustrate the injection rates of CO_2 and surfactant solution at different foam stability, respectively. When cumulative injected CO_2 reaches 0.4 hydrocarbon pore volume (16,700 MMSCF), water is the only phase which is injected to chase CO_2-foam in the reservoir as same as the case of CO_2 flooding. From the reservoir simulation, water chasing is started from 4,900-5,000 days of production.

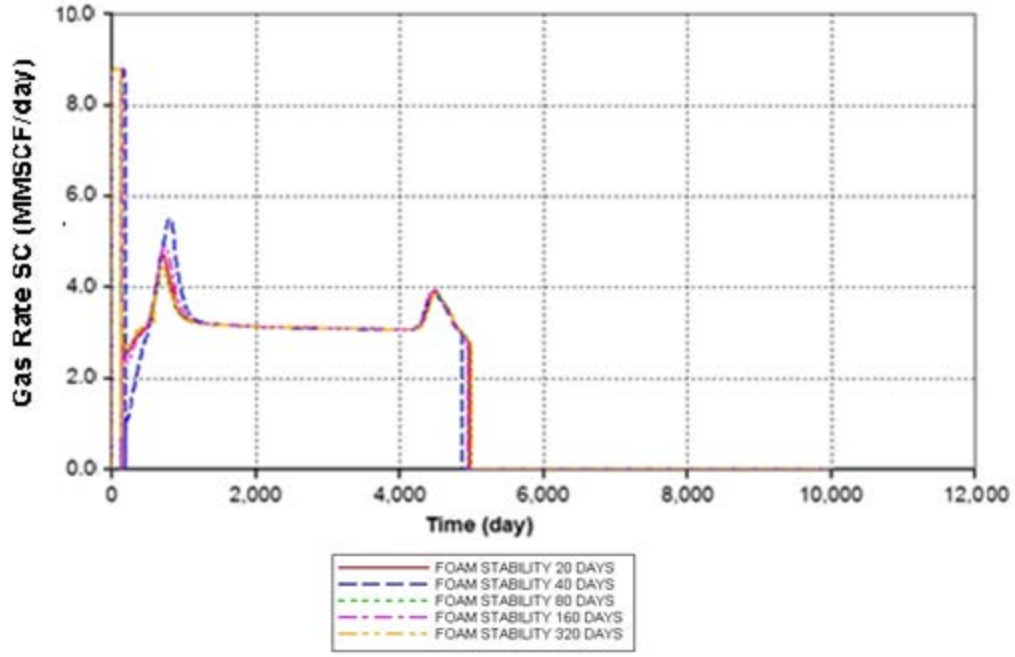

Figure 5.18 CO_2 gas injection rates of CO_2–foam flooding base case.

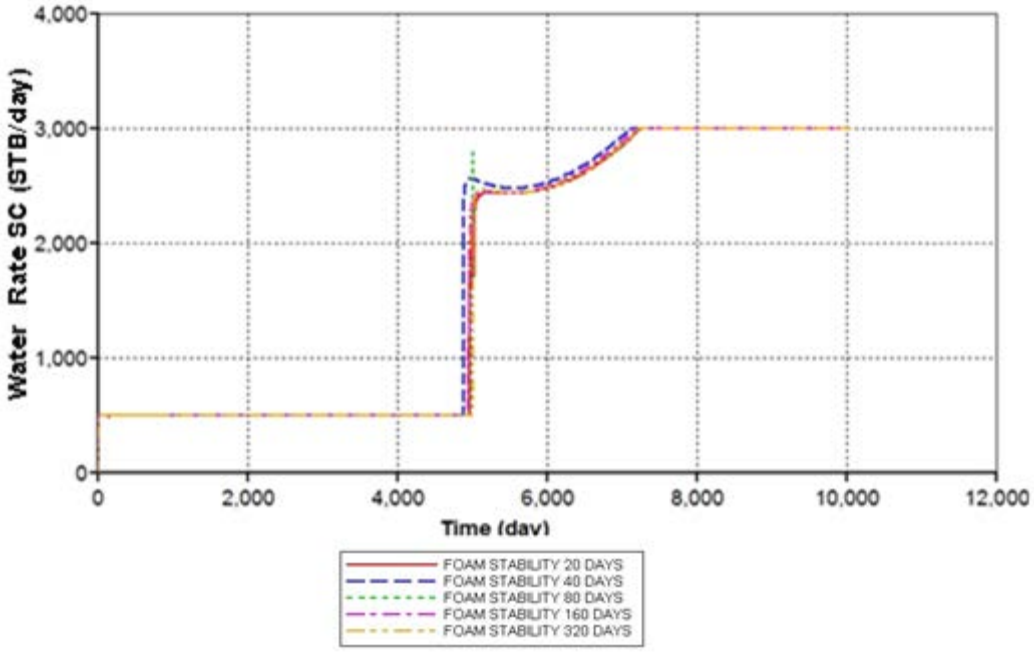

Figure 5.19 Water injection rates of CO_2–foam flooding base case.

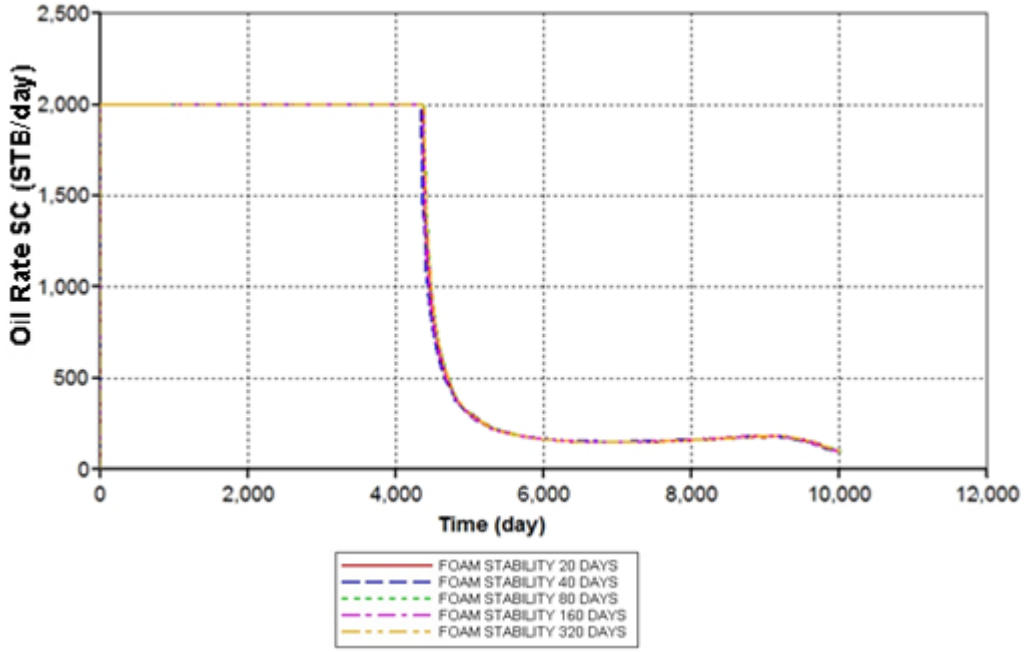

Figure 5.20 Oil production rates of CO_2–foam flooding base case.

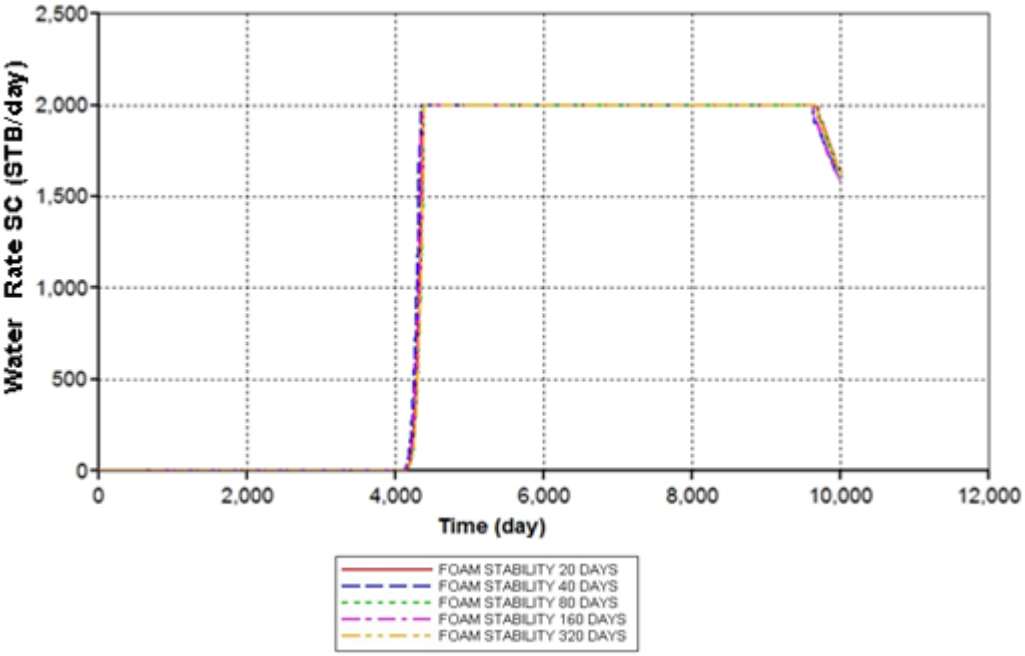

Figure 5.21 Water production rates of CO_2–foam flooding base case.

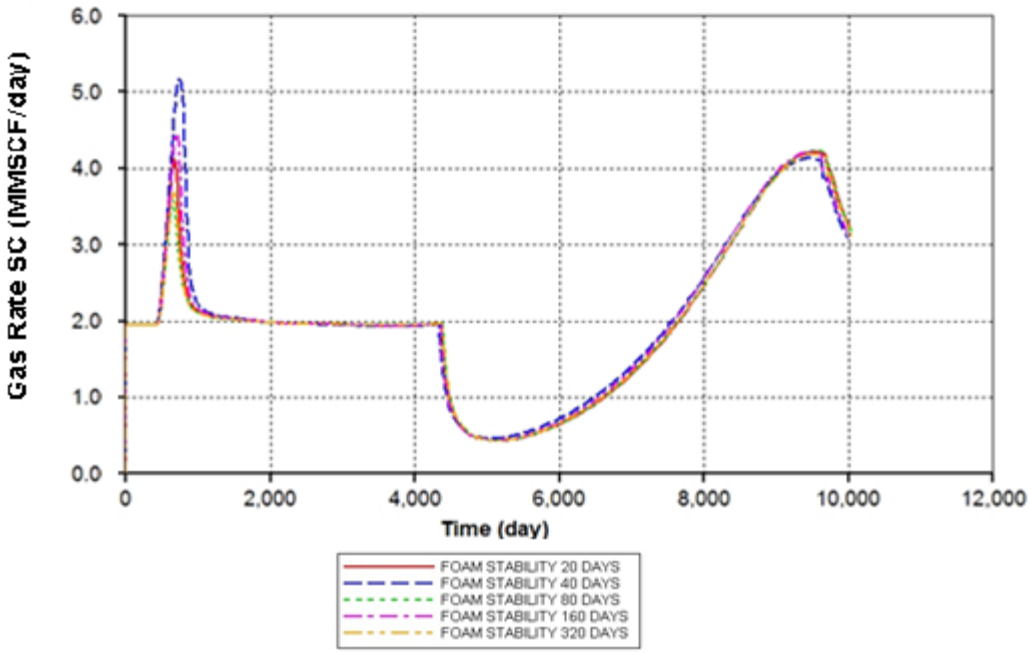

Figure 5.22 Gas production rates of CO_2–foam flooding base case.

Oil and water production rates are displayed in Figure 5.20 and 5.21, respectively. It can be seen that oil can be produced at the constant rate of 2,000 STB for 4,350 days. Afterwards, water breakthrough occurs at production well and this diminishes oil production rate, consequently oil rate drops drastically. Although water production rate reaches the maximum limit of 2,000 STB/D and oil rate decreases abruptly, oil can still be produced at a small rate at approximately 100-200 STB/D until oil rate approaches the production constraints which are 95% of water cut and 100 STB/D of oil production rate. The production period of all cases terminate within the range of 9,980-10,040 days.

Figure 5.22 there are obvious peaks of gas rate in the period of 440-1,000 days of production. These peaks result from part of CO_2 which cannot be captured by lamella. Foam therefore cannot be formed immediately at the initial of fluid injection. CO_2 that is not accounted for foam generation in the initiation stage then flows in reservoir. After that CO_2 undergoes miscibility with oil in the reservoir because of the pressure that is above the MMP. Methane and intermediates in reservoir oil are vaporized and move forward to the production well. Because there is only small amount of gas that cannot be encapsulated by foam, produced gas peaks are not high

enough to interrupt oil production rate. At about 4,320 days of production, gas production rates drop as almost the same time of where oil production rates suddenly decline. This is a result from water breakthrough. Around 700 days after that, all gas production rates rise up again. This situation occurs because CO_2 and surfactant solution injections are stopped since 4,950 days, accordingly when the existing foam in the reservoir coalescences and breaks into free CO_2 and no new foam is generated, free CO_2 is miscible with reservoir oil and so vaporized methane and intermediates in oil substantially increase. In the late period, all produced fluid rates are dropped due to declining of reservoir pressure. The bottomhole pressures of production well of all cases are shown in Figure 5.23.

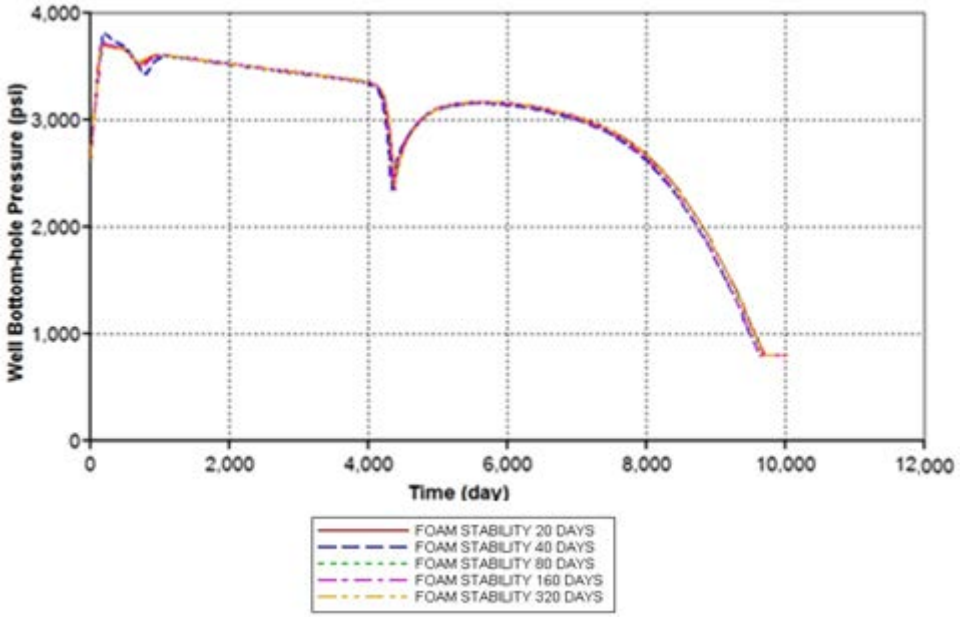

Figure 5.23 Bottomhole pressures at production well of foam flooding base case.

According to the simulation results, it is observed that variation of foam stabilities does not affect significantly production performances. This result could be from injecting too big slug of CO_2-foam. When exist foam lamella breaks, there are new foams generated continuously so an effect of foam stability cannot be seen obviously. In order to assure that injecting big slug of CO_2-foam is a cause of insensitivity of foam stability, additional simulation is performed. Foam stabilities of

20 days and 320 days are selected and applied to CO_2-foam flooding executed for 100 days then chased by water until production is terminated by the production constraint. Figure 5.24 shows that injecting small slug in short period provides different result in each foam stabilitie. Foam stability of 20 days yields faster foam degradation process. From 3D illustration, it ensures that injecting continuously big slug of CO_2-foam is a reason of insensitivity of foam stability. However, the effect of foam stability may be observed with other different conditions. Hence, variation of foam stability is carried over to the rest of study.

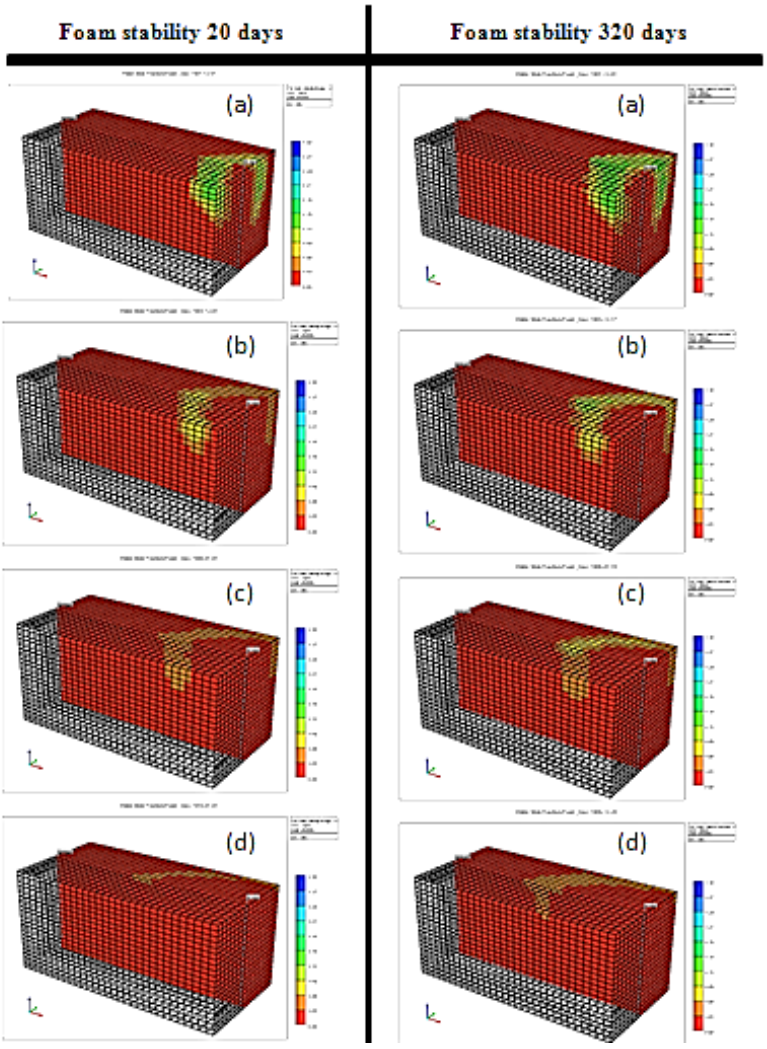

Figure 5.24 Amount of foam at different time obtained from foam stability of 20 days and 320 days case.

The cumulative oil production, water production, gas production and oil recovery factor of foam application which are compared with CO_2 flooding are illustrated in Figures 5.25 to 5.28, respectively.

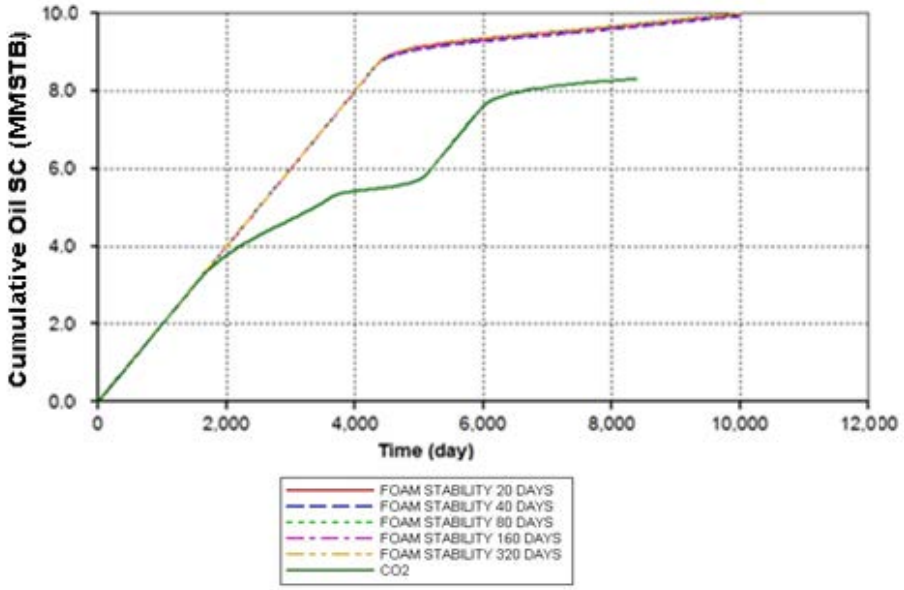

Figure 5.25 Cumulative oil productions of foam flooding base cases compared to CO_2 flooding base case.

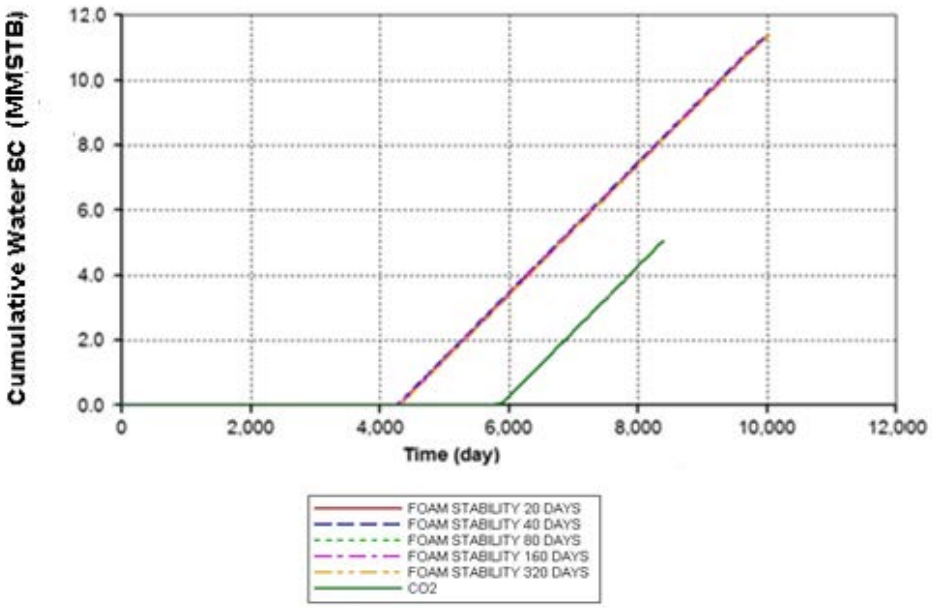

Figure 5.26 Cumulative water productions of foam flooding base cases compared to CO_2 flooding base case.

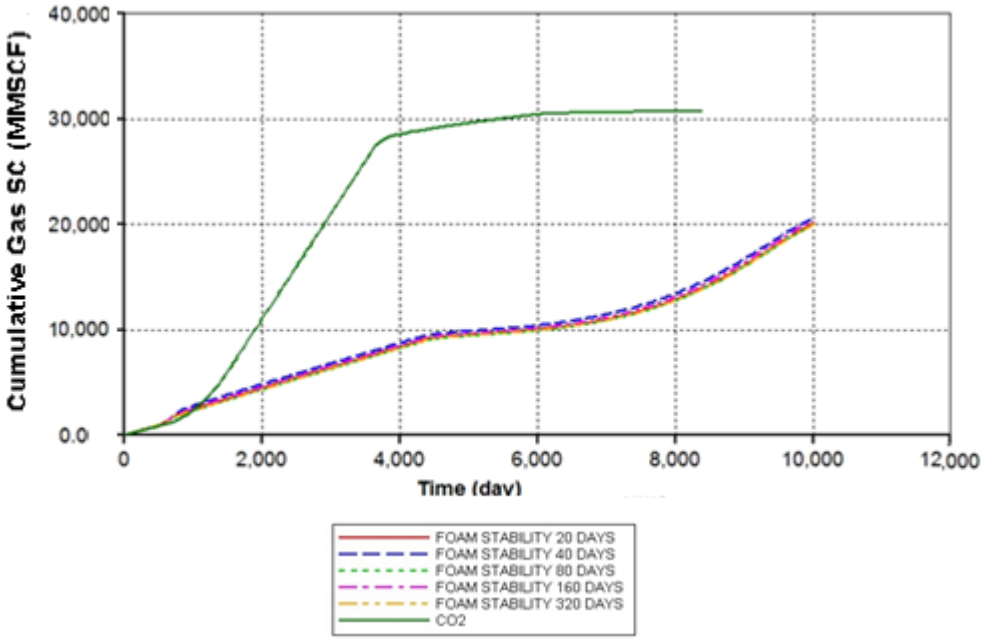

Figure 5.27 Cumulative gas productions of foam flooding base cases compared to CO_2 flooding base case.

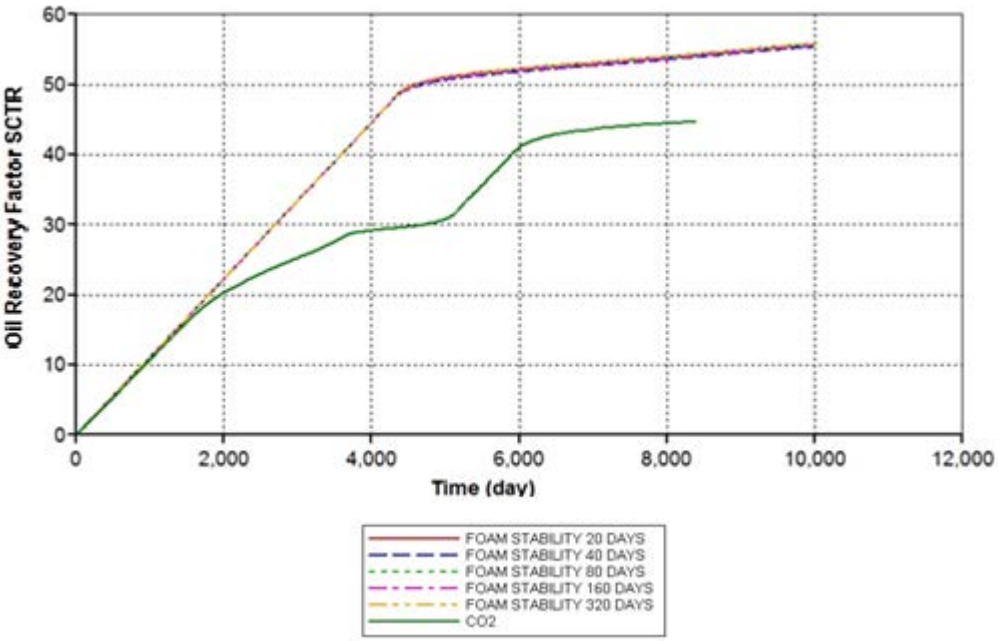

Figure 5.28 Oil recovery factors of foam flooding base cases compared to CO_2 flooding base case.

Regarding the Figures 5.25 to 5.28, it can be seen that foam flooding can recovery oil much better that CO_2 flooding. Since foam can reduce gas mobility. This yields smoother flood front compared to the case of CO_2 flooding. Since there is no direct way to visualize mobility of gas phase in STARS simulator, mobility is however an ability to move and this can be seen from flowing speed. Figure 5.29 shows an evolution of flood front of CO_2 flooding compared to CO_2-foam flooding captured at the same time. It is observed that in CO_2 flooding, flood front moves very fast but CO_2-foam flood front flows is much slower. Inside bubbles, there is CO_2 gas encapsulated. From this evidence, it confirms that CO_2-foam flooding can reduce mobility of gas phase which leads to better results than CO_2 flooding. However, it can be noticed that foam cannot perform a piston-like flooding as an ideal displacement because foam also consists of gas component tending to flow upward. The overriding anyway is not as severe as the case of CO_2 flooding.

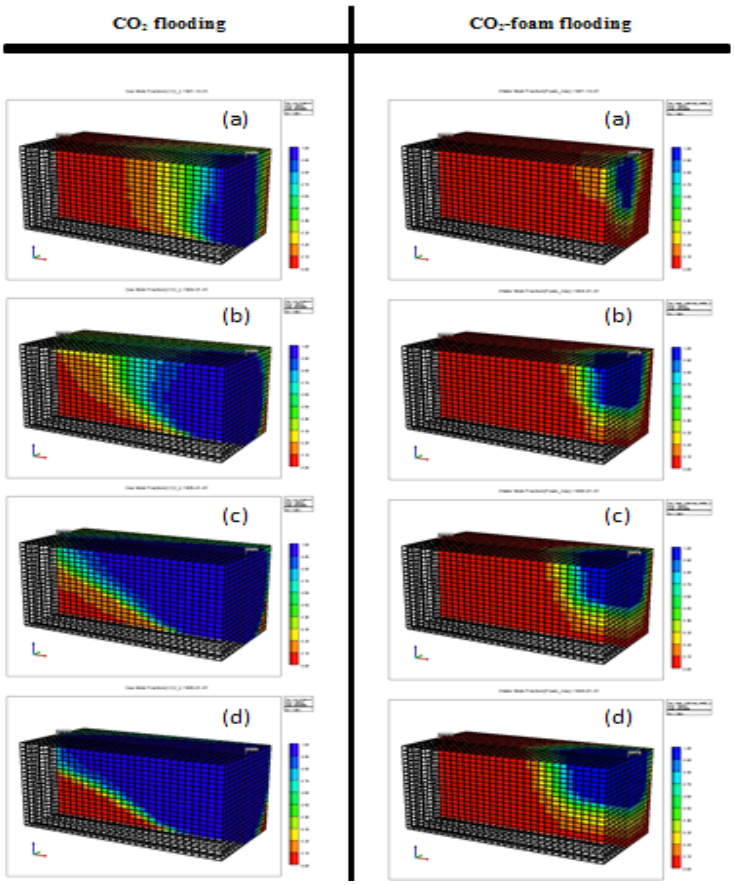

Figure 5.29 Evolution of flood front of CO_2 flooding compared to CO_2-foam flooding.

The efficiency of foam flooding can also be seen from the average oil saturation remained in the reservoir from Figure 5.30a to 5.30f. The change of oil saturation in Figure 5.30b occurs from the miscibility function of CO_2 that is not formed immediately the foam. Afterwards, oil saturation decreases from miscibility of CO_2 together with foam sweeping potential. The dark blue and purple zones in Figure 5.30 are a result from the miscibility of reservoir oil and CO_2 because it displays the overriding of gas. Nevertheless, in Figures 5.30e and 5.30f, the dark blue color in the lower zone is from the water sweeping by chasing water which flows underruning.

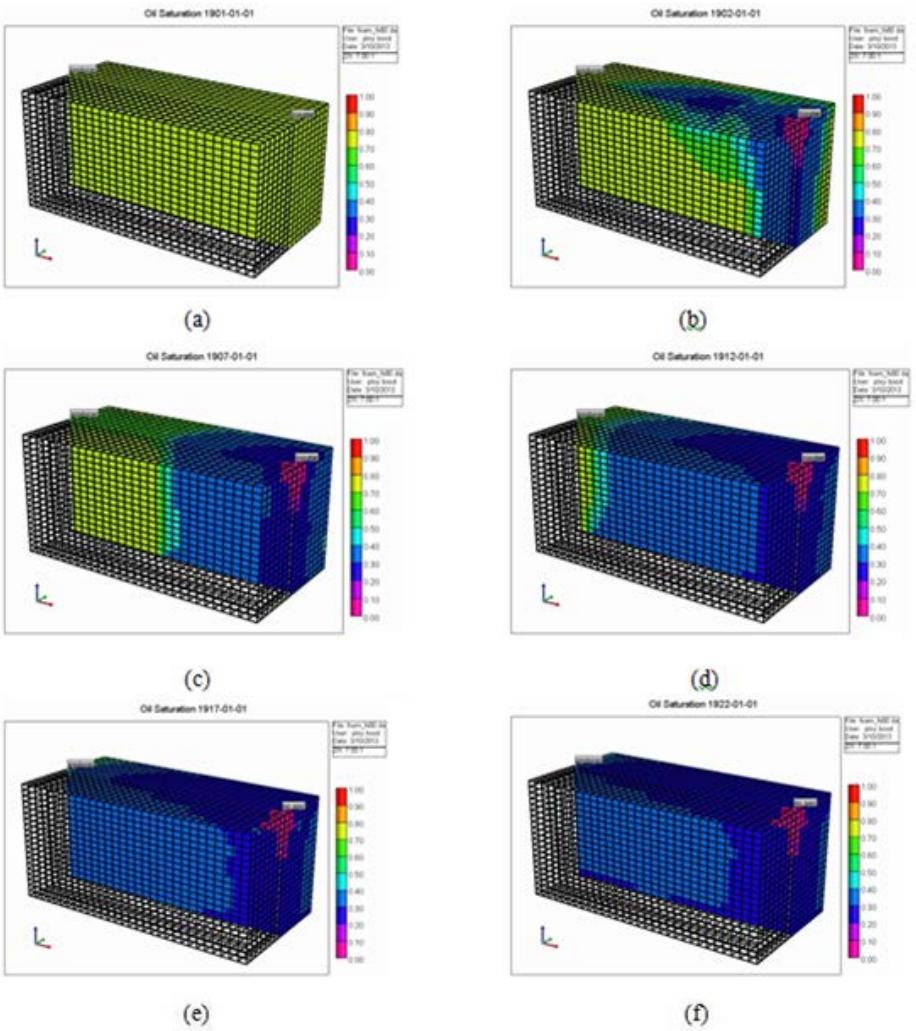

Figure 5.30 Average oil saturation remained in the reservoir of foam flooding sequence from the start to the end of production.

The miscibility of CO_2 after foam lamellas breaks can be seen in Figure 5.31. Oil mass density changes similar as in the case of CO_2 flooding, but due to amount of CO_2 released from foam is not as much as the case of CO_2 flooding, area of miscibility is much smaller. From Figure 5.29, foam is crowded in the upper zone this makes CO_2 crowded in the upper zone as well.

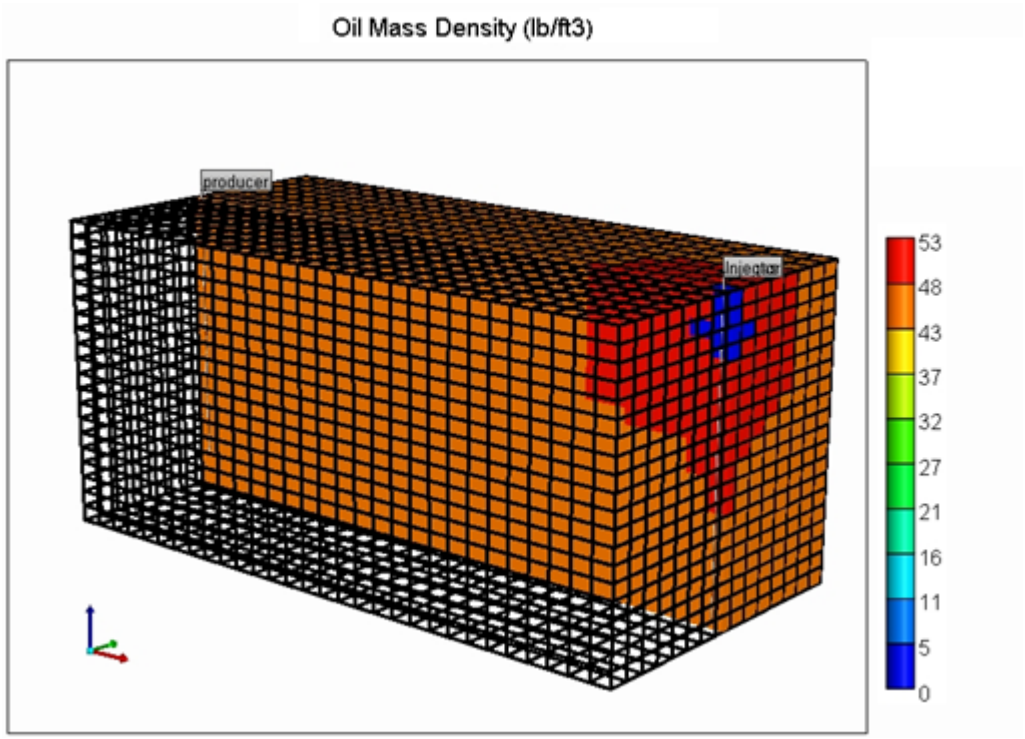

Figure 5.31 Miscibility effect on oil mass density in CO_2-foam flooding.

The comparison performances of CO_2 flooding and CO_2-foam flooding is performed at the point where equal amount of fluids are injected into the reservoir. In this study, cumulative of oil, water, and gas and ultimate oil recovery factor are detected when injected chasing water reaches 0.4 pore volume. The results are summarized in Table 5.3.

Table 5.3 Cumulative oil production, water production, gas production and oil recovery factor of CO_2-foam flooding base case.

	CO_2 flooding	**Foam flooding**				
		FS 20 days	**FS 40 days**	**FS 80 days**	**FS 160 days**	**FS 320 days**
Time for injected water to reach 0.4 PV, day	6,350	9,796	9,673	9,801	9,755	9,801
Cumulative oil production (MMSTB)	7.91	9.94	9.87	9.96	9.91	9.95
Cumulative water production, (MMSTB)	0.98	11.00	10.83	10.98	10.94	10.99
Cumulative gas production (MMSCF)	30,520	19,370	19,490	19,320	19,500	19,300
Oil recovery factor, %	42.62	55.48	55.12	55.63	55.36	55.59

Base on oil recovery factor, even through oil recovery factors obtained from each foam stability case are not much different, it can be concluded that CO_2-foam flooding with foam stability of 80 days provides the best ultimate oil recovery and it also prolongs maximally production period. However, comparing among foam flooding base cases themselves, foam stability does not show a significant effect on effectiveness of foam flooding.

5.3. Effect of varied parameters on CO_2-foam flooding

Several parameters are applied in the CO_2-foam model to evaluate their effects and sensitivity on the performance of CO_2-foam. The interested parameters include:

- Wetting condition of reservoir rock
- Intermediate percentages of hydrocarbon in volatile oil
- Injected slug size of foam

All cases are simulated under the same production constraints as well as injection rates of base case CO_2-foam model consisting of CO_2 injection rate of 8.78 MMSCF/D and surfactant solution injection rate of 500 STB/D. Each parameter is independent to others. The comparison of CO_2-foam flooding performance is performed by comparing with the result obtained from CO_2 flooding.

5.3.1 Effect of wetting condition of reservoir rock

This study is performed to evaluate the effects of wetting conditions that are varied from an original value in a direction to more oil-wet. The sensitivity analysis of wetting condition on the effectiveness of foam flooding is carried out by adjusting SCAL data. From the rule of thumb, reducing irreducible water saturation, increasing the relative permeability to water at residual oil saturation, and decreasing of crossover saturation is a sign of direction to a more oil-wet. Four types of wettability are investigated in this study. The wettability of the reservoir in the base case is considered as strongly water-wet, therefore wetting conditions which are investigated in this section are varied to moderately water-wet, neutral-wet, moderately oil-wet, and strongly oil-wet.

5.3.1.1 Moderately water-wet

A moderately water-wet is constructed by slightly adjusting a water-oil relative permeability function to be more oil-wet. Parameters that are used for creating the moderately water-wet in the simulator are shown in the Table 5.4. The data of water–oil relative permeabilities are showed in Table 5.5 and the plot is illustrated in Figure 5.32.

Table 5.4 Parameters applied in relative permeability generation in moderately water-wet.

Keyword	Description	Value
SWCON	connate Water	0.26
SWCRIT	critical Water	0.26
SOIRW	irreducible Oil for Water-Oil Table	0.28
SORW	residual Oil for Water-Oil Table	0.28
SOIRG	irreducible Oil for Gas-Liquid Table	0.05
SORG	residual Oil for Gas-Liquid Table	0.10
SGCON	connate Gas	0.00
SGCRIT	critical Gas	0.15
KROCW	k_{ro} at connate Water	0.55
KRWIRO	k_{rw} at irreducible Oil	0.23
KRGCL	k_{rg} at connate Liquid	0.6
	exponent for calculating k_{rw} from KRWIRO	3
	exponent for calculating k_{row} from KROCW	3
	exponent for calculating k_{rog} from KROGCG	3
	exponent for calculating k_{rg} from KRGCL	3

Table 5.5 Relative permeabilities to oil and water as functions of water saturation in moderately water-wet.

Water saturation (S_w)	**Relative perm. to water (k_{rw})**	**Relative perm. to oil (k_{ro})**
0.26	0.0000	0.5500
0.29	0.0001	0.4532
0.32	0.0004	0.3685
0.35	0.0015	0.2950
0.38	0.0036	0.2320
0.40	0.0070	0.1787
0.43	0.0121	0.1343
0.46	0.0193	0.0979
0.49	0.0288	0.0688
0.52	0.0409	0.0461
0.55	0.0562	0.0290
0.58	0.0747	0.0168
0.61	0.0970	0.0086
0.63	0.1234	0.0036
0.66	0.1541	0.0011
0.69	0.1895	0.0001
0.72	0.2300	0.0000

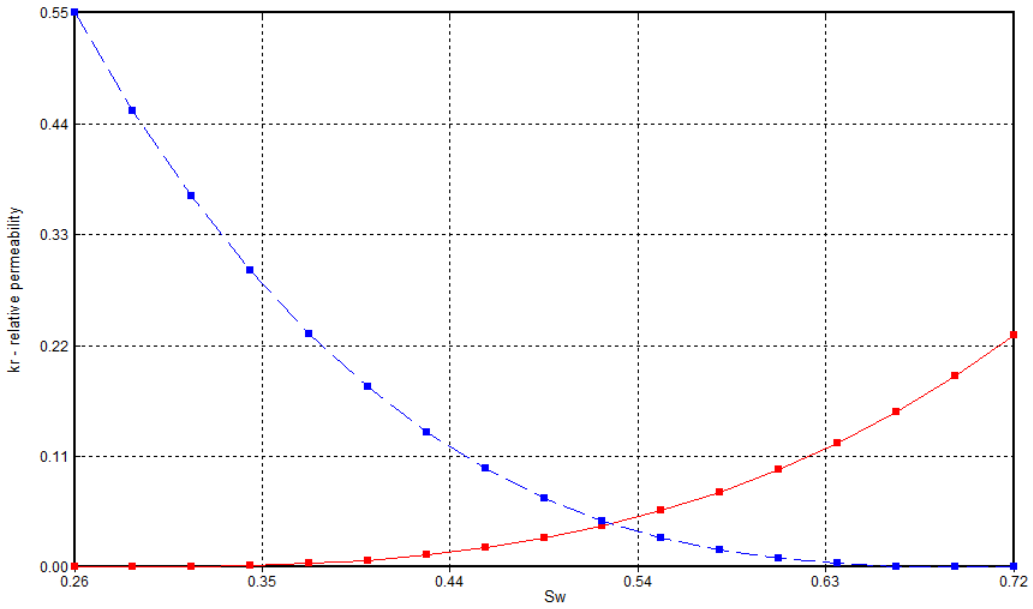

Figure 5.32 Relative permeabilities to oil and water in moderately water-wet reservoir as functions of water saturation.

The simulation outcomes such as oil production rate, water production rate and gas production rate are displayed in the Figures 5.33 to 5.35. From the figures, it shows that there is only slight variation affected by foam stability. The produced gas rates obtained when foam stabilities are 80 days and 320 days yield obvious higher peak magnitude compared to other foam stabilites as seen in Figure 5.35. The higher magnitude of gas rates at foam stabilities of 80 days and 320 days are the result from less foam generations than the others cases, leading to the bottomhole pressures at injection well to reach the preset fracture pressure slower that the cases of foam stabilities 20, 40, and 160 days. Therefore, foam stabilities of 80 and 320 days provide longer constant injection period which means larger amount of gas is injected. That leads all occurrences happen faster because the total volume of gas injected reaches 0.4 hydrocarbon pore volume quicker and the start of chasing water injection is earler as well. Water breakthrough also occurs earlier in the cases of 80 and 320 days of foam stabilities, causing the total production period to be slightly shorter. Regarding to previously mentioned reasons, the total amount of oil production obtained from

cases of 80 and 320 days foam stabilities are then lower than those of 20, 40, and 160 days.

According to Figures 5.33 to 5.35, solely CO_2 flooding behavior in moderately water-wet is similar to the CO_2 flooding performed in strongly water-wet (CO_2 base case). Oil production rate of CO_2 flooding drops raplidly due to early gas breakthrough at the producer, having the similar trend as seen in CO_2 base case performed in strongly water-wet. It is obvious that CO_2-foam flooding can extend the period of constant oil production rate at 2,000 STB/D because foam retards gas breakthrough. In moderately water-wet reservoir, water reaches producion well after 5,200 days which is more rapid than in CO_2 base case (water breakthrough at 5,570th days).

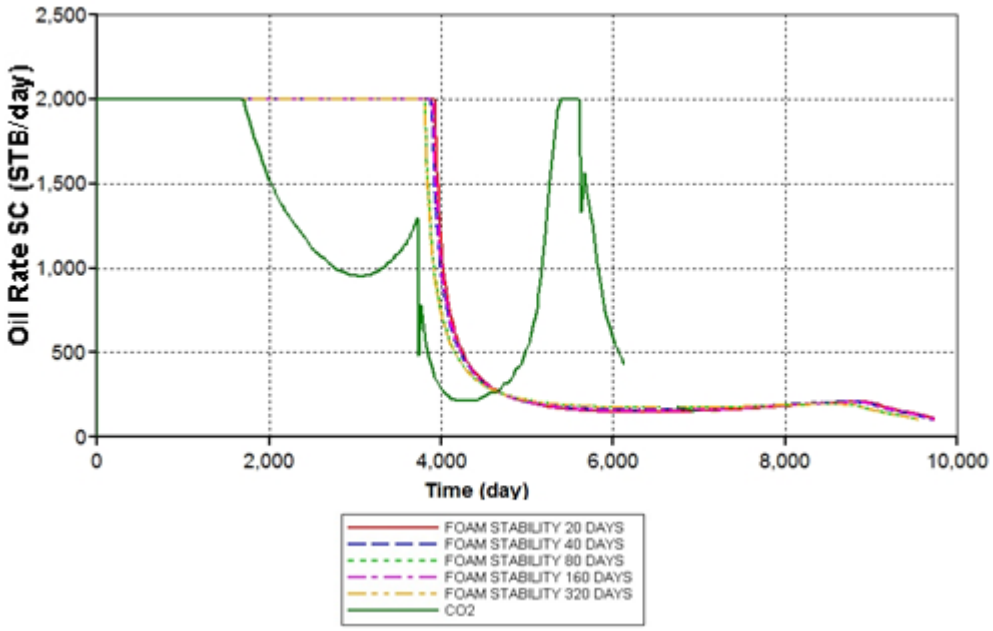

Figure 5.33 Oil production rates of CO_2–foam and CO_2 flooding cases in moderately water-wet reservoir as functions of time.

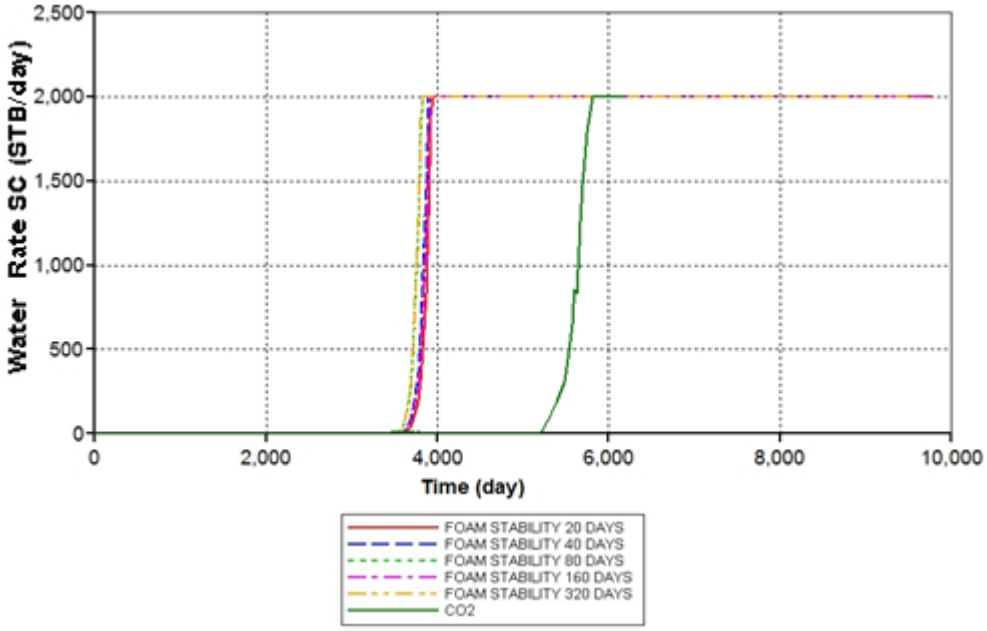

Figure 5.34 Water production rates of CO_2–foam and CO_2 flooding cases in moderately water-wet reservoir as functions of time.

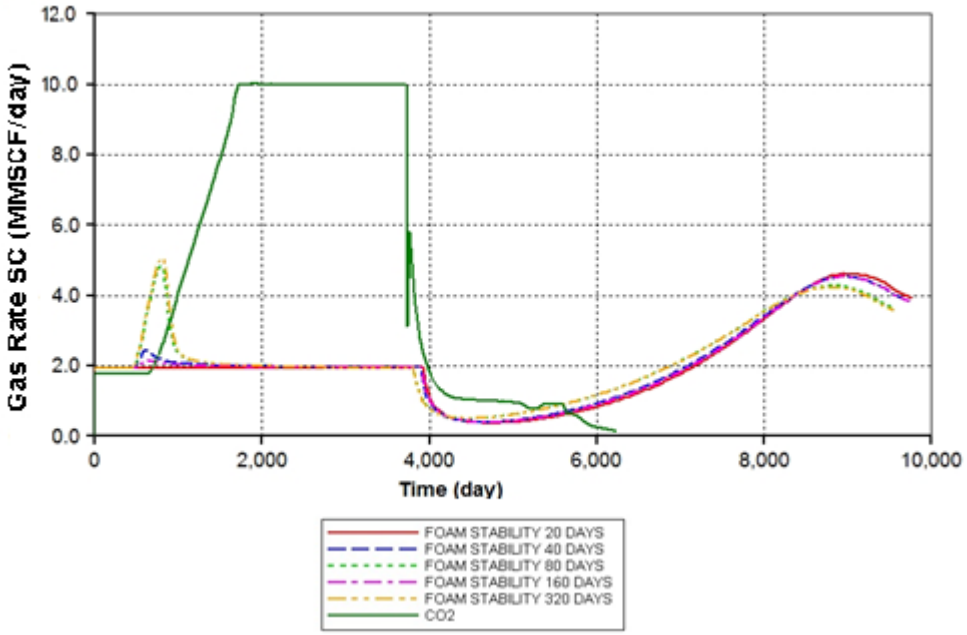

Figure 5.35 Gas production rates of CO_2–foam and CO_2 flooding cases in moderately water-wet reservoir as functions of time.

The accumulation of produced oil, water, and gas compared to CO_2 flooding in the same condition are presented in Figures 5.36 to 5.38. The extract values are then summarized in Table 5.6. From the simulation results, they show that in moderately water-wet reservoir, foam flooding is more preferable than CO_2 flooding since the cumulative oil production and oil recovery factor are greater. However, foam flooding requires the injection of aqueous phase simultaneously with gas, therefore, the water breakthrough from foam flooding cases is much earlier than CO_2 flooding case and water production trend does not drop until the end of production period. Hence, the total amount of produced water is much higher. However, the cumulative gas obtained from foam flooding is lower than that of CO_2 flooding.

Considering oil recovery factor in moderately water-wet, there is no significant difference. However, it is found that foam stability of 20 days provides the best result in CO_2-foam flooding and the benefit of this case over CO_2 flooding is approximately 10.1%.

Table 5.6 Cumulative oil production, water production, gas production and oil recovery factor of CO_2–foam and CO_2 flooding cases in moderately water- wet reservoir

	CO_2 flooding	**Foam flooding**				
		FS 20 days	**FS 40 days**	**FS 80 days**	**FS 160 days**	**FS 320 days**
Time for injected water to reach 0.4 PV, day	6,100	9,769	9,705	9,483	9,736	9,464
Cumulative oil production (MMSTB)	7.61	9.15	9.11	8.97	9.12	8.96
Cumulative water production, (MMSTB)	1.04	11.85	11.80	11.50	11.83	11.48
Cumulative gas production (MMSCF)	29,990	20,130	20,290	20,460	20,160	20,410
Oil recovery factor, %	41.01	51.11	50.88	50.15	50.93	50.09

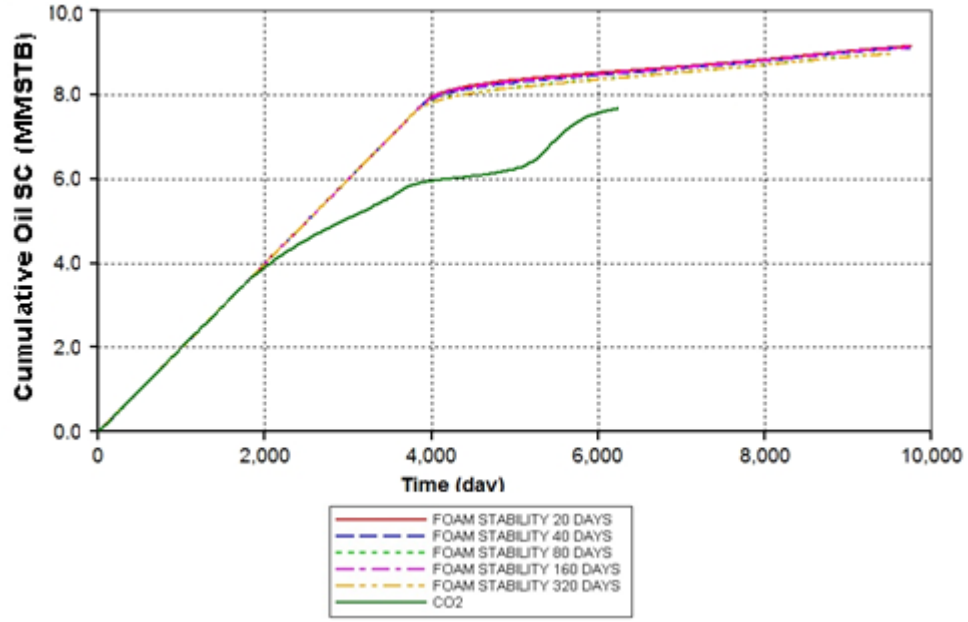

Figure 5.36 Cumulative oil productions of CO_2–foam and CO_2 flooding cases in moderate water-wet reservoir as functions of time.

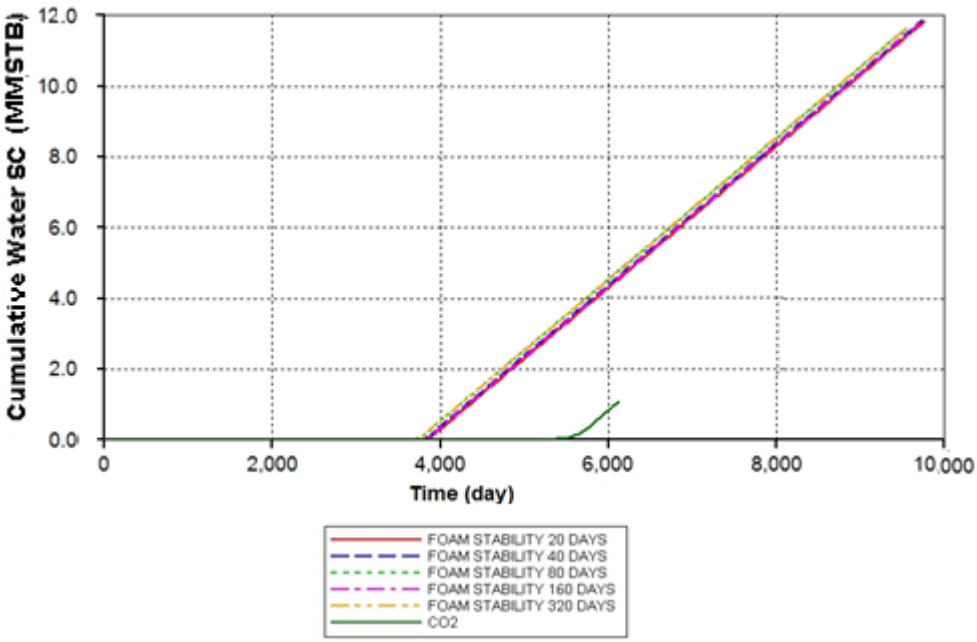

Figure 5.37 Cumulative water productions of CO_2–foam and CO_2 flooding cases in moderate water-wet reservoir as functions of time.

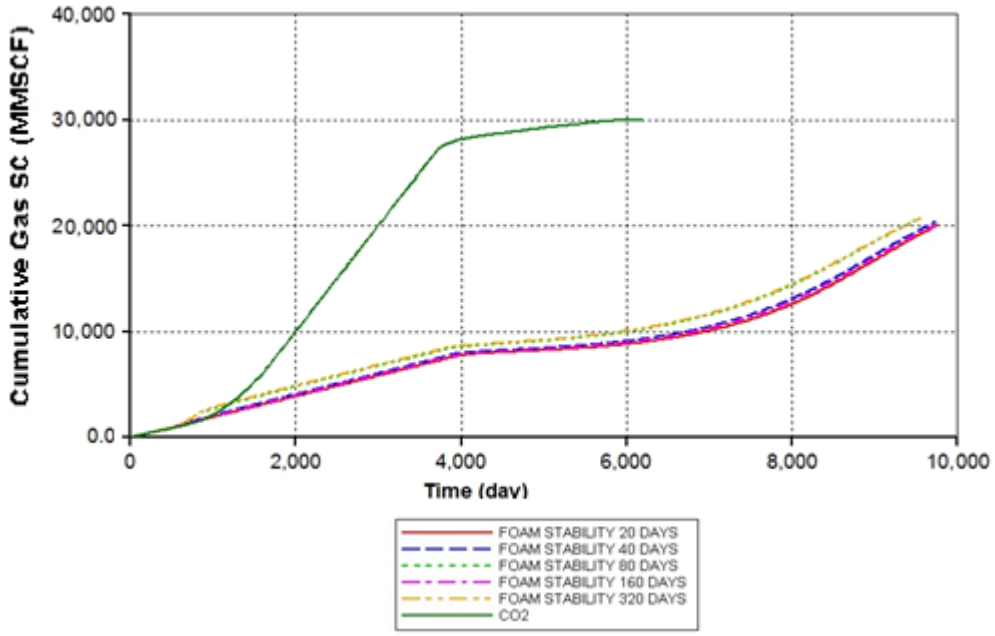

Figure 5.38 Cumulative gas productions of CO_2–foam and CO_2 flooding cases in moderate water-wet reservoirs as functions of time.

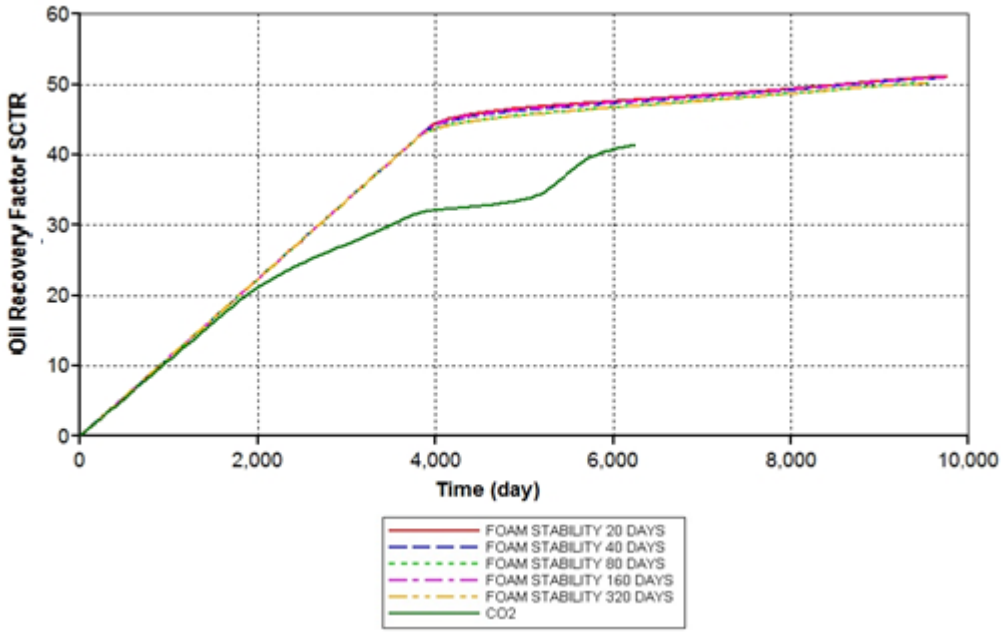

Figure 5.39 Oil recovery factors of CO_2–foam and CO_2 flooding cases in moderate water-wet reservoir as functions of time.

5.3.1.2 Neutral-wet

Water-oil relative permeabilities are adjusted in order to generate neutral-wet condition by changing several parameters as shown in Table 5.7. The calculated relative permeabilities are showed in Table 5.8 and the plot is shown in Figure 5.40.

Table 5.7 Parameters applied in relative permeability generation in neutral-wet reservoir.

Keyword	**Description**	**Value**
SWCON	connate Water	0.2
SWCRIT	critical Water	0.2
SOIRW	irreducible Oil for Water-Oil Table	0.32
SORW	residual Oil for Water-Oil Table	0.32
SOIRG	irreducible Oil for Gas-Liquid Table	0.05
SORG	residual Oil for Gas-Liquid Table	0.10
SGCON	connate Gas	0.00
SGCRIT	critical Gas	0.15
KROCW	k_{ro} at connate Water	0.7
KRWIRO	k_{rw} at irreducible Oil	0.35
KRGCL	k_{rg} at connate Liquid	0.6
	exponent for calculating k_{rw} from KRWIRO	3
	exponent for calculating k_{row} from KROCW	3
	exponent for calculating k_{rog} from KROGCG	3
	exponent for calculating k_{rg} from KRGCL	3

Table 5.8 Relative permeabilities to oil and water as functions of water saturation in neutral-wet reservoir.

Water saturation (S_w)	**Relative perm. to water (k_{rw})**	**Relative perm. to oil (k_{ro})**
0.20	0.0000	0.7000
0.23	0.0001	0.5768
0.26	0.0007	0.4689
0.29	0.0023	0.3755
0.32	0.0055	0.2953
0.35	0.0107	0.2275
0.38	0.0185	0.1709
0.41	0.0293	0.1246
0.44	0.0438	0.0875
0.47	0.0623	0.0586
0.50	0.0854	0.0369
0.53	0.1137	0.0214
0.56	0.1477	0.0109
0.59	0.1877	0.0046
0.62	0.2345	0.0014
0.65	0.2884	0.0002
0.68	0.3500	0.0000

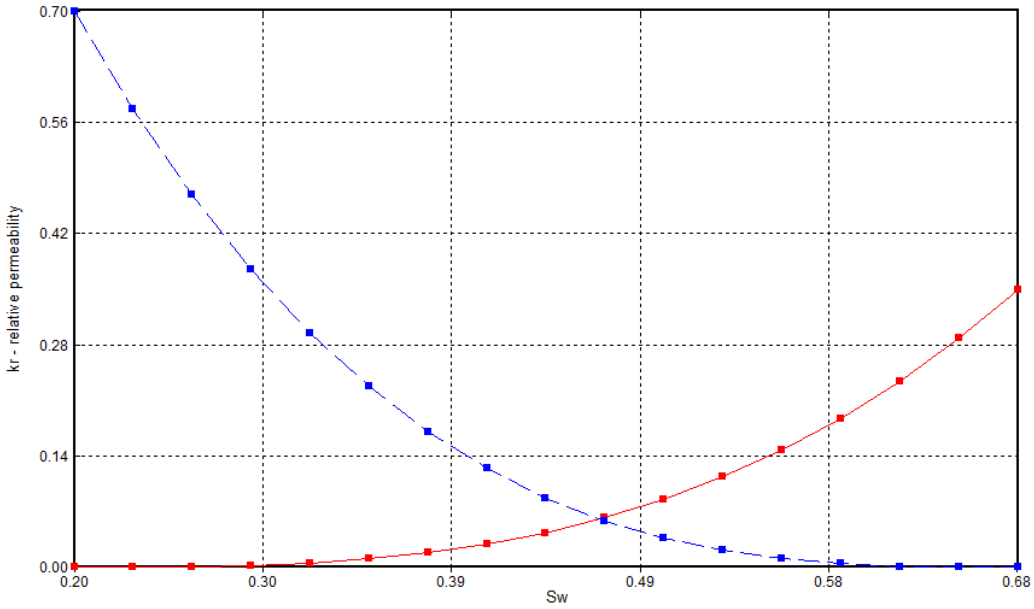

Figure 5.40 Relative permeabilities to oil and water in neutral-wet reservoir as functions of water saturation.

In the neutral-wet case, it is observed that foam stability of 160 days shows the highest peak at the day 820th while other foam stabilities do now show any peak during the same period (more or less constant rate). Gas production rates of all cases are displayed in Figure 5.41. The high produced gas rate causes the same results as discussed in the moderately water-wet, accelerating all events to occur quicker which results in the lowest cumulative oil production and the shortest production period as shown in Figure 5.41. Oil production rates and water production rates of CO_2–foam cases together with CO_2 flooding are illustrated in Figures 5.42 and 5.43. From Figure 5.42, oil rates of CO_2–foam flooding cases drop quicker than the cases of moderately water-wet because water breakthrough occurs earlier.

For CO_2 flooding in neutral-wet reservoir, the second rising of oil rate in Figure 5.42 is a result of chasing water, sweeping the lower oil zone of the reservoir. However, this is not as high as the second oil rate peak in moderately water-wet because in this neutral-wet case water flows easier and spends shorter time to reach the production well.

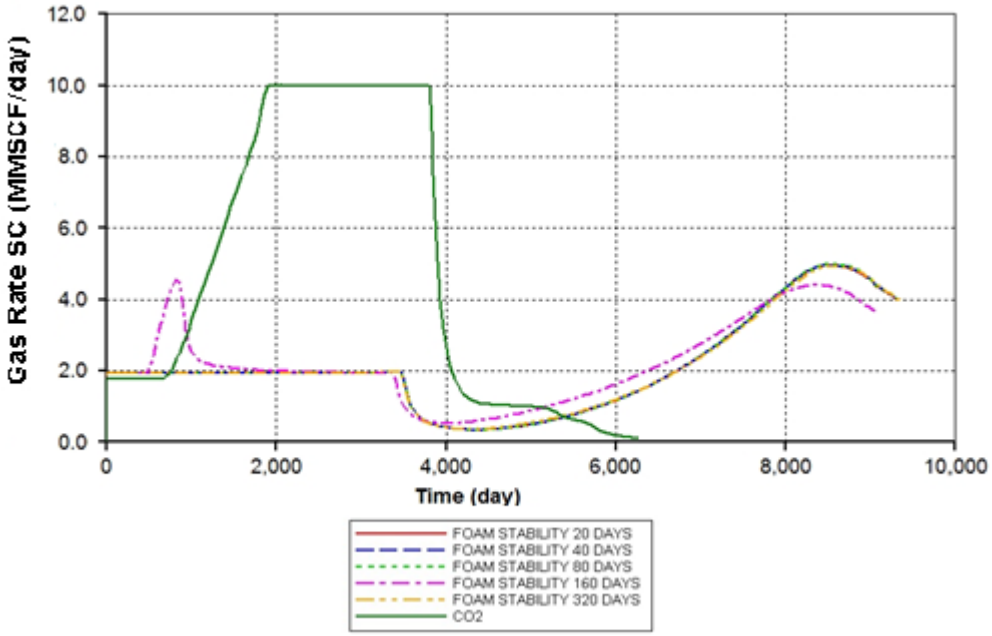

Figure 5.41 Gas production rates of CO_2–foam and CO_2 flooding cases in neutral wet reservoir as functions of time.

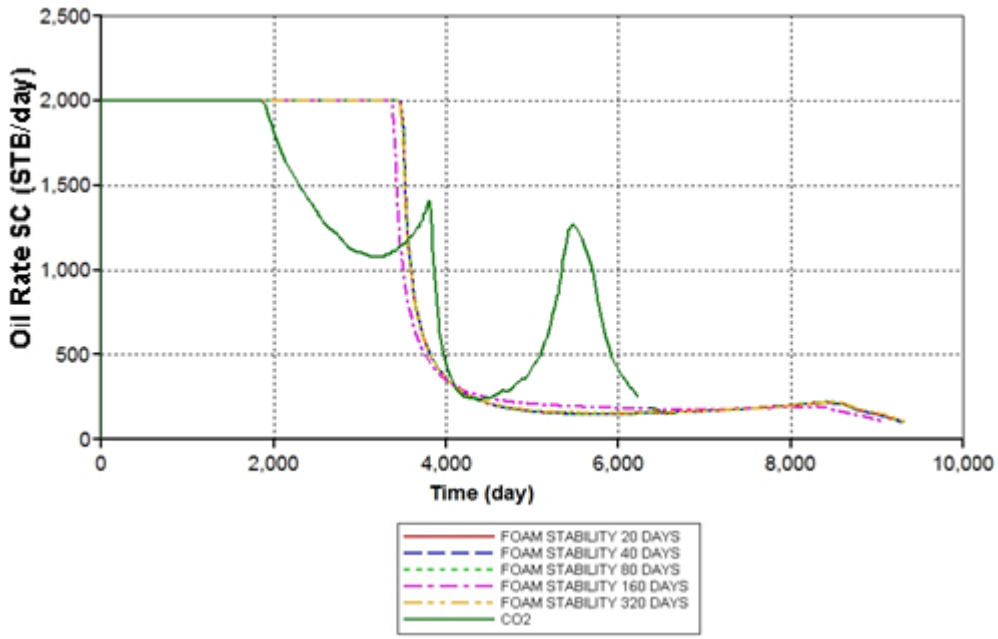

Figure 5.42 Oil production rates of CO_2–foam and CO_2 flooding cases in neutral-wet reservoir as functions of time.

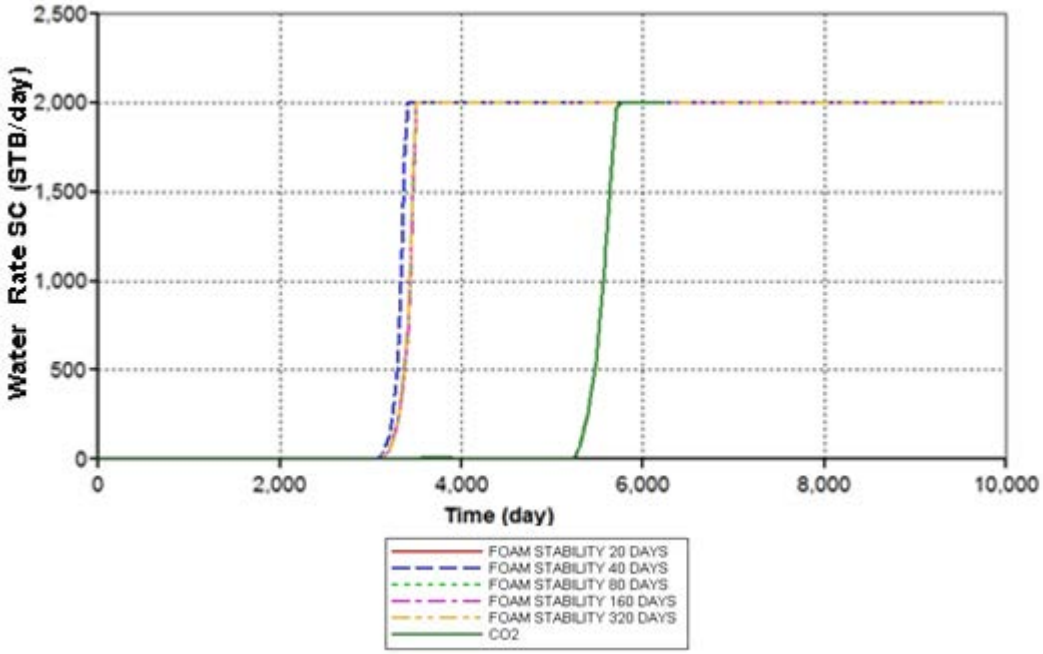

Figure 5.43 Water production rates of CO_2–foam and CO_2 flooding cases in neutral-wet reservoir as functions of time.

Summary of simulation outcomes are shown in Table 5.9. From the table together with results shown in Figures 5.44 to 5.45, variation of foam stability does not impact on oil recovery factor. The best outcome of CO_2-foam flooding in neutral-wet is the case where foam stability of 320 days is applied. It yields the highest cumulative oil production of about 8.29 MMSTB and the longest production period of 9,343 days. The benefit of CO_2-foam flooding over solely CO_2 flooding is approximately 5.37%.

Table 5.9 Cumulative oil production, water production, gas production and oil recovery factor of CO_2–foam and CO_2 flooding cases in neutral wet reservoir.

	CO_2 flooding	**Foam flooding**				
		FS 20 days	**FS 40 days**	**FS 80 days**	**FS 160 days**	**FS 320 days**
Time for injected water to reach 0.4 PV, day	6,136	9,312	9,282	9,312	9,070	9,343
Cumulative oil production (MMSTB)	7.6	8.28	8.28	8.28	8.17	8.29
Cumulative water production, (MMSTB)	1.24	11.84	11.78	11.84	11.53	11.91
Cumulative gas production (MMSCF)	29,900	19,590	19,500	19,630	20,100	19,680
Oil recovery factor, %	40.94	46.25	46.23	46.27	45.60	46.31

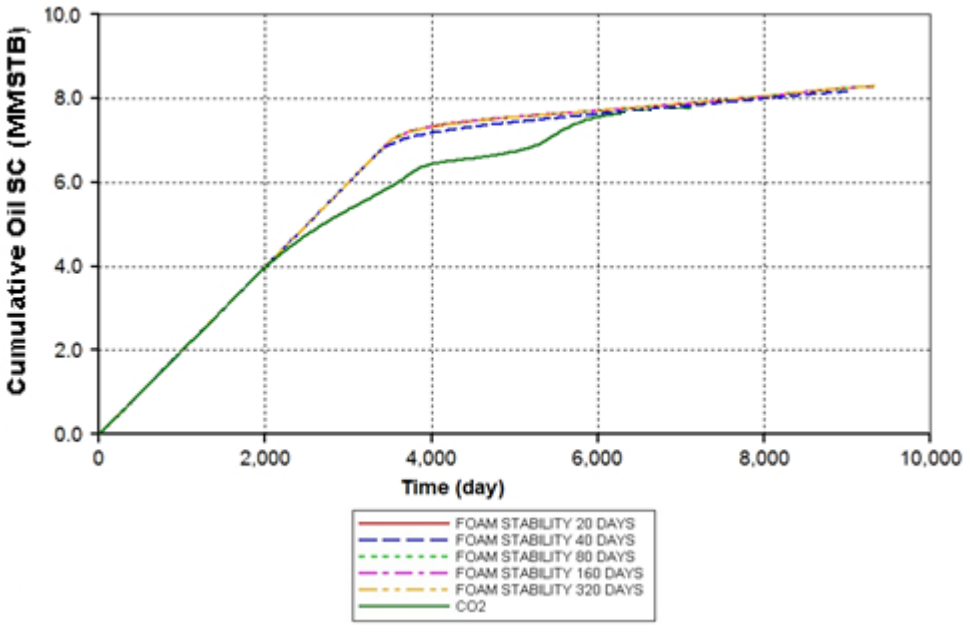

Figure 5.44 Cumulative oil productions of CO_2–foam and CO_2 flooding in neutral-wet reservoir as functions of time.

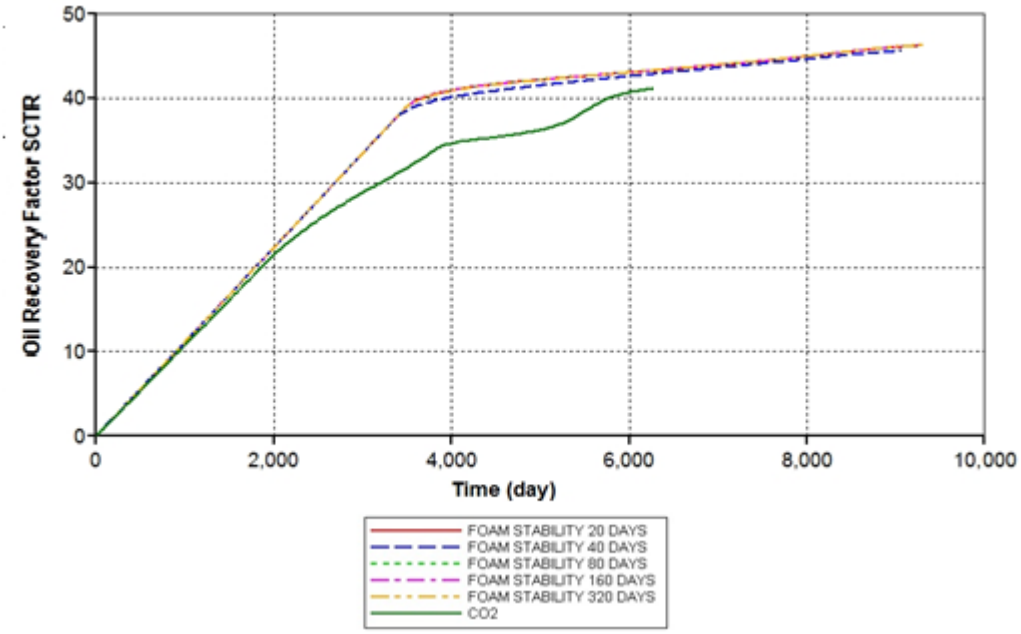

Figure 5.45 Oil recovery factors of CO_2–foam and CO_2 flooding cases in neutral-wet reservoir as functions of time.

5.3.1.3 Moderately oil-wet

In order to generate moderately oil-wet reservoir, the water-oil relative permeabilities are modified by adjusting several parameters as in cases of moderately water-wet and neutral-wet. The modified parameters are indicated in Table 5.10 and the values of calculated relative permeabilities are displayed in Table 5.11 and consecutively plotted in Figure 5.46.

Table 5.10 Parameters applied in relative permeability generation in moderately oil-wet reservoir.

Keyword	Description	Value
SWCON	connate Water	0.1
SWCRIT	critical Water	0.1
SOIRW	irreducible Oil for Water-Oil Table	0.35
SORW	residual Oil for Water-Oil Table	0.35
SOIRG	irreducible Oil for Gas-Liquid Table	0.05
SORG	residual Oil for Gas-Liquid Table	0.10
SGCON	connate Gas	0.00
SGCRIT	critical Gas	0.15
KROCW	k_{ro} at connate Water	0.8
KRWIRO	k_{rw} at irreducible Oil	0.65
KRGCL	k_{rg} at connate Liquid	0.6
	exponent for calculating k_{rw} from KRWIRO	3
	exponent for calculating k_{row} from KROCW	3
	exponent for calculating k_{rog} from KROGCG	3
	exponent for calculating k_{rg} from KRGCL	3

Table 5.11 Relative permeabilities to oil and water as functions of water saturation in moderately oil-wet reservoir.

Water saturation (S_w)	**Relative perm. to water (k_{rw})**	**Relative perm. to oil (k_{ro})**
0.10	0.0000	0.8000
0.13	0.0002	0.6592
0.17	0.0013	0.5359
0.20	0.0043	0.4291
0.24	0.0102	0.3375
0.27	0.0198	0.2600
0.31	0.0343	0.1953
0.34	0.0544	0.1424
0.38	0.0813	0.1000
0.41	0.1157	0.0670
0.44	0.1587	0.0422
0.48	0.2112	0.0244
0.51	0.2742	0.0125
0.55	0.3486	0.0053
0.58	0.4354	0.0016
0.62	0.5356	0.0002
0.65	0.6500	0.0000

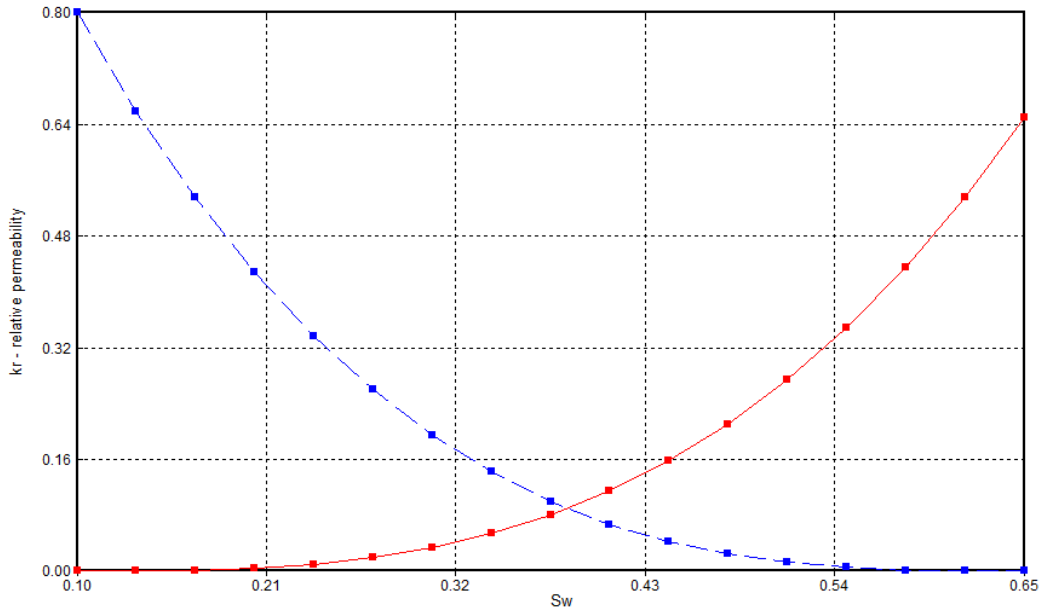

Figure 5.46 Relative permeabilities to oil and water in moderately oil-wet reservoir.

For moderately oil-wet case, all results are mostly the same in appearance. The difference however is observed in Figure 5.47. The order of highest magnitude of produced gas appears at approximately the day 730th of production in the cases of foam stabilities 40, 20, and 320 days, respectively. The cases of foam stabilities 80 and 160 days do not show any increment of produced gas rate during that period. The rising of produced gas rate results in similar effects as mentioned in the moderately water-wet and neutral wet.

Figures 5.48 and 5.49 show produced oil rate and produced water rate, respectively. The period that oil rate is maintained at 2,000 STB/D by using CO_2-foam in this case is shorter than the case of neutral-wet which is a result of early water breakthrough. However, more oil-wet condition also affects the CO_2 flooding. Since water moves quiker in this formation, therefore when water displaces the left oil in the lower zone of reservoir, oil is displaced just a little because water arrives to production well easier and become the major fluid that flows into production well.

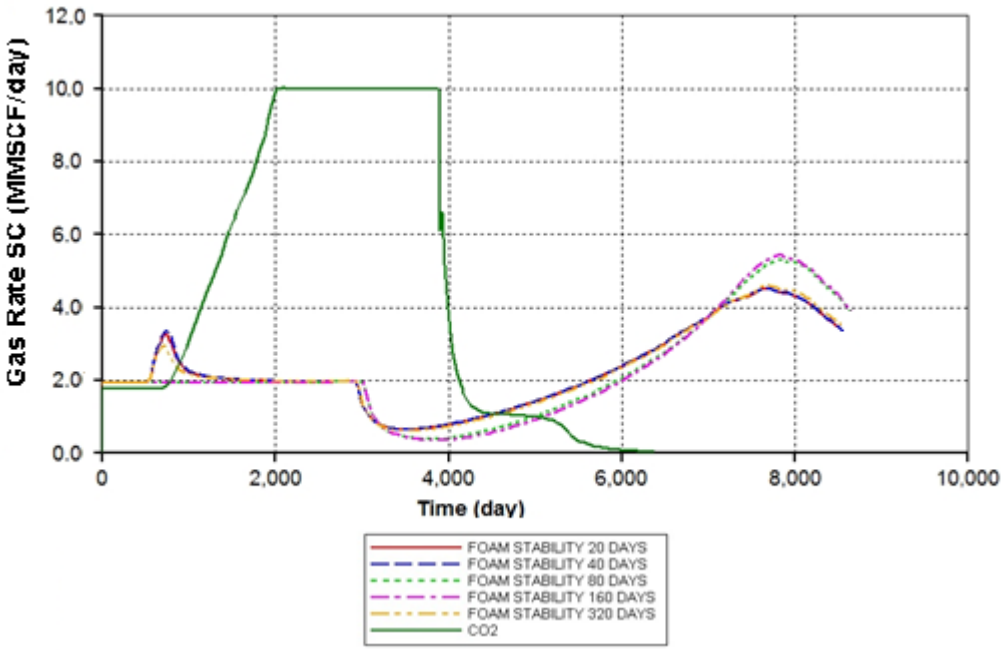

Figure 5.47 Gas production rates of CO_2–foam and CO_2 flooding cases in moderately oil-wet reservoir as functions of time.

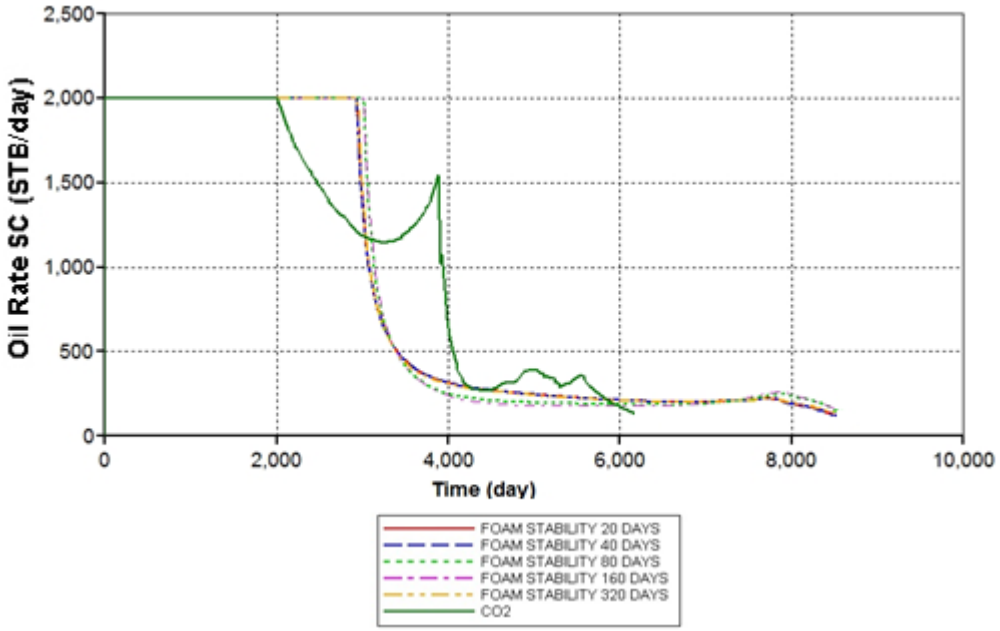

Figure 5.48 Oil production rates of CO_2–foam and CO_2 flooding cases in moderately oil-wet reservoir as functions of time.

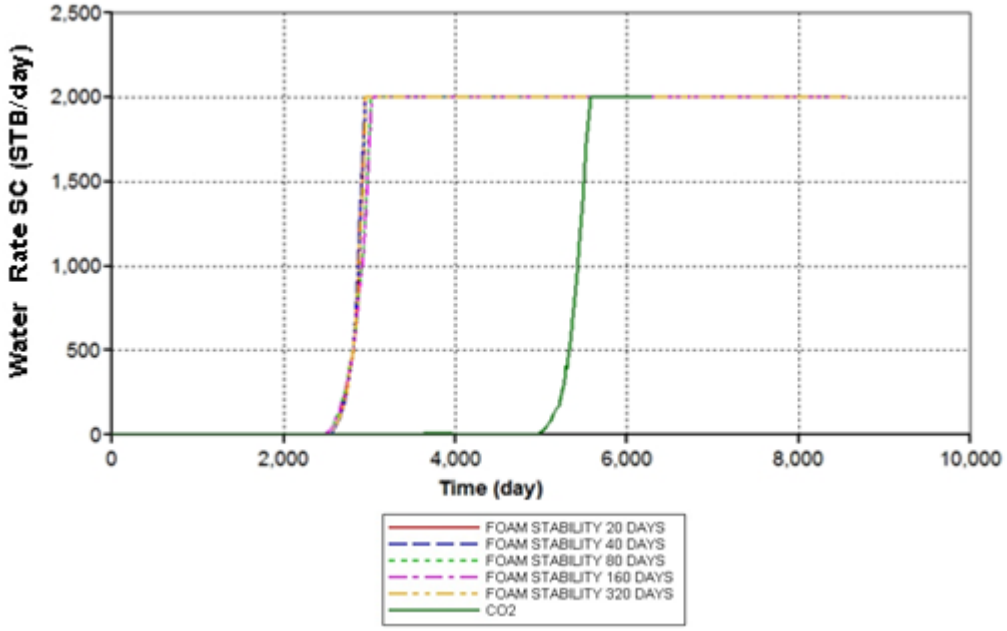

Figure 5.49 Water production rates of CO_2–foam and CO_2 flooding cases in moderately oil-wet reservoir as functions of time.

Table 5.12 Cumulative oil production, water production, gas production and oil recovery factor of CO_2–foam and CO_2 flooding cases in moderately oil- wet reservoir.

	CO_2 flooding	**Foam flooding**				
		FS 20 days	**FS 40 days**	**FS 80 days**	**FS 160 days**	**FS 320 days**
Time for injected water to reach 0.4 PV, day	6,136	8,613	8,613	8,705	8,705	8,674
Cumulative oil production (MMSTB)	7.50	7.51	7.50	7.49	7.47	7.51
Cumulative water production, (MMSTB)	1.24	11.57	11.57	11.70	11.17	11.68
Cumulative gas production (MMSCF)	29,900	19,670	19,750	19,490	19,400	19,740
Oil recovery factor, %	40.94	41.92	41.89	41.86	41.75	41.95

Table 5.12 presents the cumulative oil production, water production, gas production and oil recovery of CO_2-foam flooding in moderately oil-wet reservoir. Althrough all foam stabilities provides similar oil recovery factor, foam stability of 320 days is the best case for moderately oil-wet reservoir. This is because it can recover oil approximately 7.51 MMSTB and ultimate oil recovery reaches 41.95%, higher that oil recovery obtained from solely CO_2 flooding about 1.01% at the time that cumulative injected water reaches 0.4 hydrocarbon pore volume. Cummulative oil production and oil recovery factor are depicted in Figures 5.50 and 5.51, respectively.

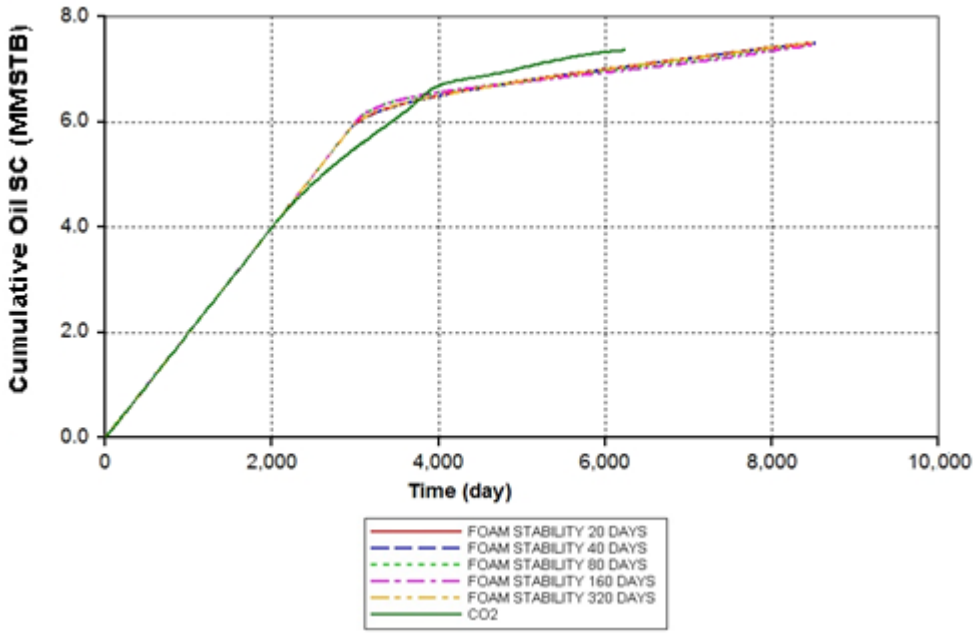

Figure 5.50 Cumulative oil productions of CO_2–foam and CO_2 flooding cases in moderately oil- wet reservoir as functions of time.

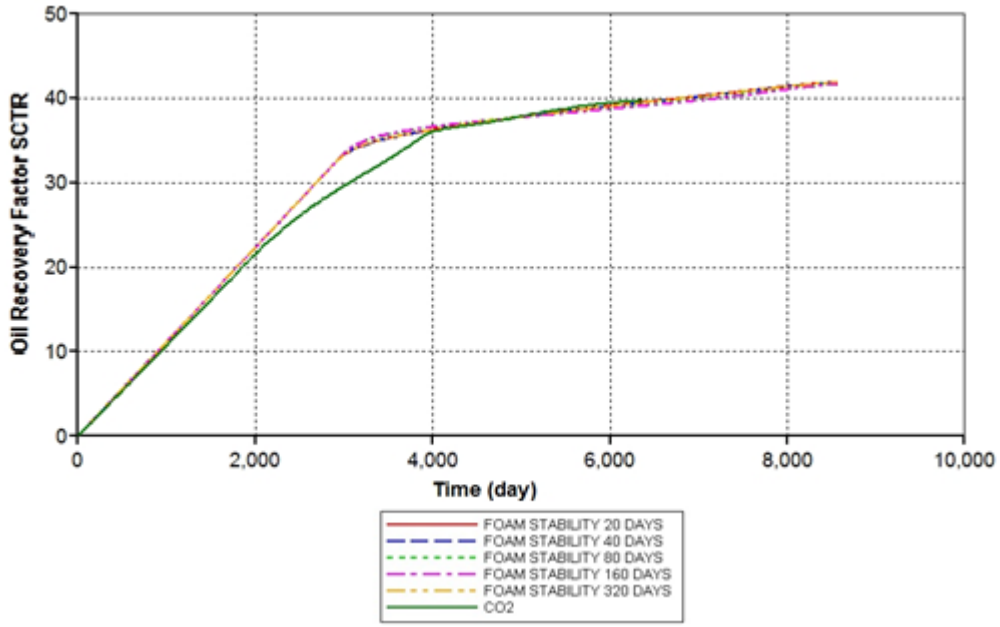

Figure 5.51 Oil recovery factors of CO_2–foam and CO_2 flooding cases in moderately oil- wet reservoir as functions of time.

5.3.1.4 Strongly oil-wet

The parameters used to generate the relative permeabilities in strongly oil-wet are summarized in Table 5.13. The calculated relative permeabilities are then tabulated in Table 5.15 and displayed graphically in Figure 5.52.

Table 5.13 Parameters applied in relative permeability generation in strongly oil-wet.

Keyword	Description	Value
SWCON	connate Water	0.08
SWCRIT	critical Water	0.08
SOIRW	irreducible Oil for Water-Oil Table	0.4
SORW	residual Oil for Water-Oil Table	0.4
SOIRG	irreducible Oil for Gas-Liquid Table	0.05
SORG	residual Oil for Gas-Liquid Table	0.10
SGCON	connate Gas	0.00
SGCRIT	critical Gas	0.15
KROCW	k_{ro} at connate Water	0.91
KRWIRO	k_{rw} at irreducible Oil	0.85
KRGCL	k_{rg} at connate Liquid	0.6
	exponent for calculating k_{rw} from KRWIRO	3
	exponent for calculating k_{row} from KROCW	3
	exponent for calculating k_{rog} from KROGCG	3
	exponent for calculating k_{rg} from KRGCL	3

Table 5.14 Relative permeabilities to oil and water as functions of water saturation in strongly oil-wet reservoir.

Water saturation (S_w)	**Relative perm. to water (k_{rw})**	**Relative perm. to oil (k_{ro})**
0.08	0.0000	0.9100
0.11	0.0002	0.7498
0.15	0.0017	0.6096
0.18	0.0056	0.4881
0.21	0.0133	0.3839
0.24	0.0259	0.2957
0.28	0.0448	0.2222
0.31	0.0712	0.1620
0.34	0.1063	0.1138
0.37	0.1513	0.0762
0.41	0.2075	0.0480
0.44	0.2762	0.0278
0.47	0.3586	0.0142
0.50	0.4559	0.0060
0.54	0.5694	0.0018
0.57	0.7004	0.0002
0.60	0.8500	0.0000

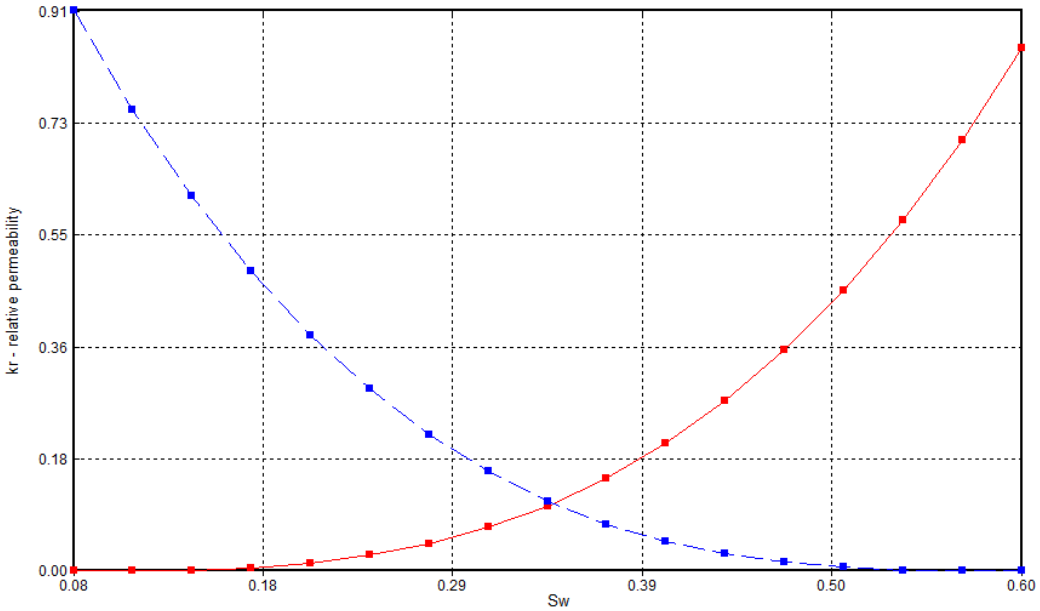

Figure 5.52 Relative permeabilities to oil and water in strongly oil-wet reservoir.

For the strongly oil-wet case, there is no gas production during the first 2,540 days as seen in Figure 5.53 because foam in all cases are created quickly. But after approximately 5,000 days, gas rate of foam stability of 160 days is noticed that makes the plot separating from other cases. This gas rate is produced slightly higher than other cases but it drops quicker than others either. This appearance results in the higher oil rate at the late period of production as seen in Figure 5.54. For strongly oil-wet condition, it is noticeable that the period that oil is produced with constant rate of CO_2-foam is not much longer than solely CO_2 injection. So an advantage of CO_2-foam is not obviously seen because in later time water breakthroughs at production well and drastically reduces oil rate of CO_2-foam flooding. Summary of water production rates are shown in Figure 5.55.

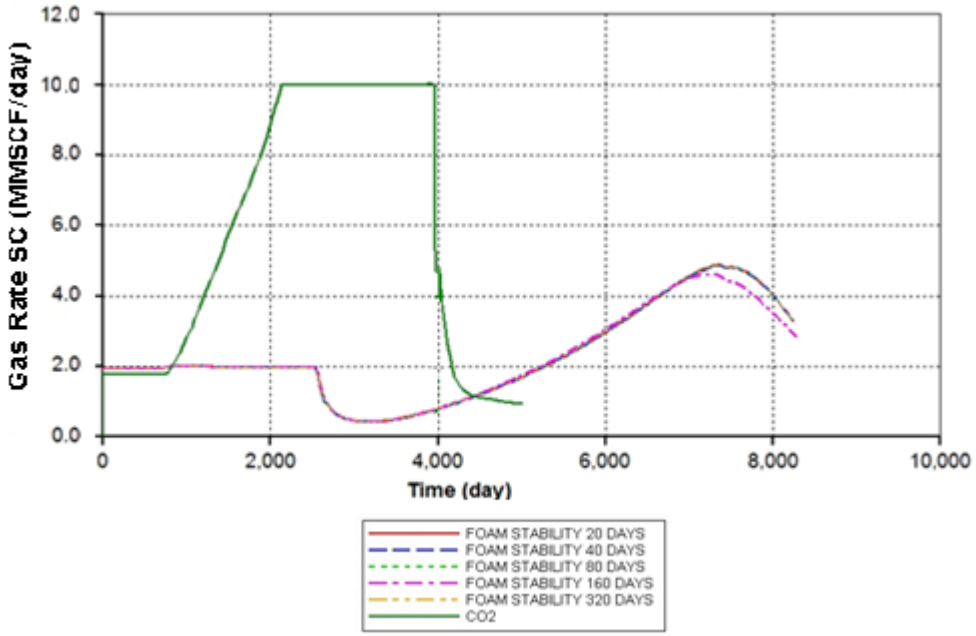

Figure 5.53 Gas production rates of CO_2–foam and CO_2 flooding cases in strongly oil-wet reservoir as functions of time.

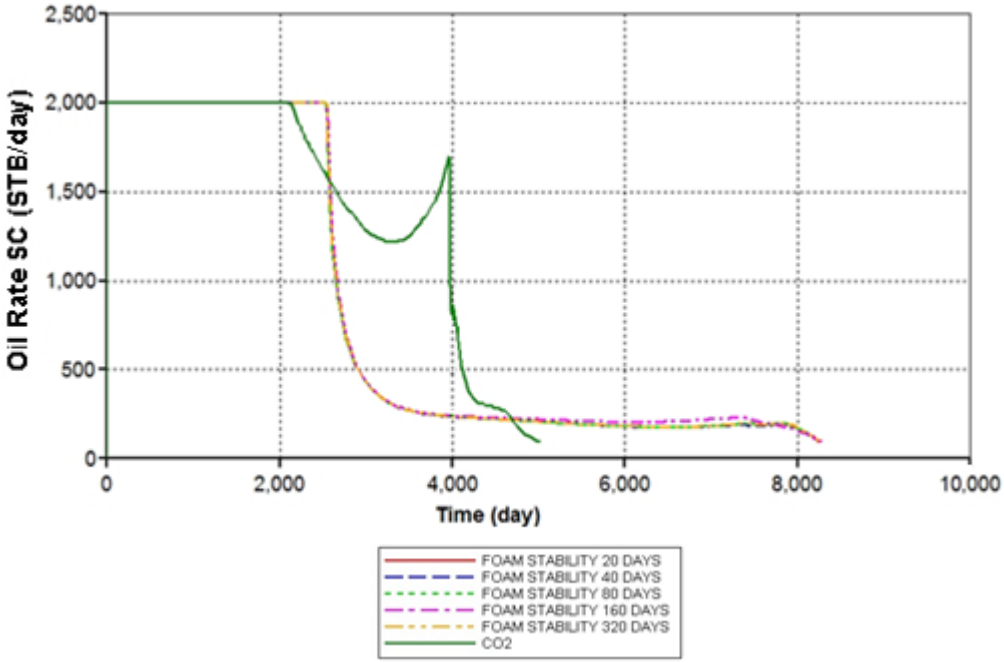

Figure 5.54 Oil production rates of CO_2–foam and CO_2 flooding cases in strongly oil-wet reservoir as functions of time.

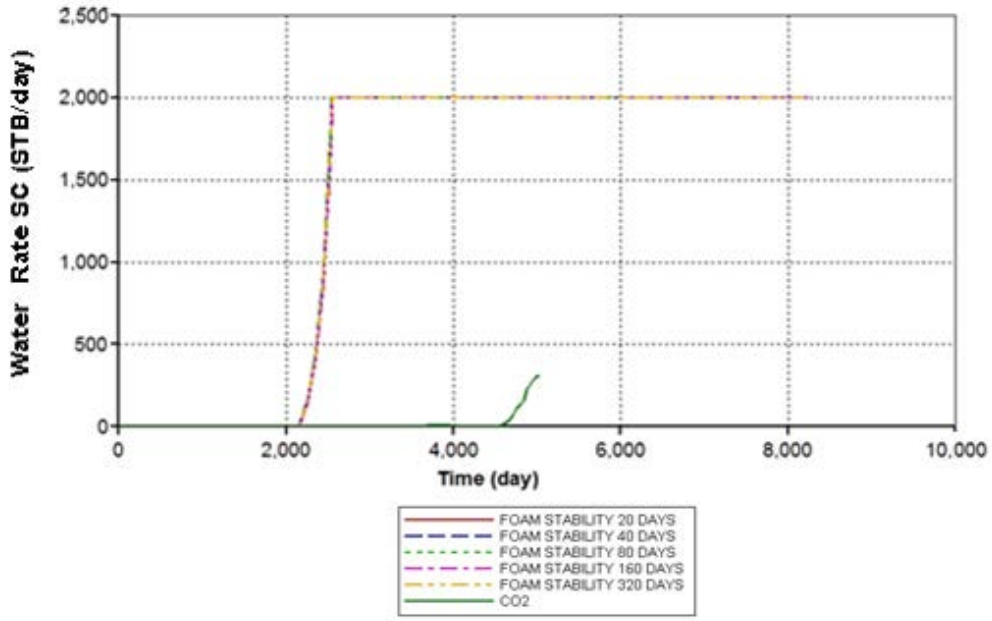

Figure 5.55 Water production rates of CO_2–foam and CO_2 flooding cases in strongly oil-wet reservoir as functions of time.

Table 5.15 Cumulative oil production, water production, gas production and oil recovery factor of CO_2–foam and CO_2 flooding cases in strongly oil - wet reservoir.

	CO_2 flooding	**Foam flooding**				
		FS 20 days	**FS 40 days**	**FS 80 days**	**FS 160 days**	**FS 320 days**
Time for injected water to reach 0.4 PV, day	5,021	8,247	8,247	8,247	8,278	8,247
Cumulative oil production (MMSTB)	7.22	6.54	6.53	6.53	6.63	6.54
Cumulative water production, (MMSTB)	0.08	11.67	11.67	11.68	11.72	11.67
Cumulative gas production (MMSCF)	28,850	18,800	18,780	18,820	18,540	18,800
Oil recovery factor, %	38.88	36.52	36.47	36.48	37.01	36.53

The summary of simulation outcomes is shown in Table 5.15. From the table it can be indicated that all foam stabilities yield similar oil recovery factor. But the best result of CO_2-foam flooding in strongly oil-wet formation is when foam stability is 160 days. The cumulative oil production from this foam stability is 6.63 MMSTB and oil recovery factor is about 37.01%. Solely CO_2 flooding, however, shows a better performance than every case of CO_2-foam flooding. The best CO_2-foam flooding case is still inferior to solely CO_2 case around 1.87%. A cumulative oil production and ultimate oil recovery of CO_2-foam flooding in the strongly oil-wet condition compared with CO_2 flooding are depicted in Figures 5.56 and 5.57, respectively.

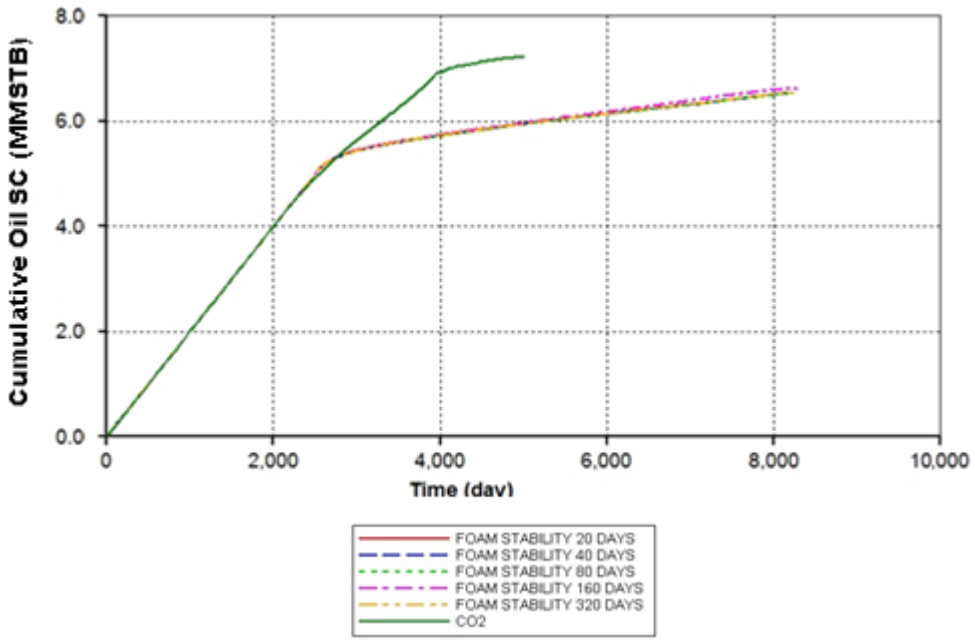

Figure 5.56 Cumulative oil productions of CO_2–foam and CO_2 flooding cases in strongly oil-wet reservoir as functions of time.

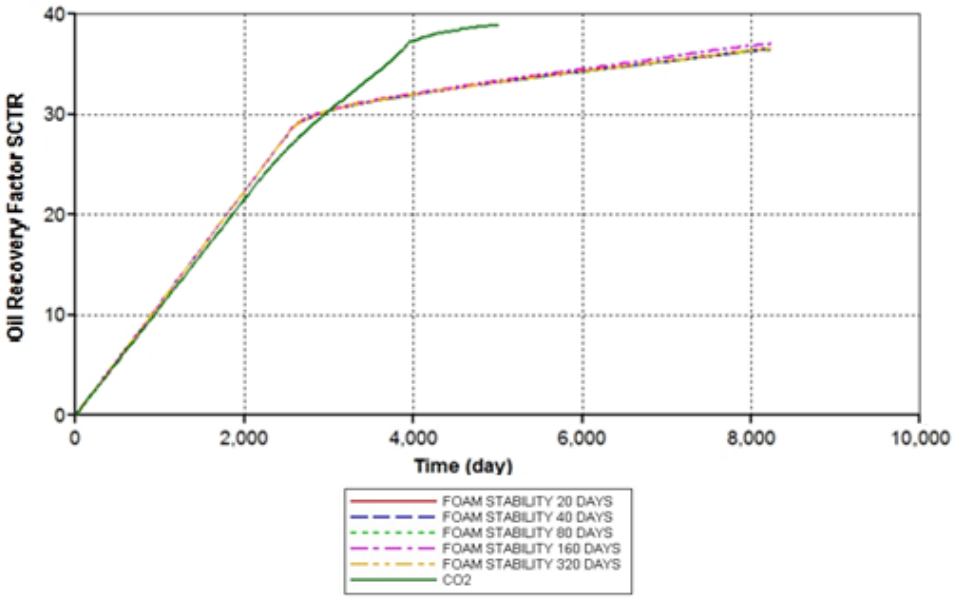

Figure 5.57 Oil recovery factors of CO_2–foam and CO_2 flooding cases in strongly oil- wet reservoir as functions of time.

5.3.1.5 Summary of effects of wettability on CO_2-foam flooding

The comparison of the effects obtained from all wettabilities on effectiveness of CO_2-foam flooding is summarized in this section. Because the performance obtained by any foam stability does not show much different, only one of five foam stabilities is a representative for all cases. In this section, foam stability of 320 days is chosen. From Figures 5.58 and 5.59 which illustrate produced oil rates and produced water rates in each wettability condition, it can be summarized that the more oil wet, the earlier water breakthrough at production well and hence, the lower ultimately oil recovery factor. This is because stronger oil-wet tends to attach less water onto the surface than water-wet condition, therefore water moves quicker and reaches earlier to production well. Late water breakthrough causes longer production period and results in greater oil recover factor. The effect of late water breakthrough is shown in Figure 5.59.

Regarding the simulation results, it can be concluded that CO_2-foam flooding is suitable for a reservoir that its wettability is in the range of neutral-wet to strongly

water-wet. For oil-wet formation, solely CO_2 flooding is preferable due to no effect of water breakthrough during gas injection period.

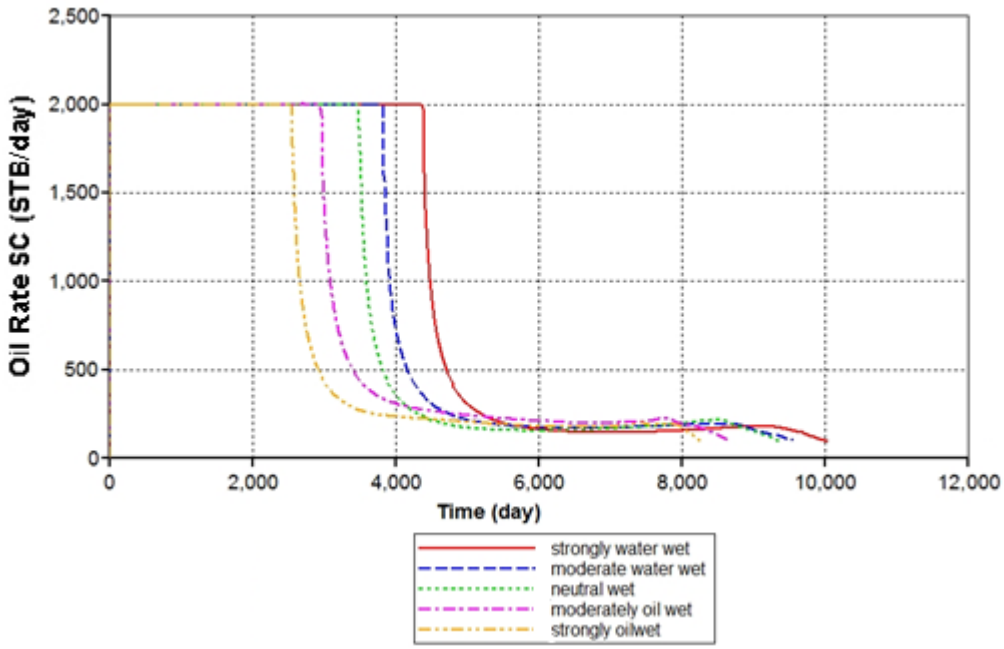

Figure 5.58 Oil production rates of CO_2–foam flooding cases with variation of wettability conditions as functions of time.

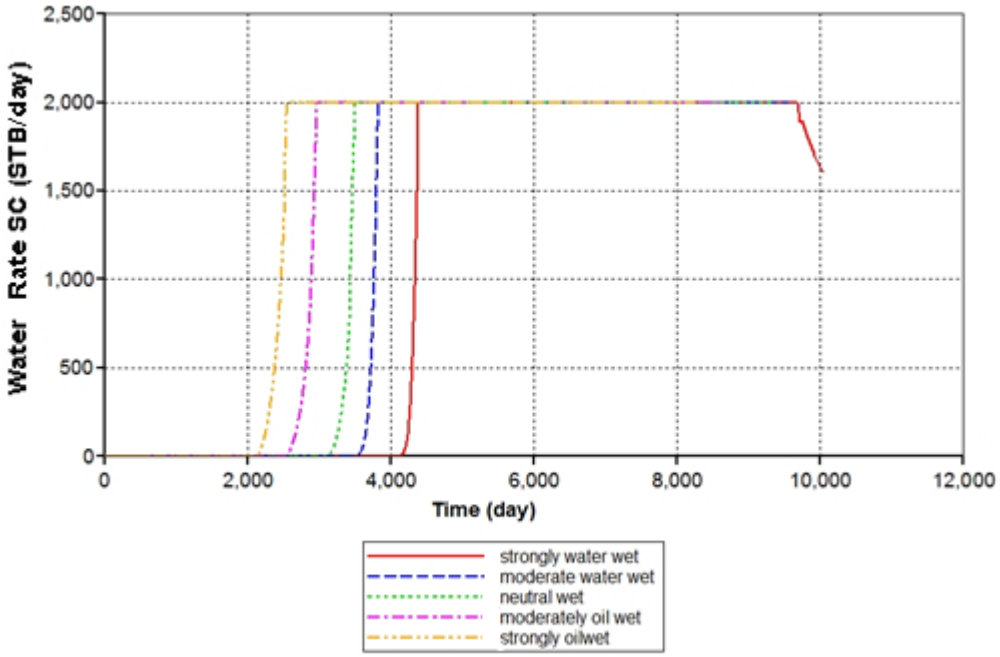

Figure 5.59 Water production rates of CO_2–foam flooding cases with variation of wettability conditions as functions of time.

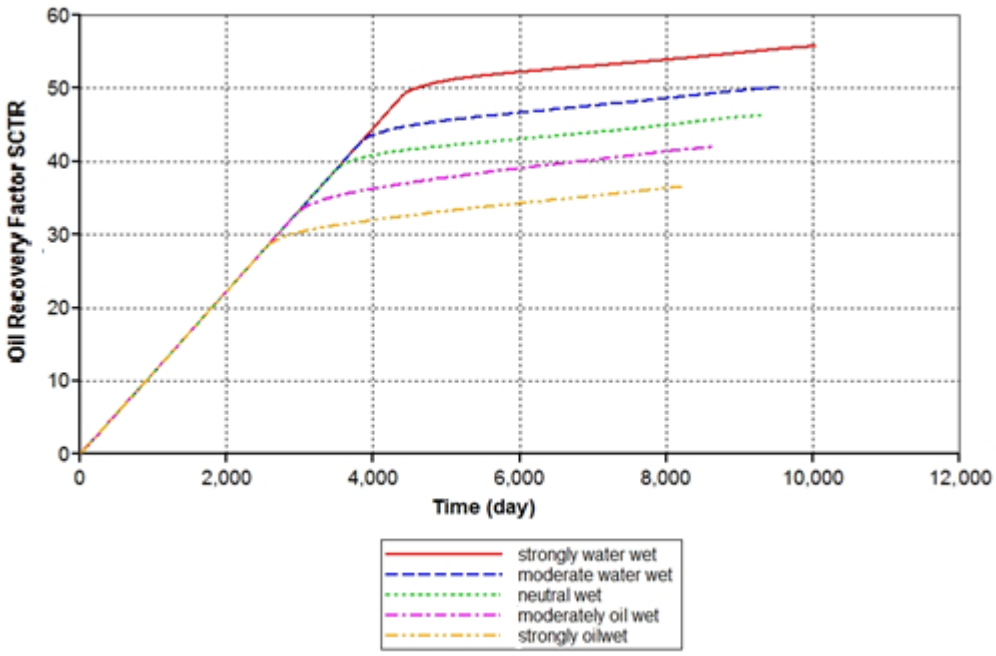

Figure 5.40 Oil recovery factors of CO_2–foam flooding cases with variation of wettability conditions as a function of time.

5.3.2 Effect of intermediate percentages of hydrocarbon in volatile oil

In this section, effects of intermediate component on ultimate oil recovery obtained by CO_2-foam flooding are studied. The percentage of intermediate component is varied from oil composition data obtained from S1 oil field by increasing the percentage of intermediate compounds about 10% and 20% compared to the base case. When the intermediate content is increased, part of heavy compounds (C_{7+}) is decreased proportionally. Other two additional cases of lower percentage of intermediate component of about 10% and 20% are also investigated. Similarly, the part of heavy compounds is increased in these cases.

5.3.2.1 Increasing percentage of intermediate component 10%

Winprop is used to generate the new oil composition by increasing the intermediate component approximately 10%. The new hydrocarbon composition is shown in Table 5.16.

Table 5.16 Hydrocarbon composition with increasing intermediate component 10%.

Component	**Mole fraction**
Carbon dioxide (CO_2)	0.0091
Nitrogen (N_2)	0.0006
Methane (C_1)	0.3383
Ethane-Hexane ($C_2 – C_6$)	0.4608
Heptane plus (C_{7+})	0.1912

Simulation results in Figure 5.61 to 5.64 illustrate oil production rates, water production rates, gas production rates, and well bottomhole pressures at the production well, respectively. However, these results have similar trend compared to the base case. But it is visible that the initial gas production rates are approximately 3.8 MMSCF/D which are much greater than the initial gas production rates in the base

case (about 1.9 MMSCF/D). This is a result from increment of intermediate component. The bubble point pressure is higher compared to the base case, resulting liberation of dissolved gas in bubbles. Moreover, water breakthrough occurs earlier than that obtained from base case because when intermediate part in oil is 10% more, this part of intermediate can be vaporized CO_2. Oil saturation is further reduced with the portion of vaporized intermediate hydrocarbon. Therefore oil saturation in this case is decreased more than in the base case CO_2-foam flooding. As relative permeability values are kept constant, lower oil saturation leads to higher relative permeability to water. Therefore, underunning water flows quicker in this case.

From Figure 5.63, the peak of high gas rates obtained by varying foam stability during 350 – 700 days of production can be sorted from the highest to the lowest rate as follows: 320 days, 160 days, 20 days, 80 days, and 40 days. The rising of gas production rate results in the same explanation as discussed in the moderately water-wet condition.

For solely CO_2 flooding, the oil production rate, illustrated in Figure 5.61, rapidly drops due to gas early breakthrough. During gas breakthrough period, oil is produced at the rate of 660-500 STB/D. Nevertheless, the rate further drops until economic oil rate is reached because bottomhole pressure is reduced to the minimum possible value.

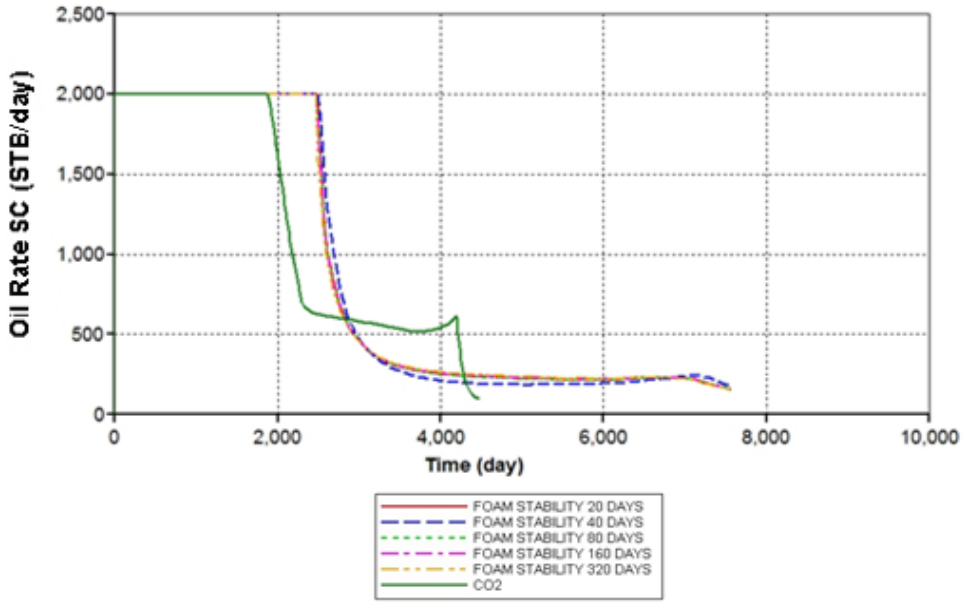

Figure 5.61 Oil production rates of CO_2–foam and CO_2 flooding cases when increasing intermediate component in oil approximately 10%.

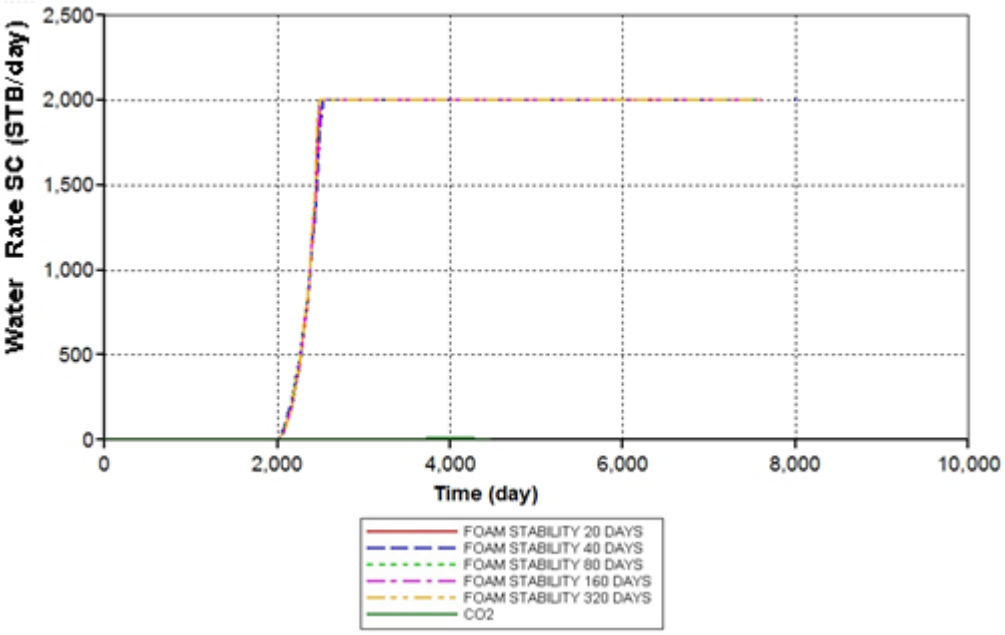

Figure 5.62Water production rates of CO_2–foam and CO_2 flooding cases when increasing intermediate component in oil approximately10%.

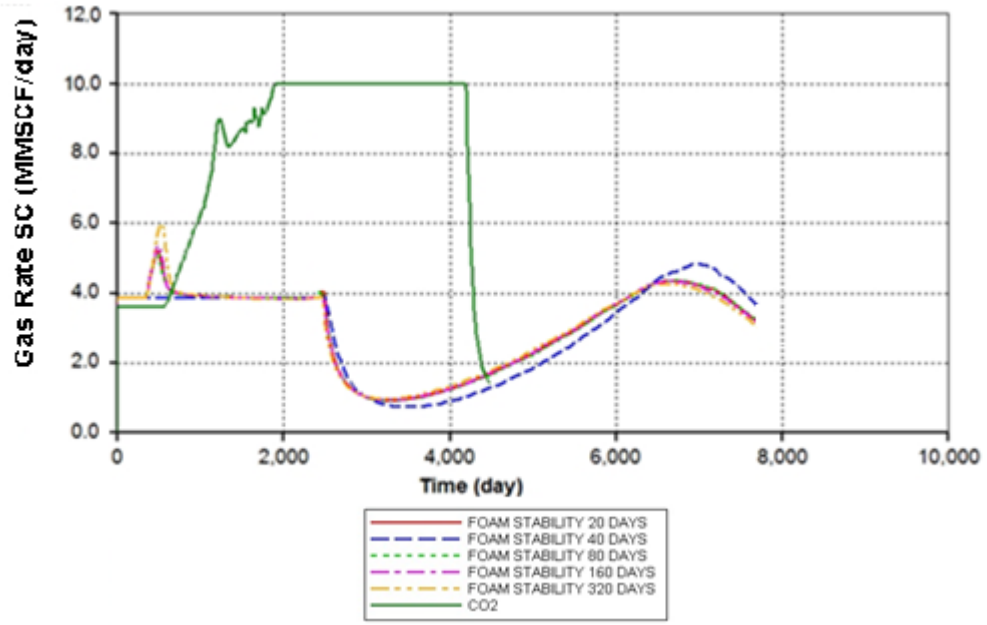

Figure 5.63 Gas production rates of CO_2–foam and CO_2 flooding cases when increasing intermediate component in oil approximately 10%.

.

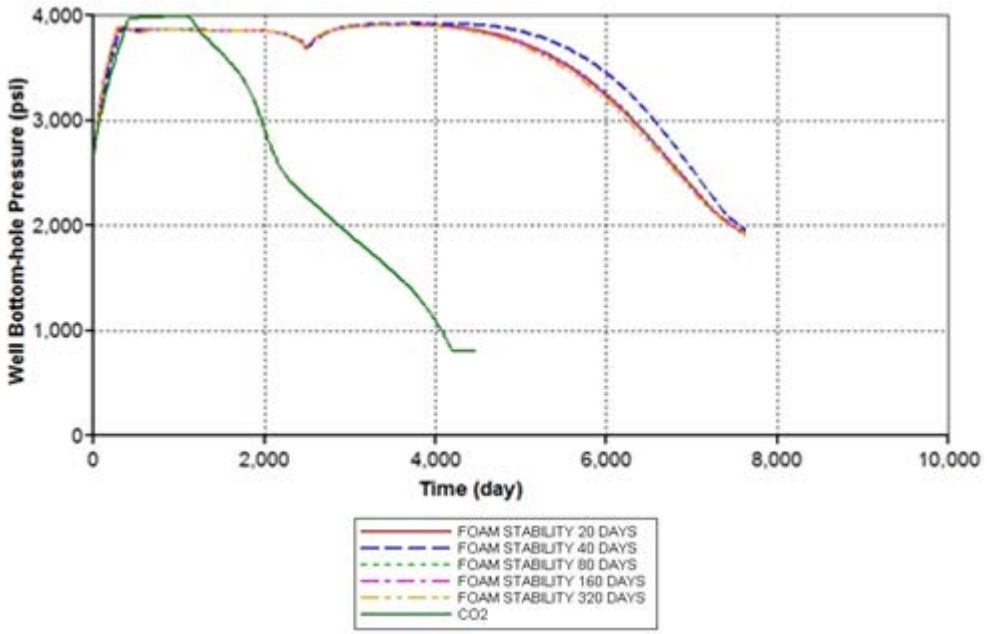

Figure 5.64 Bottomhole pressures at production well of CO_2–foam and CO_2 cases flooding when increasing intermediate component in oil approximately 10%.

The summary of simulation outcomes obtained from CO_2-foam flooding in 10% higher intermediate component in oil is listed in Table 5.17. When intermediate component in oil is increased approximately 10%, the best performance is obtained from the case where foam stability is 20 days with cumulative oil production of 6.52 MMSTB and oil recovery factor is 50.79%. But change of foam stability does not actually affect on oil recovery factor. Benefit of this case over CO_2 flooding is about 9.93%. Cumulative oil production and ultimate oil recovery of CO_2-foam flooding of this situation compared with CO_2 flooding are displayed in Figures 5.65 and 5.66, respectively.

Table 5.17 Cumulative oil production, water production, gas production and oil recovery factor of CO_2–foam and CO_2 flooding cases when increasing intermediate component in oil approximately 10%.

	CO_2 flooding	**Foam flooding**				
		FS 20 days	**FS 40 days**	**FS 80 days**	**FS 160 days**	**FS 320 days**
Time for injected water to reach 0.4 PV, day	4,473	7,670	7,639	7,670	7,670	7,729
Cumulative oil production (MMSTB)	5.44	6.52	6.47	6.50	6.50	6.51
Cumulative water production, (MMSTB)	0.01	10.69	10.64	10.69	10.70	10.82
Cumulative gas production (MMSCF)	35,710	24,100	24,010	24,010	23,900	23,950
Oil recovery factor, %	40.86	50.79	50.53	50.70	50.77	50.73

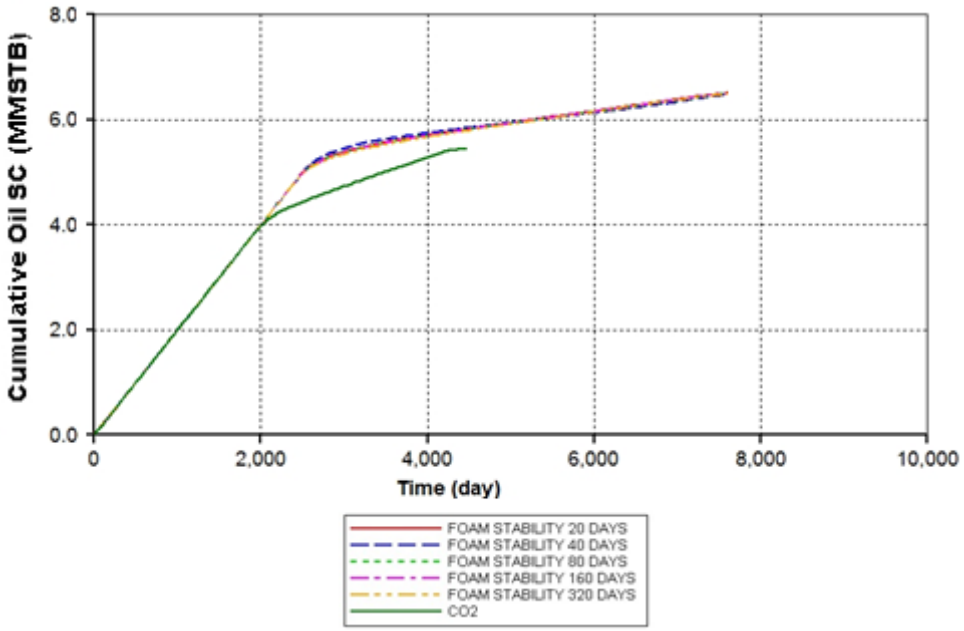

Figure 5.65 Cumulative oil productions of CO_2–foam and CO_2 flooding cases when increasing intermediate component in oil approximately 10%.

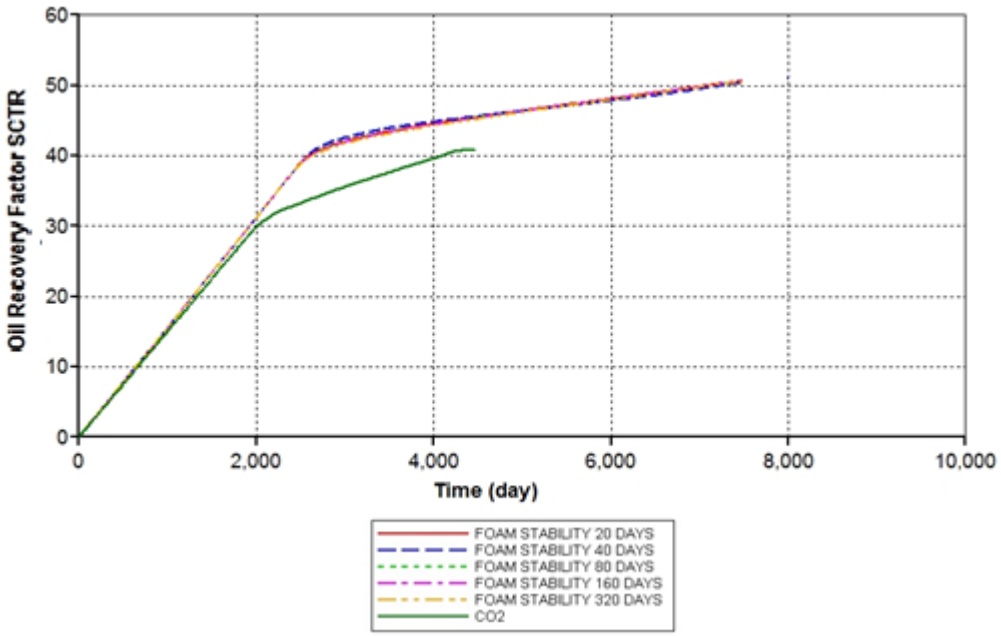

Figure 5.66 Oil recovery factors of CO_2–foam and CO_2 flooding cases when increasing intermediate component in oil approximately 10%.

5.3.2.2 Increasing percentage of intermediate component 20%

In order to create the oil composition where the intermediate component is increased approximately 20%, Winprop is utilized. The new hydrocarbon composition is listed in Table 5.18.

Table 5.18 Hydrocarbon composition with increasing intermediate component 20%.

Component	**Mole fraction**
Carbon dioxide (CO_2)	0.0091
Nitrogen (N_2)	0.0006
Methane (C_1)	0.3383
Ethane-Hexane ($C_2 – C_6$)	0.5408
Heptane plus (C_{7+})	0.1112

Figures 5.67 to 5.70 show oil production rate, water production rate, gas production rate and bottomhole pressure at production well, respectively. For CO_2-foam flooding, it is found that the initial produced gas rates are about 7.2 MMSCF/D which is already close to the limit gas production rate at 10 MMSCF/D. Small increment of gas rates are observed during 340-695 days however they do not impact oil production rates. Oil rates starts to decline at about 2,130 days due to gas and water breakthroughs which both come from CO_2-foam breakthrough. The arrival of CO_2-foam at production well is shown in Figure 5.71. Foam moves quickly in the reservoir in this case because the flow property of foam is controlled by relative permeability to water. When intermediate portion in oil is increased about 20%, the component of liquid oil after emerging of miscibility are reduced rapidly. Consider the water-oil relative permeabilities, when oil saturation reduces the relative permeability to water increases and hence, foam can flow much quicker. The effects of gas and water breakthrough can also be seen. Both gas and water compete against oil flow at production well. Therefore, oil rates fall rapidly and reach the economic limit at 100STB/D. During 2,100 to 2,970 days, produced gas and water rates strangely fluctuate. This is a result from the arrival of CO_2-foam consisting of

aqueous and gaseous phases. It is obvious that CO_2-foam can prolong the constant oil rate at 2,000 STB/D much longer than the case of solely CO_2 flooding.

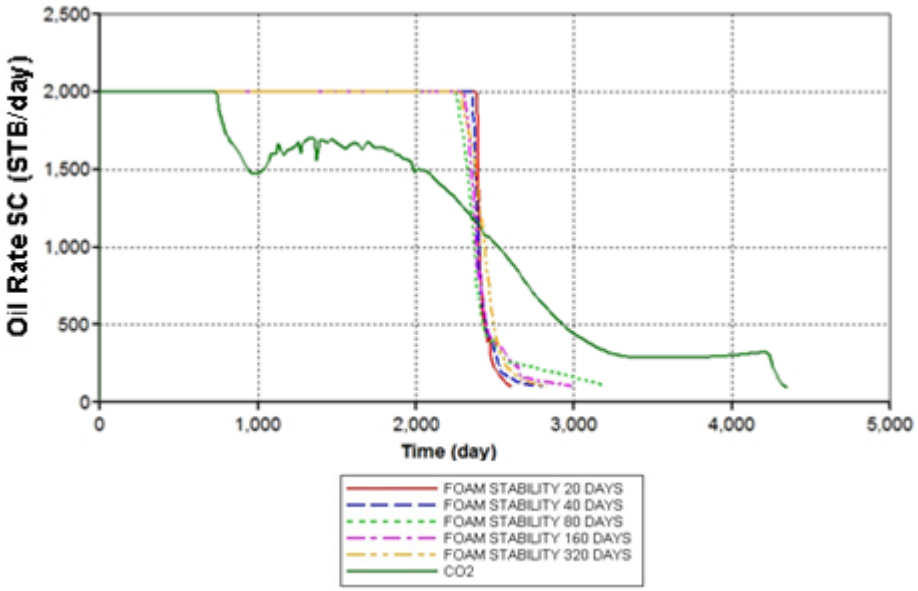

Figure 5.67 Oil production rates of CO_2–foam and CO_2 flooding cases when increasing intermediate component in oil approximately 20%.

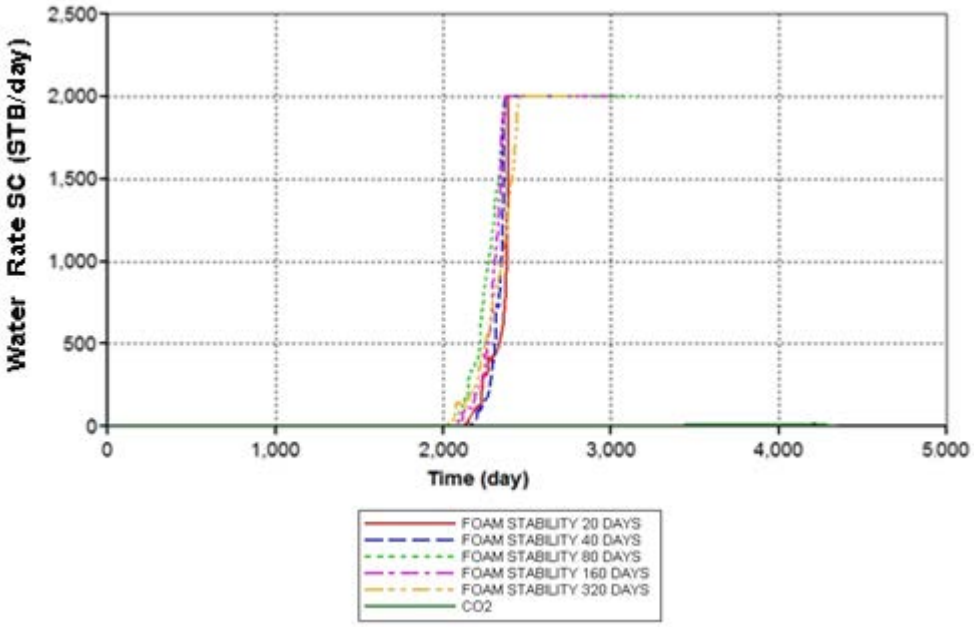

Figure 5.68 Water production rates of CO_2–foam ad CO_2 flooding cases when increasing intermediate component in oil approximately 20%.

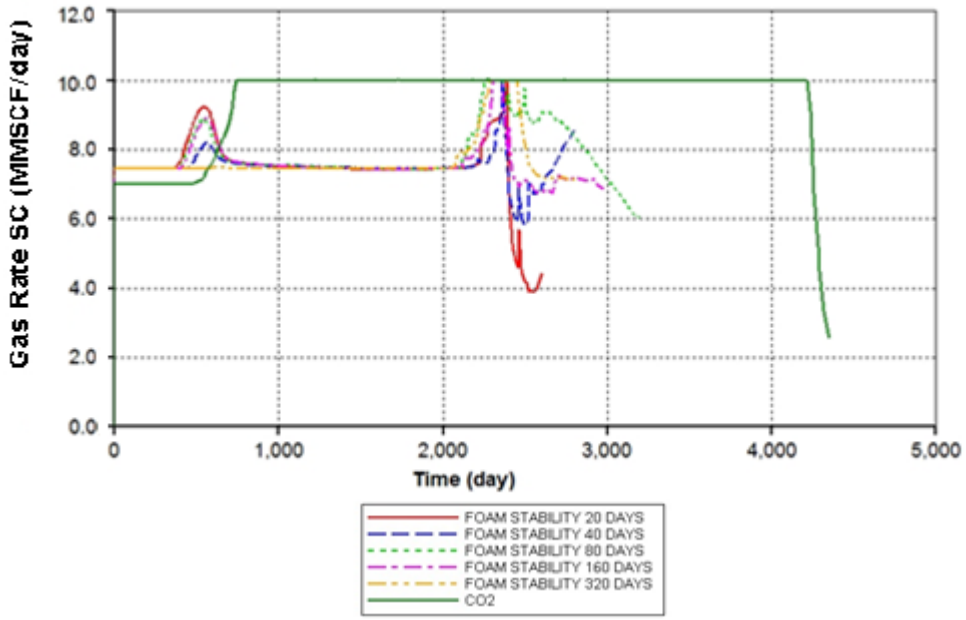

Figure 5.69 Gas production rates of CO_2–foam and CO_2 flooding cases when increasing intermediate component in oil approximately 20%.

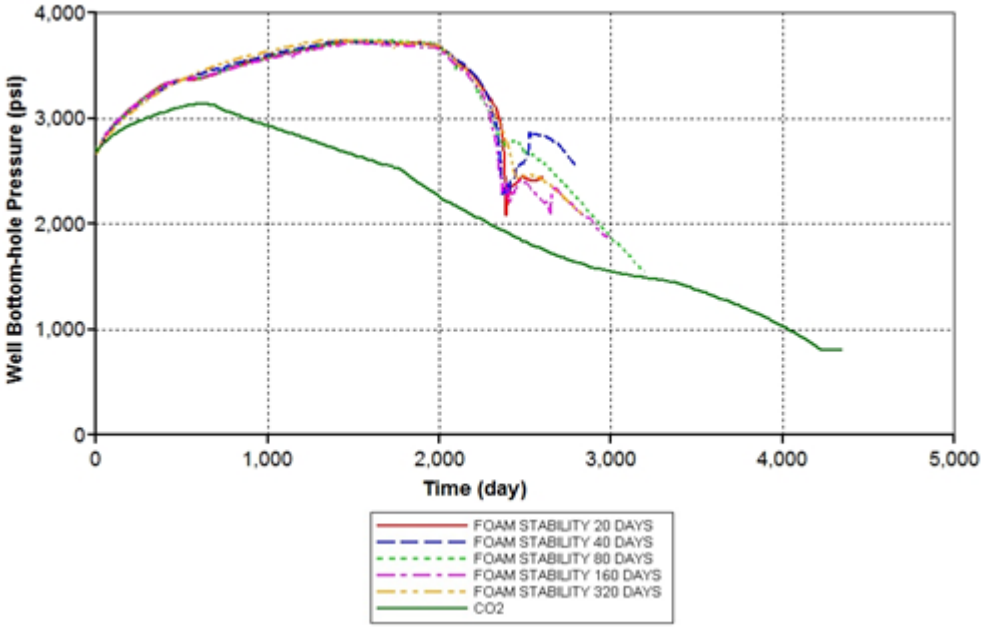

Figure 5.70 Bottomhole pressures at production well of CO_2–foam and CO_2 flooding cases when increasing intermediate component in oil approximately 20%.

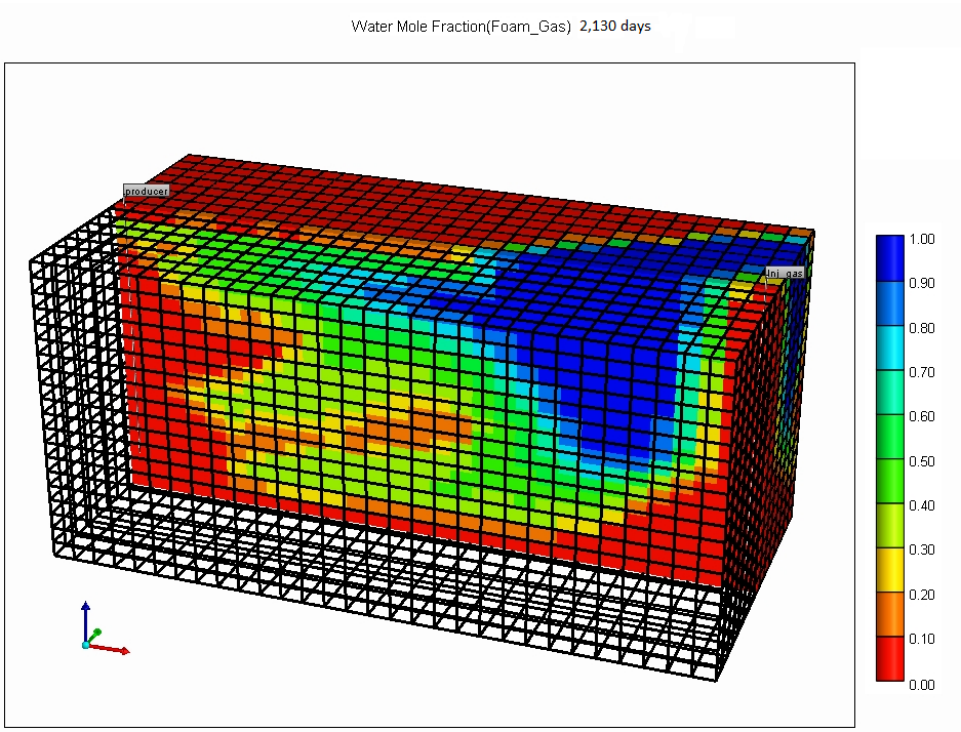

Figure 5.71 CO_2-foam breakthroughs at production well at 2,130 days.

For solely CO_2 flooding, oil production rate as shown in Figure 5.67 rapidly fall at the day 740th as a result of gas early breakthrough. But this drop is not as high as the case increased intermediate component of 10% because the initial produced gas rate is not much different from the limit gas production rate. This can be inferred that relative permeability to oil is not reduced much. Nevertheless, oil rate is continuously decreased and the production is terminated at the day 4,350th.

Results of cases obtained when intermediate component is increased of 20% are listed in Table 5.19. Even though oil recovery factors obtained from different foam stability are not much varied, the best result is obtained when foam stability is 320 days. The ultimate oil recovery obtained from this case is higher than solely CO_2 flooding approximately 2.28%. Cumulative oil production and ultimate oil recovery of CO_2-foam flooding compared with CO_2 flooding are illustrated in Figures 5.72 and 5.73, respectively.

Table 5.19 Cumulative oil production, water production, gas production and oil recovery factor of CO_2–foam and CO_2 flooding cases when increasing intermediate component in oil compound approximately 20%.

	CO_2 flooding	**Foam flooding**				
		FS 20 days	**FS 40 days**	**FS 80 days**	**FS 160 days**	**FS 320 days**
Time for injected water to reach 0.4 PV, day	4,349	2,708	2,800	3,193	2,981	2,824
Cumulative oil production (MMSTB)	4.92	4.82	4.86	4.89	4.88	4.90
Cumulative water production, (MMSTB)	0.01	0.85	0.96	1.88	1.39	1.02
Cumulative gas production (MMSCF)	40,860	21,340	21,020	25,050	22,590	21,690
Oil recovery factor, %	56.90	58.60	58.75	59.06	58.95	59.18

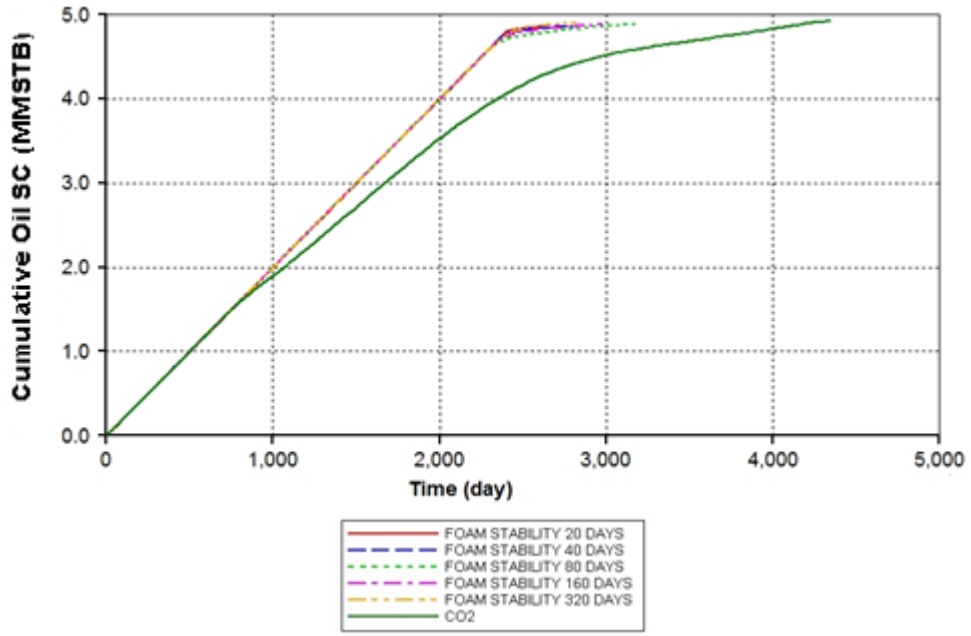

Figure 5.72 Cumulative oil productions of CO_2–foam and CO_2 flooding cases when increasing intermediate component in oil approximately 20%.

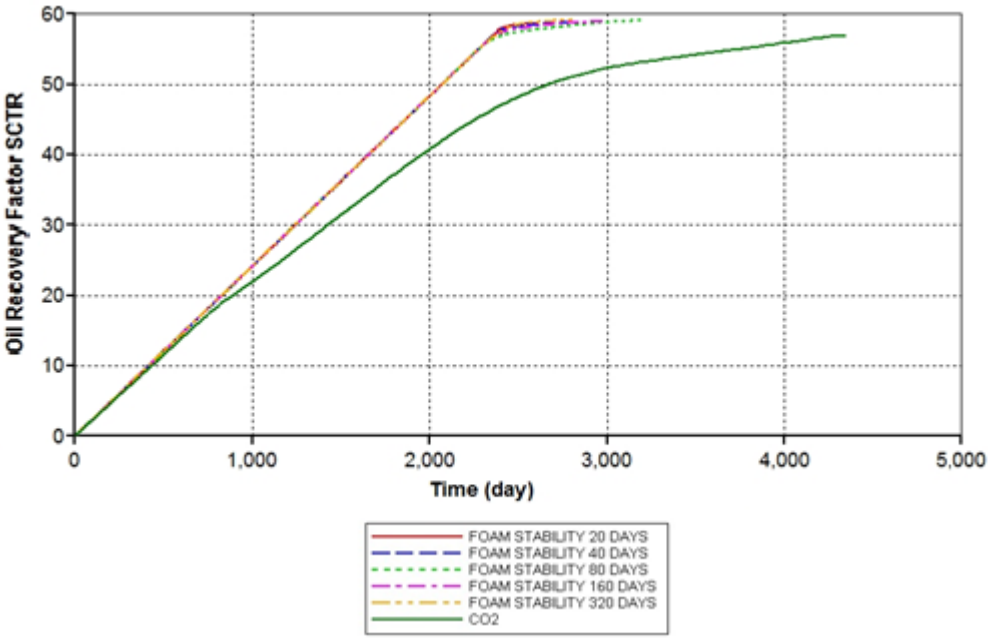

Figure 5.73 Oil recovery factors of CO_2–foam and CO_2 flooding cases when increasing intermediate component in oil approximately 20%.

5.3.2.3 Decreasing percentage of intermediate component 10%

The oil composition where intermediate is decreased about 10% is shown in Table 5.20.

Table 5.20 Hydrocarbon composition with increasing intermediate component 10%.

Component	**Mole fraction**
Carbon dioxide (CO_2)	0.0091
Nitrogen (N_2)	0.0006
Methane (C_1)	0.3383
Ethane-Hexane ($C_2 - C_6$)	0.2308
Heptane plus (C_{7+})	0.4212

Oil production rate, water production rate, gas production rate and well bottomhole pressure of the production well are depicted in Figures 5.74 to 5.77, respectively. For CO_2-foam flooding, oil production rate of all case can be kept operated constantly for approximately 4,870 days. After that, the rates fall roughly due to the arrival of CO_2-foam at around 3,850 days of production period as shown in Figure 5.78. The reason that most of foam does not break during travelling in the reservoir is that foam tends to be more stable in heavier oil. Lighter oil composing of short chain alkanes has the ability to enter into CO_2 and surfactant interfaces of lamellae. This leads to weakening of foam bubble and eventually, foam ruptures. Therefore, more heavy oil component causes higher stability of foam. Fluctuation of produced gas rate and produced water rate during 4,000-7,000 days is a result from breakthrough of CO_2-foam consisting of both gaseous and aqueous phase. It can be noticed that cases of foam stabilities of 20 days, 80 days, 160 days, and 320 days water production rates are controlled at the maximum value (2,000 STB/D). So, cumulative produced water is higher than the case of foam stability of 40 days. On the other hands, a case of 40 days foam stability is controlled by produced gas rate since it reaches the maximum gas rate of 10 MMSCF/D. Therefore cumulative produced gas of this case is higher than other cases. Afterwards, produced gas rates and

produced water rates drop again due to reduction of reservoir pressure. Hence, fluids are produced at small rates. At approximately 7,000 days after production, water rates increase again. The increment of water rate occurs from chasing water that approaches to production well.

For CO_2 flooding with decreasing in intermediate component of 10%, it shows similar trend as in CO_2 base case but a period that water sweeps oil in the lower zone this case (day 4,750th to 5,880th) can produce more oil than base case. This is because saturation of remaining oil that is not vaporized by CO_2 is higher than that of CO_2 base case.

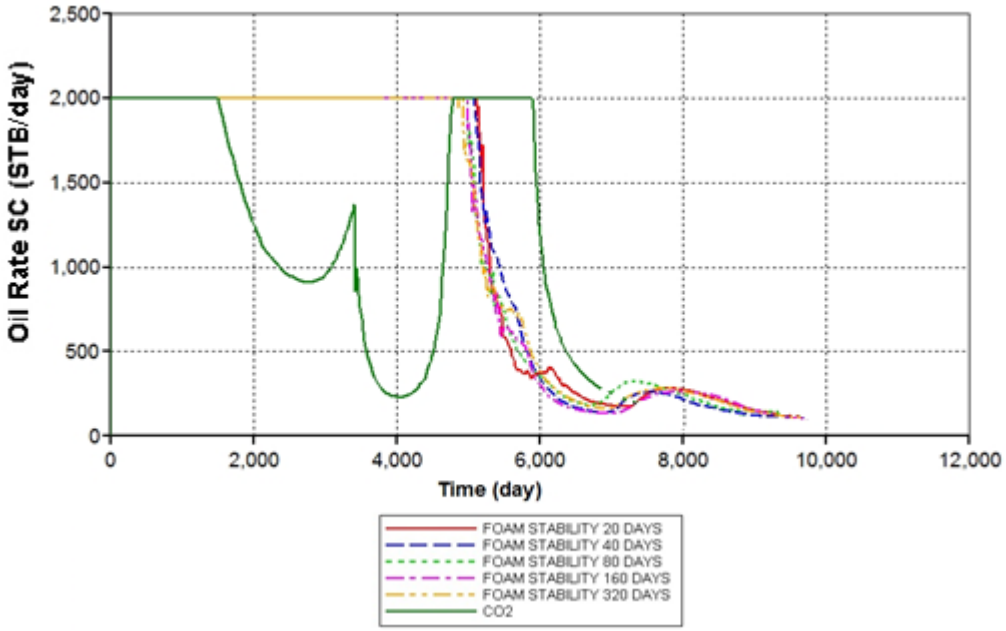

Figure 5.74 Oil production rates of CO_2–foam and CO_2 flooding cases when decreasing intermediate component in oil approximately 10%.

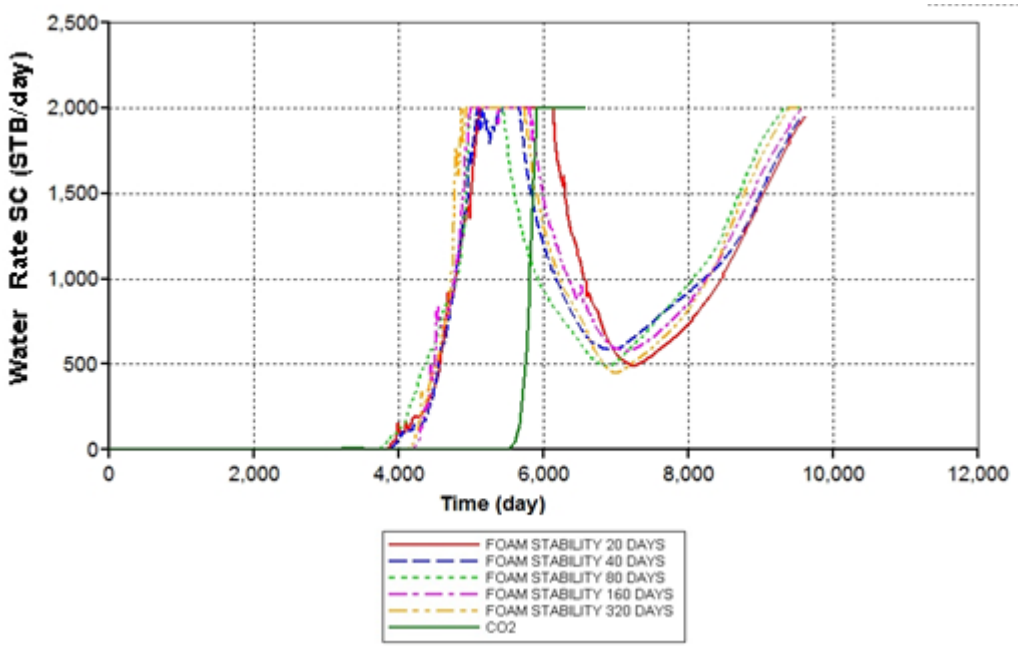

Figure 5.75 Water production rates of CO_2–foam and CO_2 flooding cases when decreasing intermediate component in oil approximately 10%.

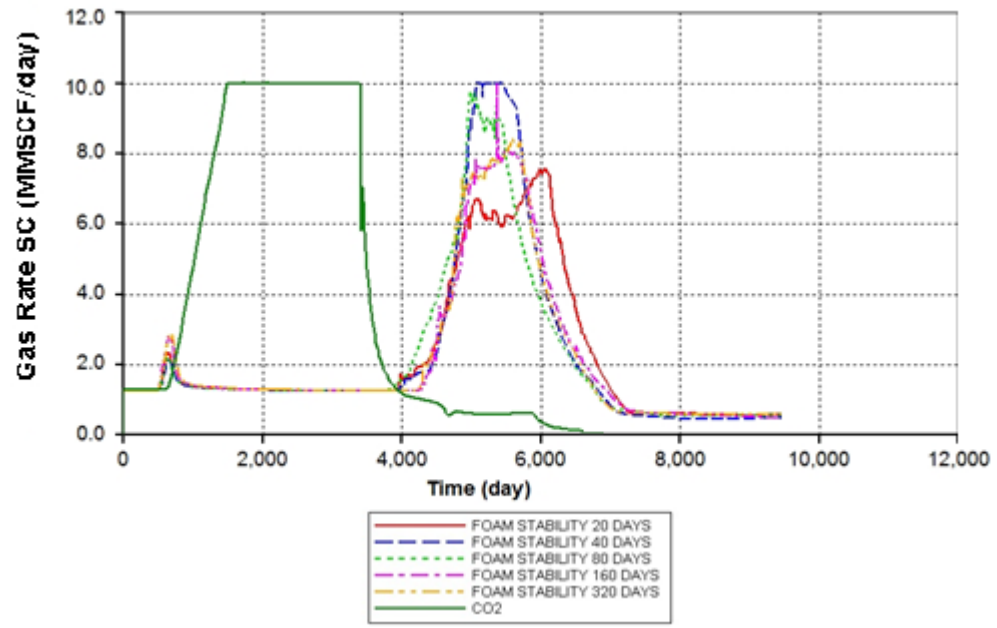

Figure 5.76 Gas production rates of CO_2–foam and CO_2 flooding cases when decreasing intermediate component in oil approximately 10%.

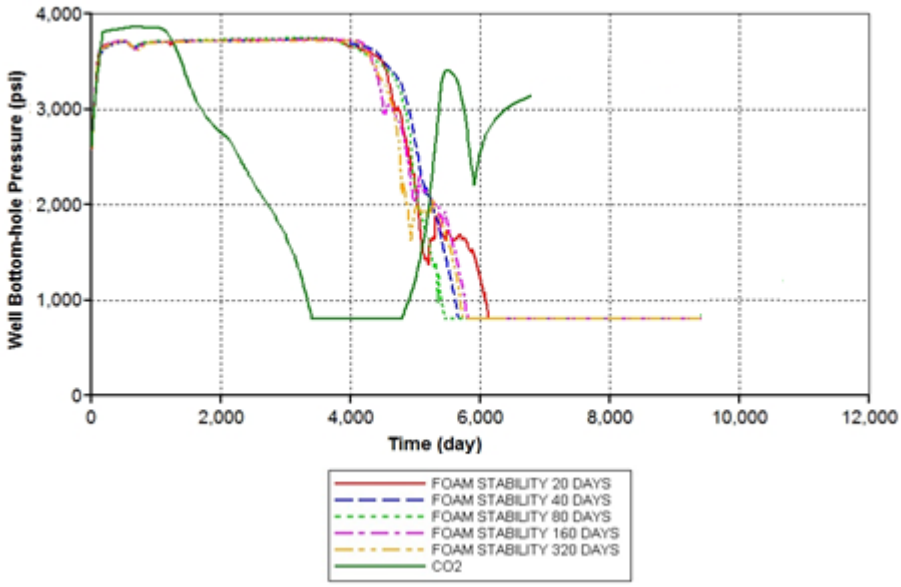

Figure 5.77 Bottomhole pressures at production well of CO_2–foam and CO_2 flooding cases when decreasing intermediate component in oil approximately 10%.

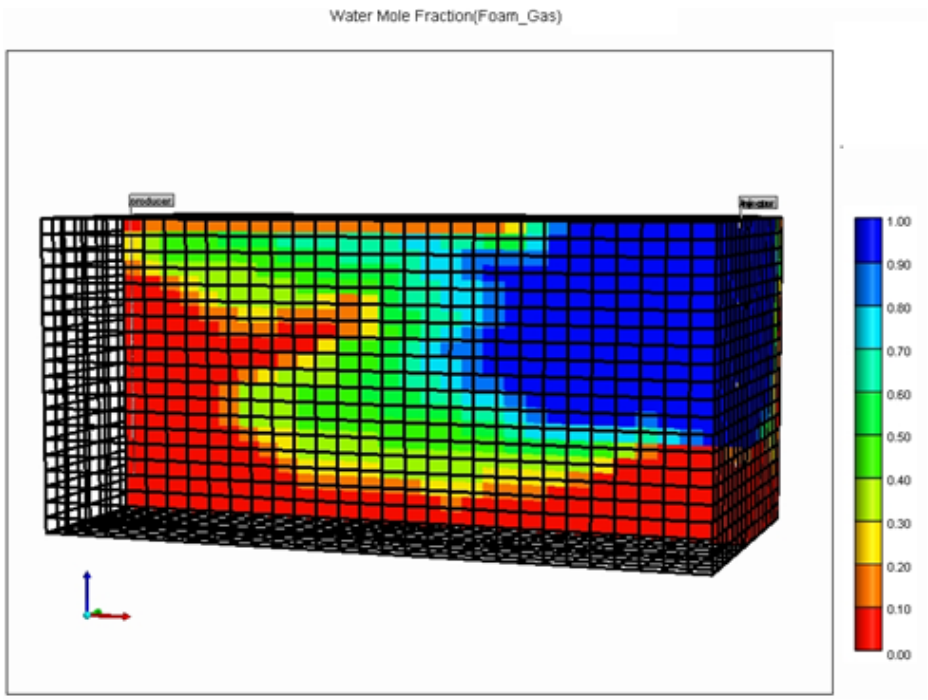

Figure 5.78 CO_2-foam breakthroughs at production well.

The summary of simulation results of each case simulated in 10% less intermediate component in reservoir oil are described in Table 5.21. Each foam stability yields similar oil recovery factor and the best result is obtained in a case where foam stability is 20 days. The ultimate oil recovery from this study case is higher than solely CO_2 flooding about 14.15%. Cumulative oil production and ultimate oil recovery of CO_2-foam flooding of this case compared to solely CO_2 flooding are illustrated in Figures 5.79 and 5.80, respectively.

Table 5.21 Cumulative oil production, water production, gas production and oil recovery factor of CO_2–foam and CO_2 flooding cases when decreasing intermediate component in oil approximately 10%.

	CO_2 flooding	**Foam flooding**				
		FS 20 days	**FS 40 days**	**FS 80 days**	**FS 160 days**	**FS 320 days**
Time for injected water to reach 0.4 PV, day	6,396	9,800	9,774	9,677	9,739	9,860
Cumulative oil production (MMSTB)	8.61	11.67	11.59	11.47	11.57	11.70
Cumulative water production, (MMSTB)	1.25	6.53	6.62	6.65	6.70	6.96
Cumulative gas production (MMSCF)	27,960	20,970	20,450	20,060	20,080	20,310
Oil recovery factor, %	41.53	55.98	55.61	55.04	55.53	56.10

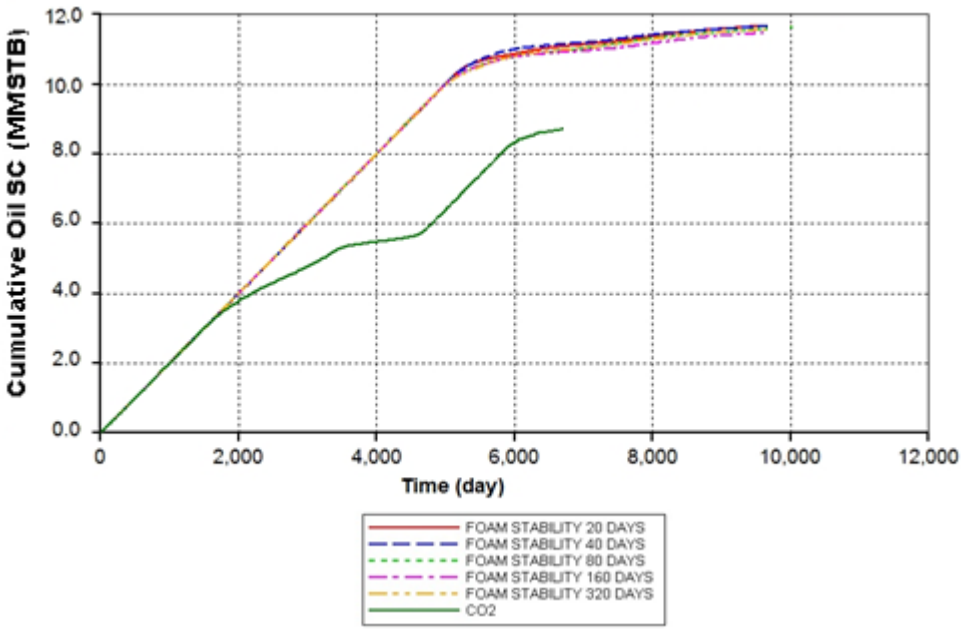

Figure 5.79 Cumulative oil productions of CO_2–foam and CO_2 flooding cases when decreasing intermediate component in oil approximately 10%.

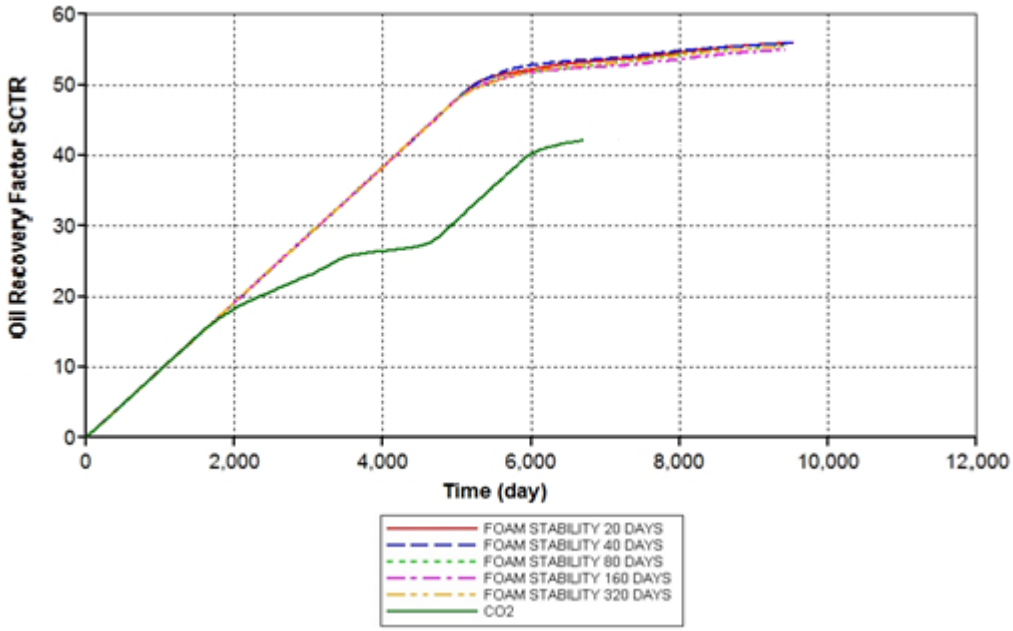

Figure 5.80 Oil recovery factors of CO_2–foam and CO_2 flooding cases when decreasing intermediate component in oil approximately 10%.

5.3.2.4 Decreasing percentage of intermediate component 20%

The oil compositions when intermediate component is decreased approximately 20% is shown in Table 5.22.

Table 5.22 Hydrocarbon composition with decreasing intermediate component 20%.

Component	**Mole fraction**
Carbon dioxide (CO_2)	0.0091
Nitrogen (N_2)	0.0006
Methane (C_1)	0.3383
Ethane-Hexane ($C_2 - C_6$)	0.1408
Heptane plus (C_{7+})	0.5112

For cases of CO_2-foam flooding in oil with decreasing of intermediate component approximately 20%, oil production rates, water production rates, and gas production rates, and well bottomhole pressure at the production well are illustrated as functions of time in Figures 5.81 to 5.84. These cases show similar results to those obtained from 10% less intermediate component but decreasing of intermediate component down to 20% can prolong the constant oil production rate period up to 5,250 days. Rapid drop of oil rate is also a result from an arrival of CO_2-foam slug. The unstable gas rate and water rate during 3,700-7,500 days are results from flowing of both gaseous and aqueous phases of foam. The cases where foam stabilities are 40 days, 80 days, 160 days, and 320 days, the productions are controlled under maximum water production rate. In a case where foam stability is 20 days production is controlled by produced gas rate since it reaches the maximum value. Because pressure reduces continuously, production of all fluids is decreased. From Figure 5.82, the increasing of water production rates can be seen around the day 7,300th. This is caused by an arrival of chasing water as same as the previous cases. Hence, oil rates are raised up a bit.

Regarding CO_2 flooding in cases where reduction of intermediate component approximately 20% is applied, the results show similar trend as seen in results of CO_2

base case and cases with 10% reduction of intermediate component. But, period of gas breakthrough is shorter than other cases. Moreover, the period that water sweeps oil in lower zone is longer than other cases. This can be described that, saturation of intermediate component which can be vaporized is lower and heavy hydrocarbon remained after vaporization is higher.

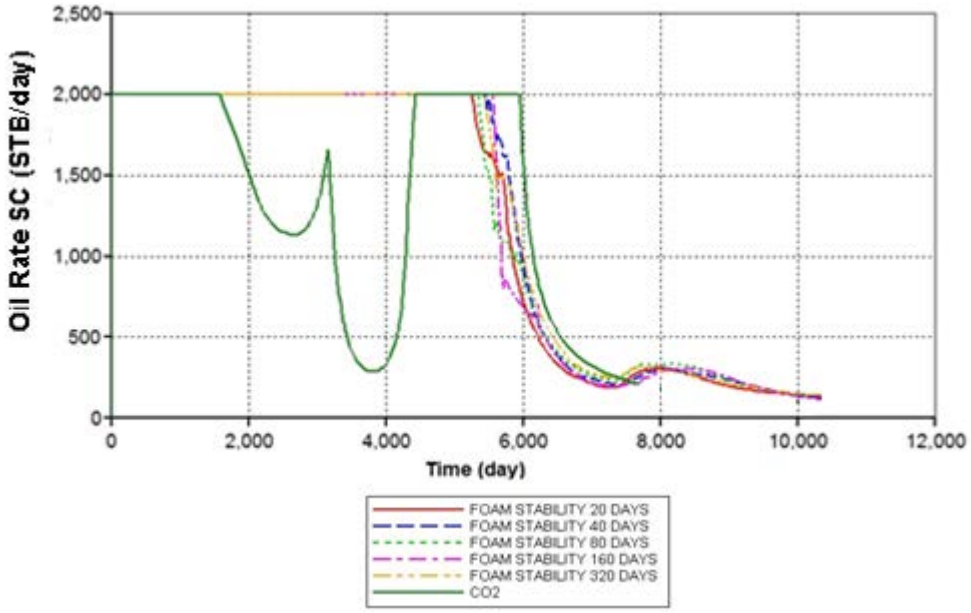

Figure 5.81 Oil production rates of CO_2–foam and CO_2 flooding cases when decreasing intermediate component in oil approximately 20%.

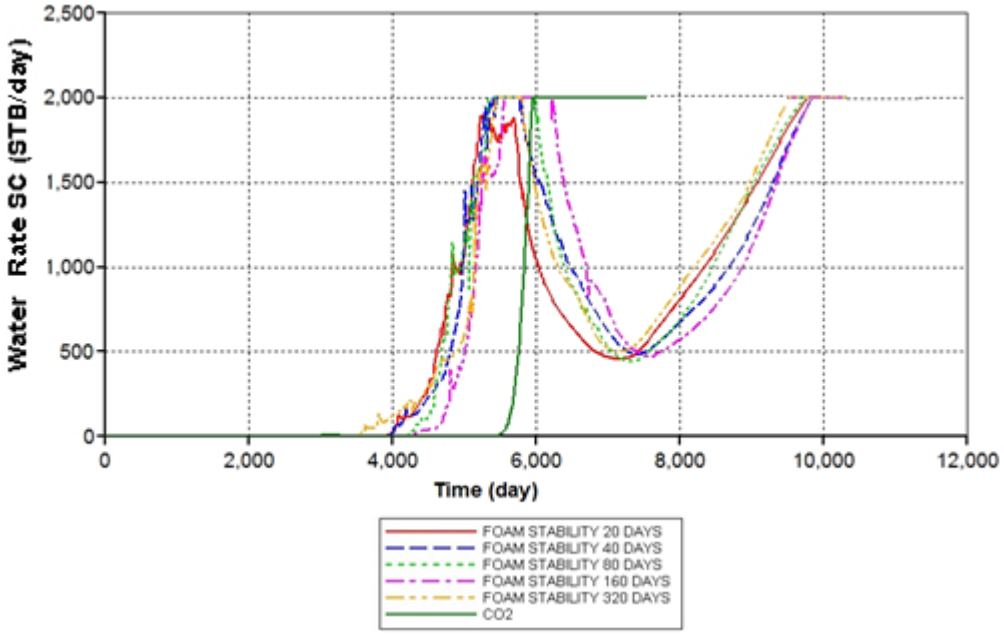

Figure 5.82 Water production rates of CO_2–foam and CO_2 flooding cases when decreasing intermediate component in oil approximately 20%.

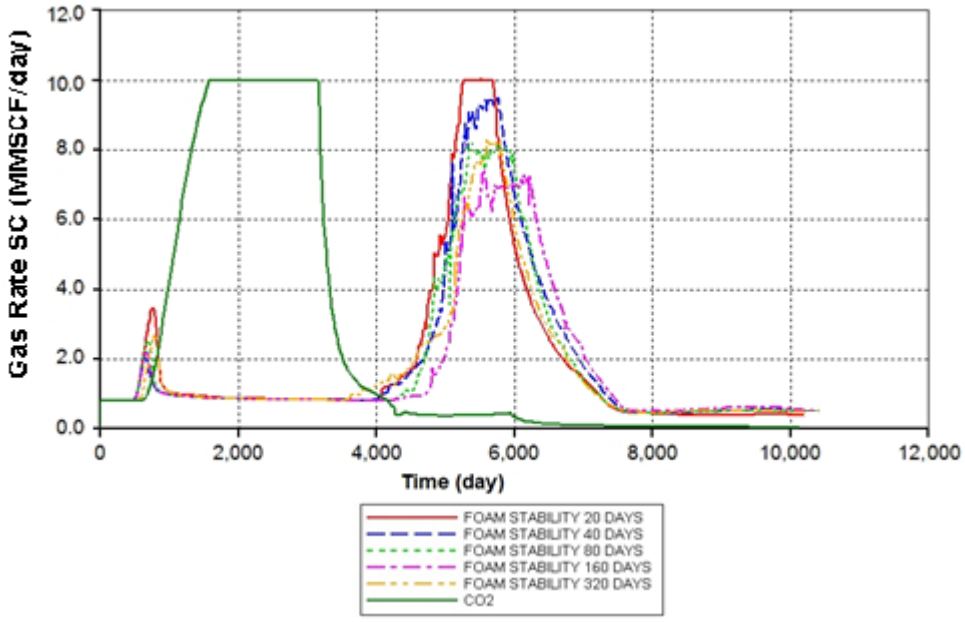

Figure 5.83 Gas production rates of CO_2–foam and CO_2 flooding cases when decreasing intermediate component in oil approximately 20%.

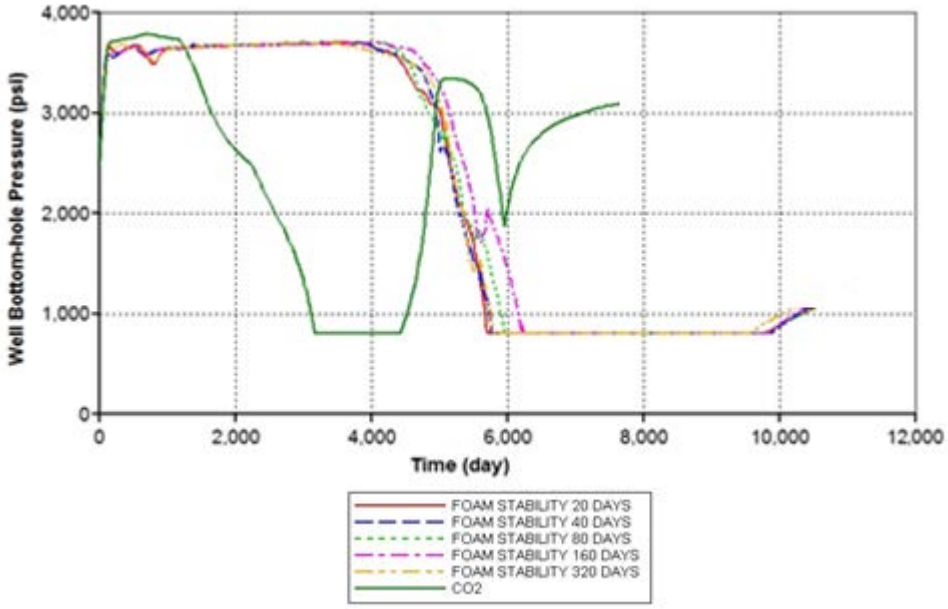

Figure 5.84 Bottomhole pressures a production well of CO_2–foam and CO_2 flooding cases when decreasing intermediate component in oil approximately 20%.

Cumulative oil production, cumulative water production, cumulative gas production and ultimate oil recovery when 20% intermediate component is reduced are listed in Table 5.23. Base on oil recovery factor, variation of foam stability affects a bit on CO_2-foam performance. Foam stability of 40 days provides the best result when CO_2-foam flooding is applied and benefit of this case over CO_2 flooding is about 11.76%.

Table 5.23 Cumulative oil production, water production, gas production and oil recovery factor of CO_2–foam and CO_2 flooding cases when decreasing intermediate component in oil approximately 20%.

	CO_2 flooding	**Foam flooding**				
		FS 20 days	**FS 40 days**	**FS 80 days**	**FS 160 days**	**FS 320 days**
Time for injected water to reach 0.4 PV, day	6,865	10,077	10,208	10,207	10,372	9,954
Cumulative oil production (MMSTB)	9.87	12.59	12.90	12.74	12.68	12.90
Cumulative water production, (MMSTB)	2.14	6.39	6.70	7.00	6.86	6.50
Cumulative gas production (MMSCF)	24,880	19,420	19,370	18,340	17,670	17,200
Oil recovery factor, %	42.05	53.81	55.14	54.44	54.22	55.12

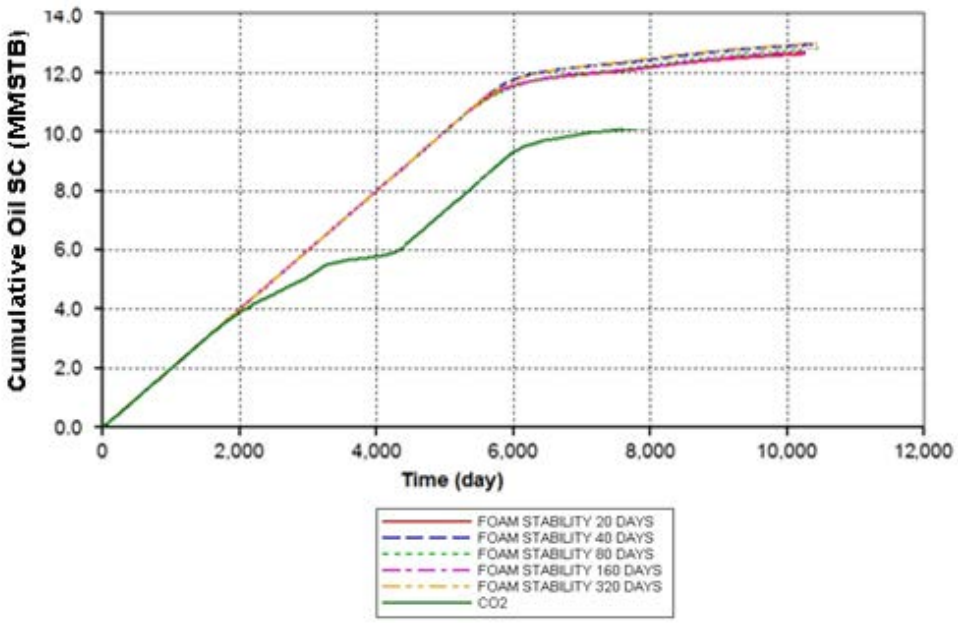

Figure 5.85 Cumulative oil productions of CO_2–foam and CO_2 flooding cases when decreasing intermediate component in oil approximately 10%.

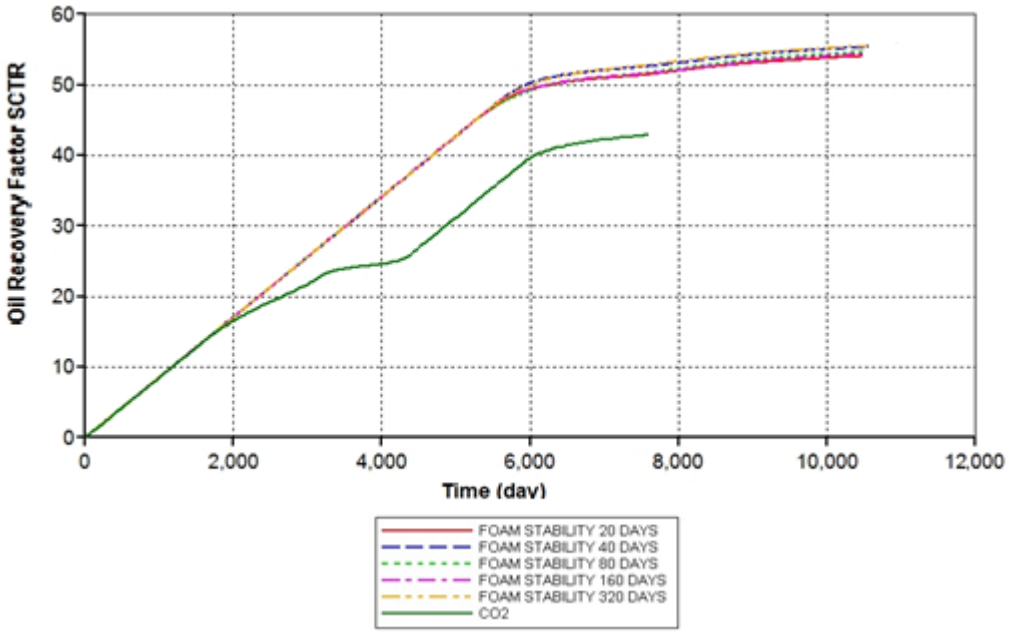

Figure 5.86 Oil recovery factors of CO_2–foam and CO_2 flooding cases when decreasing intermediate component in oil approximately 20%.

5.3.2.5 Summary of effects of intermediate percentages of hydrocarbon in volatile oil on CO_2-foam flooding

In the study of intermediate component, foam stability of 160 days is chosen to represent for all cases. From Figures 5.87 to 5.89 produced oil rates, produced water rates and produced gas rate at production well in each condition are displayed. It can be seen that higher intermediate component in oil composition induces quicker flow of CO_2-foam slug by observing an arrival of water. The quicker water breakthrough causes early termination of production. Moreover, another thing to be noticed is that low intermediate component oil does not cause rupture of CO_2-foam as much as in high intermediate component oil. In the cases of decreasing intermediate component, foam hardly ruptures and be produced simultaneously with oil. An arrival of foam at production well can be noticed from coincidence of gas and water production rate.

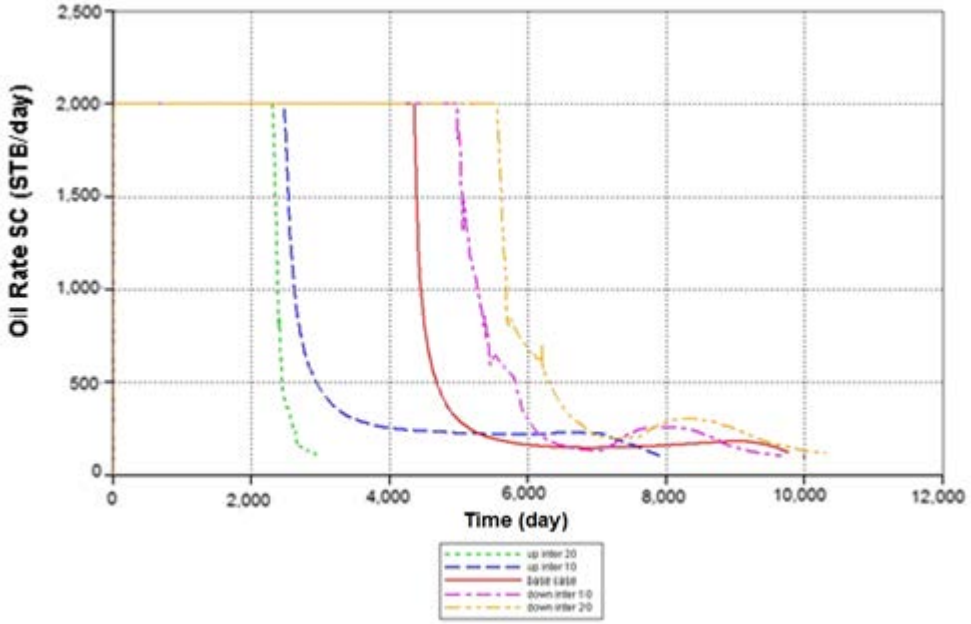

Figure 5.87 Oil production rates of CO_2–foam flooding with variation of oil composition as functions of time.

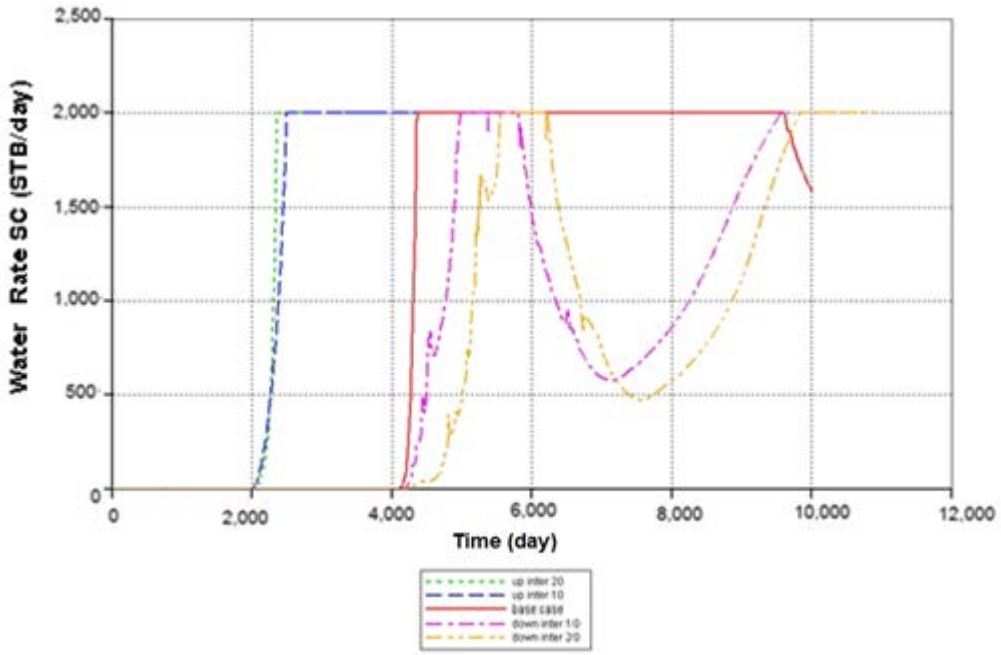

Figure 5.88 Water production rates of CO_2–foam flooding with variation of oil composition as functions of time.

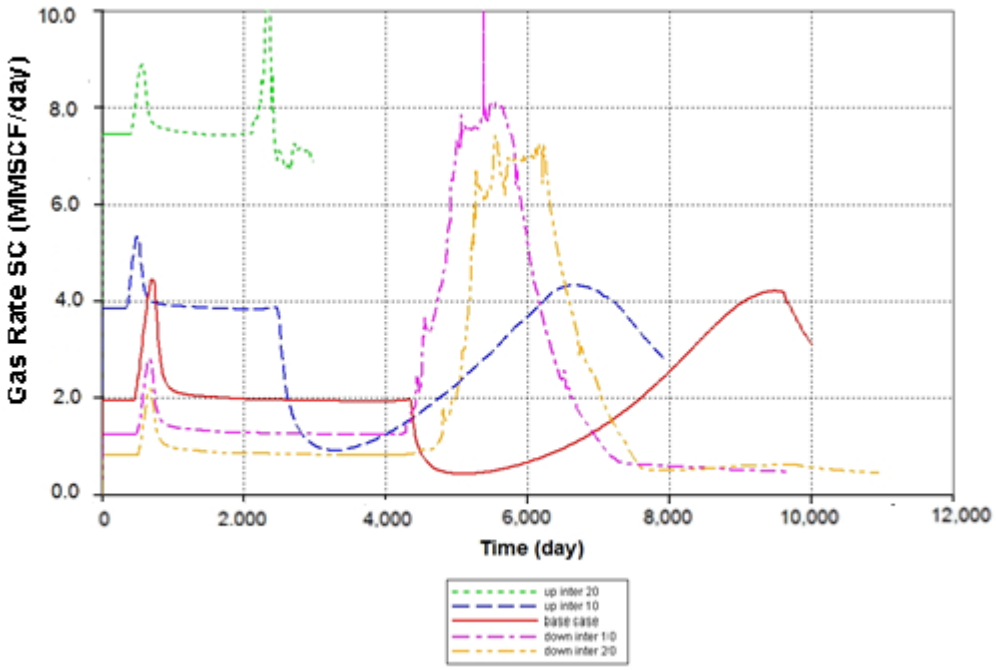

Figure 5.89 Gas production rates of CO_2–foam flooding with variation of oil composition as functions of time.

5.3.3 Effect of foam slug size

The effect of slug size is studied by dividing foam injection from 0.4 pore volume into two slugs of 0.2 pore volume and three slugs of 0.133 pore volume. Each slug is alternated with chasing water slugs. The total foam volume must be equal in all cases and also the ratio between foam and alternating water slug is kept constant.

5.3.3.1 Double slugs with 0.2 pore volume

CO_2-foam injection or CO_2 injection (for solely CO_2 injection) is started at the first day of production. Chasing water is started when amount of CO_2-foam or CO_2 injection reaches 0.2 hydrocarbon pore volume (8,330 MMSCF). Water is injected until cumulative water injection is 0.2 pore volume (8.01 MMSTB). Afterwards, CO_2-foam or CO_2 is injected again and chased by water respectively with

the same amounts of the first slug. The sequences of injection are exhibited by time in Table 5.24.

Table 5.24 Injection time sequence of CO_2-foam and CO_2 flooding cases in double-slug scheme.

Injection time sequence	**CO_2-foam flooding**	**CO_2 flooding**
Start injection 1st CO_2/ CO_2-foam, day	1	1
Start injection 1st water chasing, day	2,342	1,188
Start injection 2nd CO_2/ CO_2-foam, day	4,656	3,180
Start injection 2nd water chasing, day	7,548	4,060

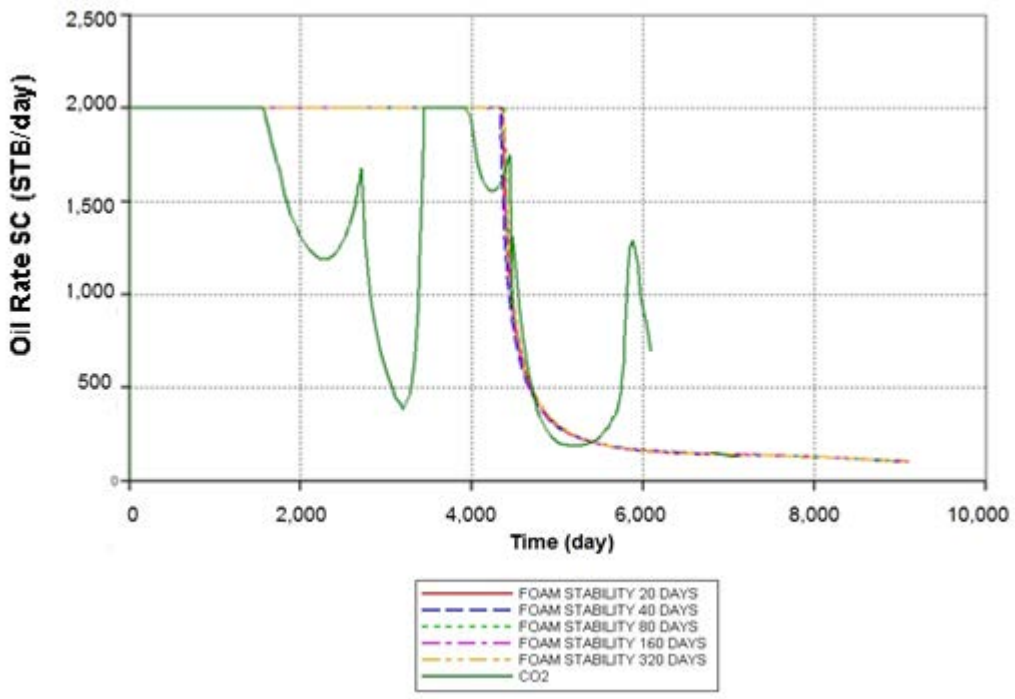

Figure 5.90 Oil production rates of CO_2–foam and CO_2 flooding cases in double-slug scheme.

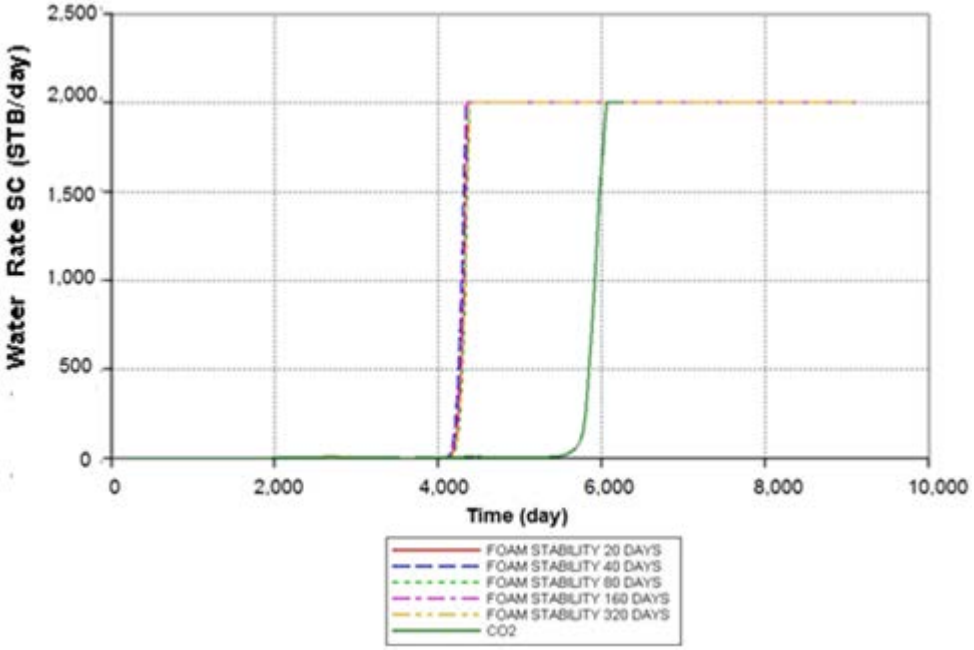

Figure 5.91 Water production rates of CO_2–foam and CO_2 flooding cases in double-slug scheme.

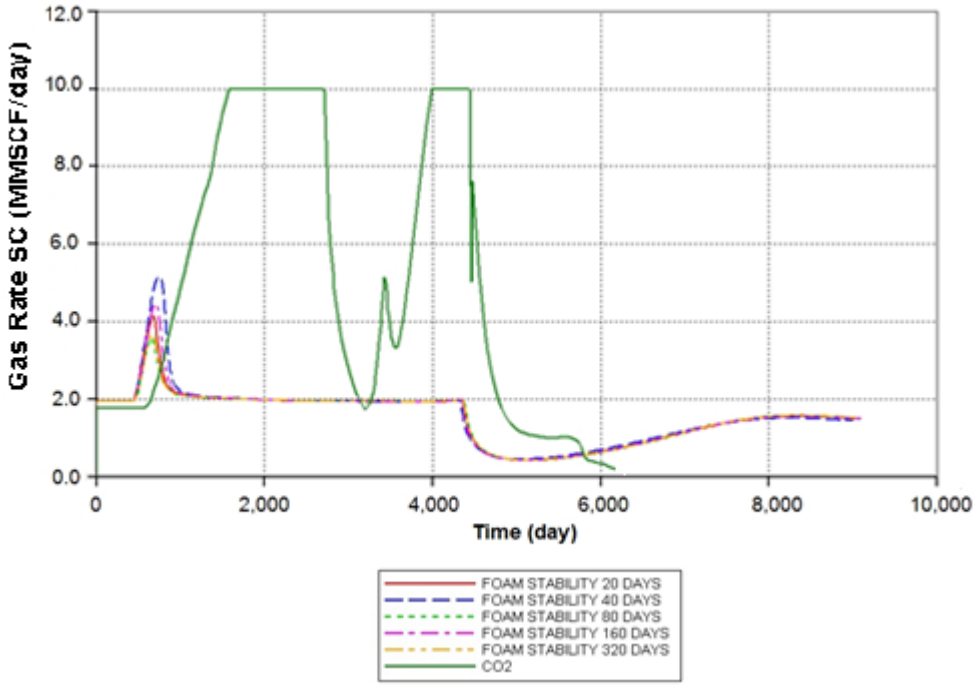

Figure 5.92 Gas production rates of CO_2–foam and CO_2 flooding cases in double-slug scheme.

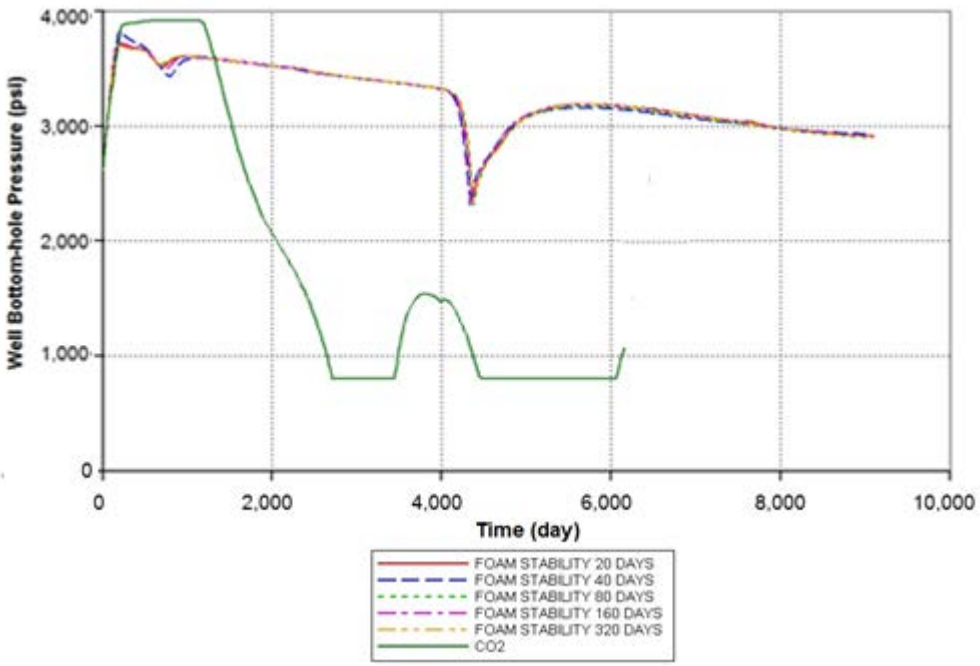

Figure 5.93 Bottomhole pressures at production well of CO_2–foam and CO_2 flooding cases in double-slug scheme.

The simulation outcomes including oil production rate, water production rate, gas production rate, and well bottomhole pressure of production well are depicted in Figures 5.90 to 5.93, respectively. It is obvious that behaviors of CO_2-foam flooding in double slugs are not much different from CO_2-foam flooding in single slug (base case). The period of water breakthrough of both cases is almost the same but that of double-slug case may be slightly retarded (4,110 days). This is because foam is able to maintain pressure better than water. In double-slug case, foam slug is divided into two slugs and therefore, pressure in double-slug case is slightly lower than that of single-slug CO_2-foam base case. This leads to slightly retarding of water breakthrough. From water production rates illustrated in Figure 5.91, it is observed that water rates of CO_2-foam flooding do not drop as in the cases of CO_2-foam base case because dividing foam into two slugs can maintain pressure not to fall quickly. However, this is not good for oil production. Since water is kept to produce at the maximum rate of 2,000 STB/D; in a mean time, oil production rate is slightly decreased. So that production is shut off due to water cut reaching constraint of 95%.

In CO_2-foam base case, pressure drops dramatically at the last stage of production, water production rate also drops because of pressure. The production is remained due to lower water cut that 95% and production is prolonged until oil rate approaches economic limit of 100 STB/D then production is terminated. For gas production rates, small increasing rates at the day about 5,000th result from rupture of foam bubbles and previously captured gas comes out. Nevertheless, amount of gas at is not as high as the CO_2-foam base case because of lower pressure drop.

Regarding CO_2 flooding, the injection CO_2 in double-slug mode impacts oil production rate as shown in Figure 5.90. An oil rate is kept constant at 2,000 STB/D for 1,572 days and falls due to gas breakthrough as seen in Figure 5.90. Oil rate rises up again during 2,280-2,710 days from the effect of chasing water (reduce relative permeability of gas). However, water cannot maintain pressure therefore; pressure drops quickly and results in decreasing of oil rate. At 3,195 days oil rate starts to increase again because chasing water sweeps oil in lower zone. The second slug of CO_2 is initially injected at the day 3,180th, leading to increment of pressure. Gas reaches production well at 3,925 days; therefore oil rates drop a little bit. Afterwards, second chasing water is injected at the day 4,060th which is not able to maintain pressure and causing the drop of oil rate. Before water reaching production well, it chases the oil and results in small oil elevation at 5,350 days.

The simulation outcomes are summarized in Table 5.25. From ultimate oil recovery factor which is shown in Figure 5.94, foam stability slightly influences on oil recovery factor. The best performance in CO_2-foam flooding is the case of foam stability at 80 days, providing improvement compared to CO_2 flooding in the same conditions around 11.79%.

Table 5.25 Cumulative oil production, water production, gas production and oil recovery factor of CO_2–foam and CO_2 flooding cases in double-slug scheme.

	CO_2 flooding	**Foam flooding**				
		FS 20 days	**FS 40 days**	**FS 80 days**	**FS 160 days**	**FS 320 days**
Time for injected water to reach 0.4 PV, day	6,066	9,100	9,009	9,070	9,070	9,070
Cumulative oil production (MMSTB)	7.94	9.75	9.68	9.76	9.73	9.76
Cumulative water production, (MMSTB)	0.375	9.62	9.57	9.53	9.58	9.54
Cumulative gas production (MMSCF)	31,040	14,010	14,300	13,860	14,080	13,890
Oil recovery factor, %	42.75	54.43	54.06	54.54	54.26	54.46

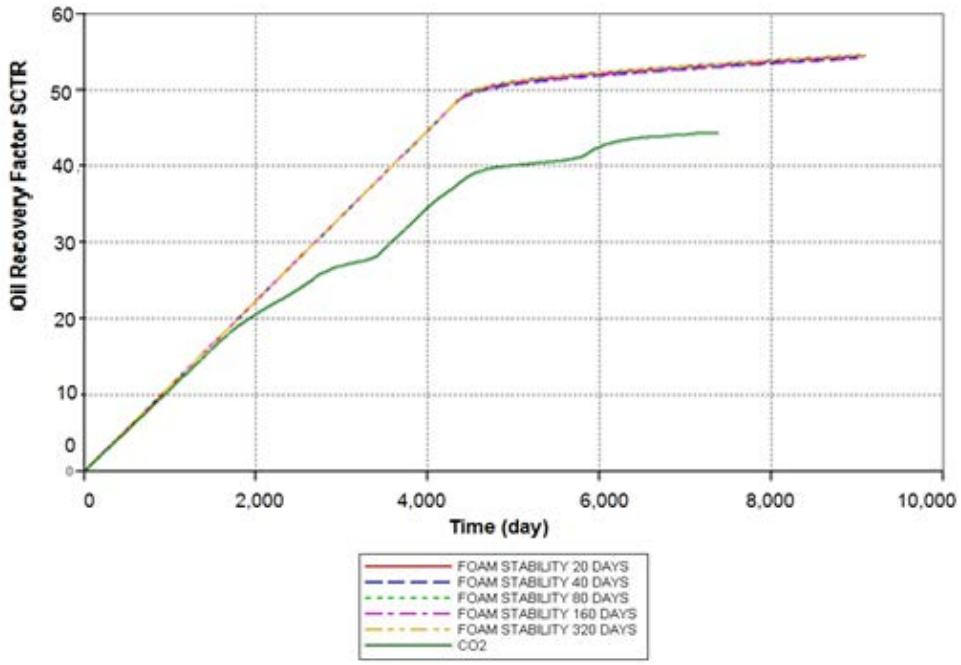

Figure 5.94 Oil recovery factors of CO_2–foam and CO_2 flooding cases in double-slug scheme.

5.3.3.2 Triple slugs with 0.13 pore volume

Injection CO_2-foam or CO_2 starts since the first day of production and continues injecting until cumulative CO_2 injection reaches 0.13 hydrocarbon pore volume (5,540 MMSCF). Then, the process is altered by injecting chasing water of 0.13 pore volume (5.33MMSTB). These operations are totally called one slug. In this section, three slugs are required to execute. Nevertheless, triple-slug operation is not completed in CO_2-foam flooding because the third slug of water cannot be finished), because water cut reaches 95% during injection of third chasing water slug, leading to termination of production.

Table 5.26 Injection time sequence of CO_2-foam and CO_2 flooding cases in triple-slug scheme.

Injection time sequence	**CO_2-foam flooding**	**CO_2 flooding**
Start injection 1st CO_2/ CO_2-foam, day	1	1
Start injection 1st water chasing, day	1,460	862
Start injection 2nd CO_2/ CO_2-foam, day	2,990	2,220
Start injection 2nd water chasing, day	4,656	2,806
Start injection 3rd CO_2/ CO_2-foam, day	6,478	4,143
Start injection 3rd water chasing, day	8,400	4,790

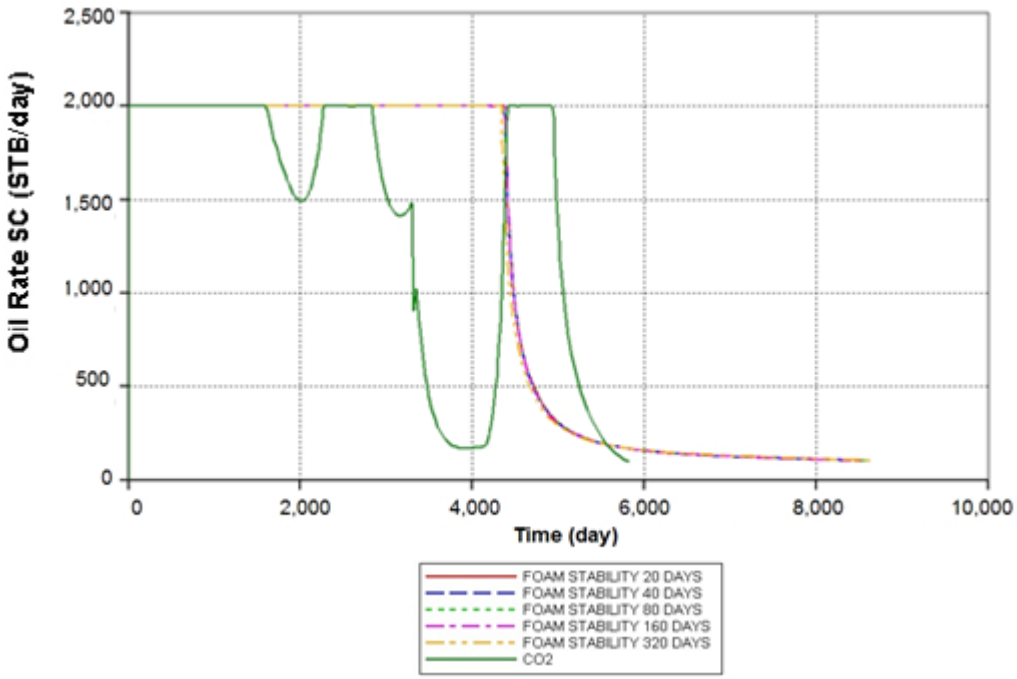

Figure 5.95 Oil production rates of CO_2–foam and CO_2 flooding cases in triple-slug scheme.

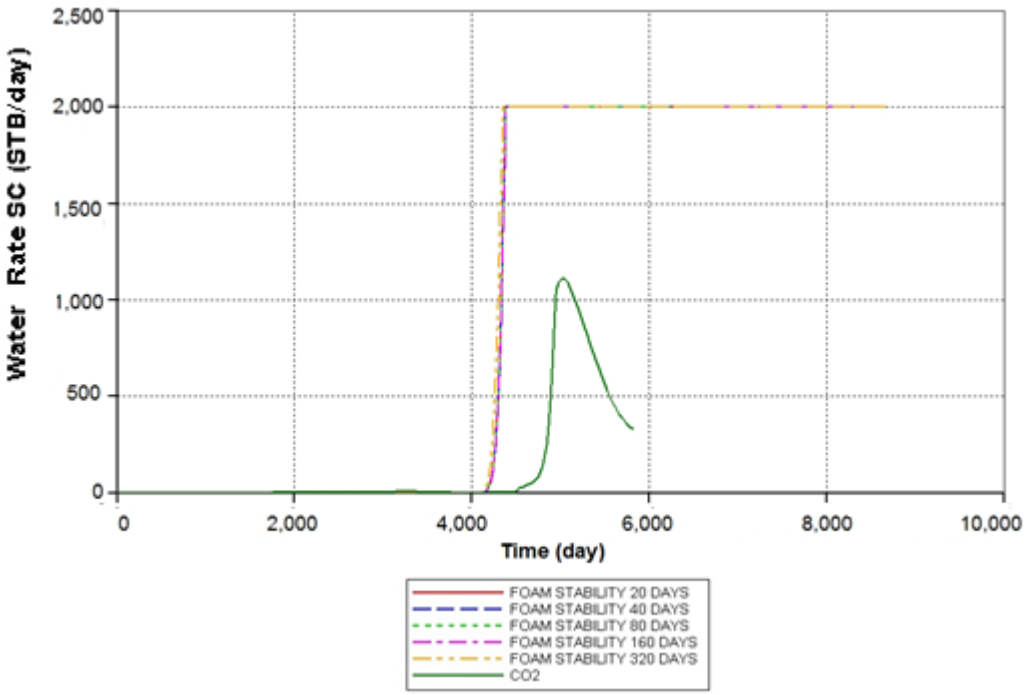

Figure 5.96 Water production rates of CO_2–foam and CO_2 flooding cases in triple-slug scheme.

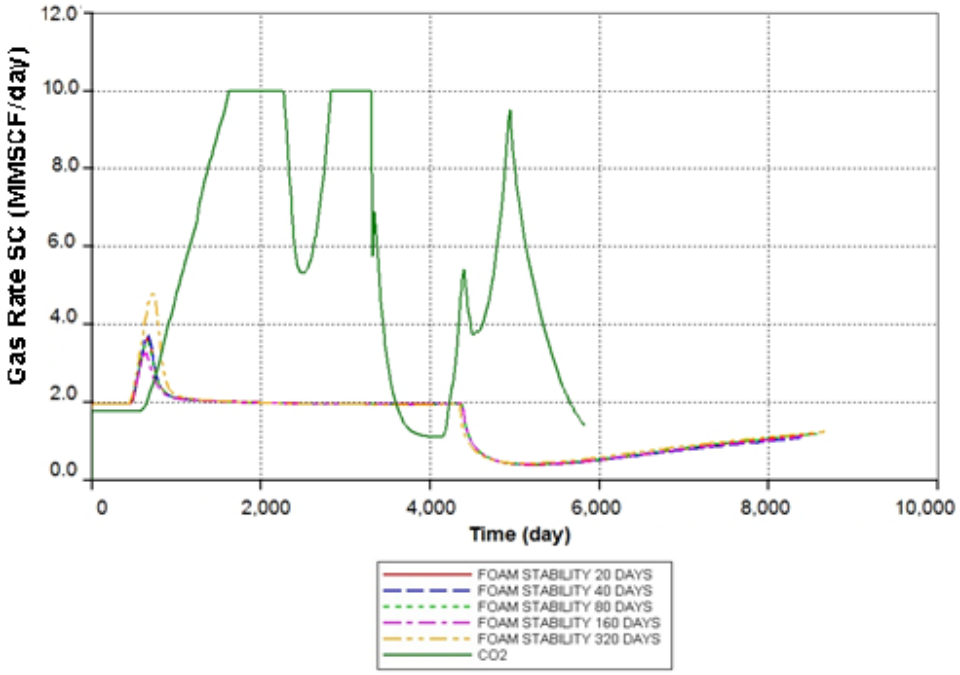

Figure 5.97 Gas production rates of CO_2–foam and CO_2 flooding cases in triple-slugs scheme.

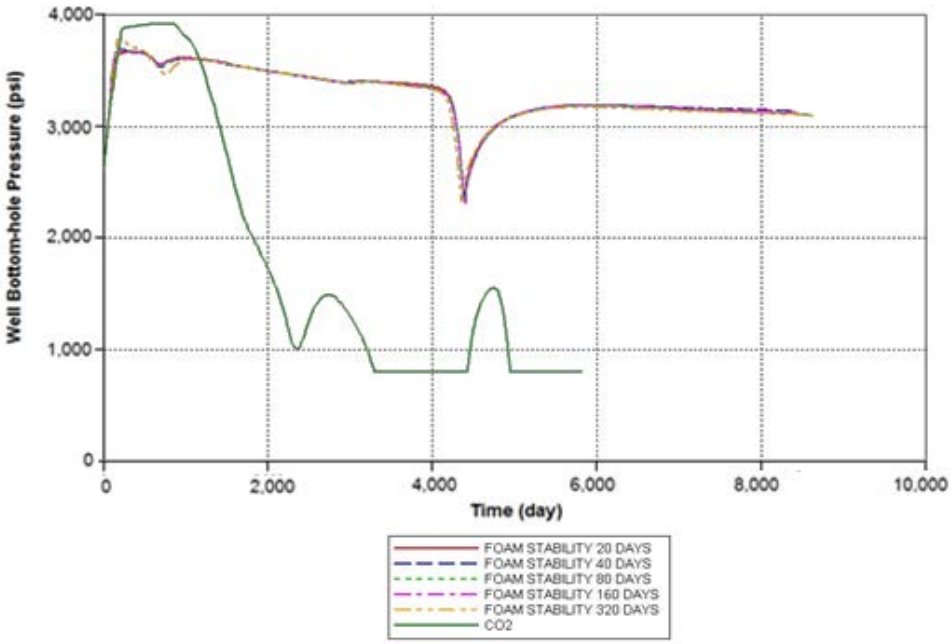

Figure 5.98 Bottomhole pressures at production well of CO_2–foam and CO_2 flooding cases in triple-slug scheme.

Figures 5.95 to 5.98 illustrates oil production rate, water production rate, gas production rate, and well bottomhole pressure of production well, respectively. The simulation results of CO_2-foam flooding in triple-slug mode are similar to CO_2-foam flooding in one slug (base case) and two slugs. But for triple-slug cases, water reaches production well slower than other cases because foam slug is divided into three slugs, so ability to maintain pressure is slightly reduced. This causes reservoir pressure of triple-slug case to be lower than one slug and two slugs. Since pressure is lower, fluids in reservoir loss driving force and hence move slower as well. Nonetheless, production stops producing due to water cut that exceeds production constraint of 95%.

From simulation results of solely CO_2 flooding, triple-slug injection is very helpful to production oil rate because it minimizes the effect from gas breakthrough as can be seen in Figure 5.95. Oil is produced at constant rate 2,000 STB/D for 1,605 days and decreases for while due to gas breakthrough as shown in Figure 5.99. As chasing water is injected, oil rate increases again during 2,268-2,830 days. However, second slug of CO_2 causes the gas breakthrough again. Therefore oil rate subsides and drops down rapidly due to lower reservoir pressure in Figure 5.100. At the day 4,161st, oil production rate rises up again, resulting from injection of CO_2 and it can maintain oil production rate constant for a while. Gas production rate and water production rate at this stage also rise up but due to low reservoir pressure, all production fluids reduce and cannot be longer produced. It should be noted that second and third slugs of CO_2 do not cause miscibility but it swells and reduces viscosity of oil. This is due to too low pressure that minimum miscibility pressure of 2,800 psi cannot be achieved.

Table 5.27 Cumulative oil production, water production, gas production and oil recovery factor of CO_2–foam and CO_2 flooding cases in triple-slug scheme.

	CO_2 flooding	**Foam flooding**				
		FS 20 days	**FS 40 days**	**FS 80 days**	**FS 160 days**	**FS 320 days**
Time for injected water to reach 0.4 PV, day	5,825	8,582	8,369	8,552	8,412	8,674
Cumulative oil production (MMSTB)	8.09	9.68	9.65	9.67	9.66	9.63
Cumulative water production, (MMSTB)	0.725	8.56	8.13	8.50	8.21	8.81
Cumulative gas production (MMSCF)	31,170	12,120	11,820	12,160	11,810	12,740
Oil recovery factor, %	44.56	54.02	53.90	54.05	53.92	53.77

Table 5.27 indicates results obtained from for triple-slug cases. Base on ultimate oil recovery factor, foam stability of 80 days provides the best result in CO_2-foam flooding. However, there is no significant difference from each case of foam stability. The benefit of this case over CO_2 flooding is about 9.49%.

5.3.3.3 Summary of effects of foam slug size on CO_2-foam flooding

Division of CO_2-foam into smaller slugs, alternating with chasing water slightly impacts on the production characteristic of CO_2-foam flooding. The small size of CO_2-foam reduces capability of pressure maintenance by foam. Injecting of one slug of CO_2-foam followed by one slug of water, results in maintaining high pressure at first period and sudden drop of pressure in latter period. On the other hand, splitting CO_2-foam into small slugs causes lower reservoir pressure at the first and higher

pressure is followed. Figure 5.99 displays bottomhole pressures at production well which is previously mentioned.

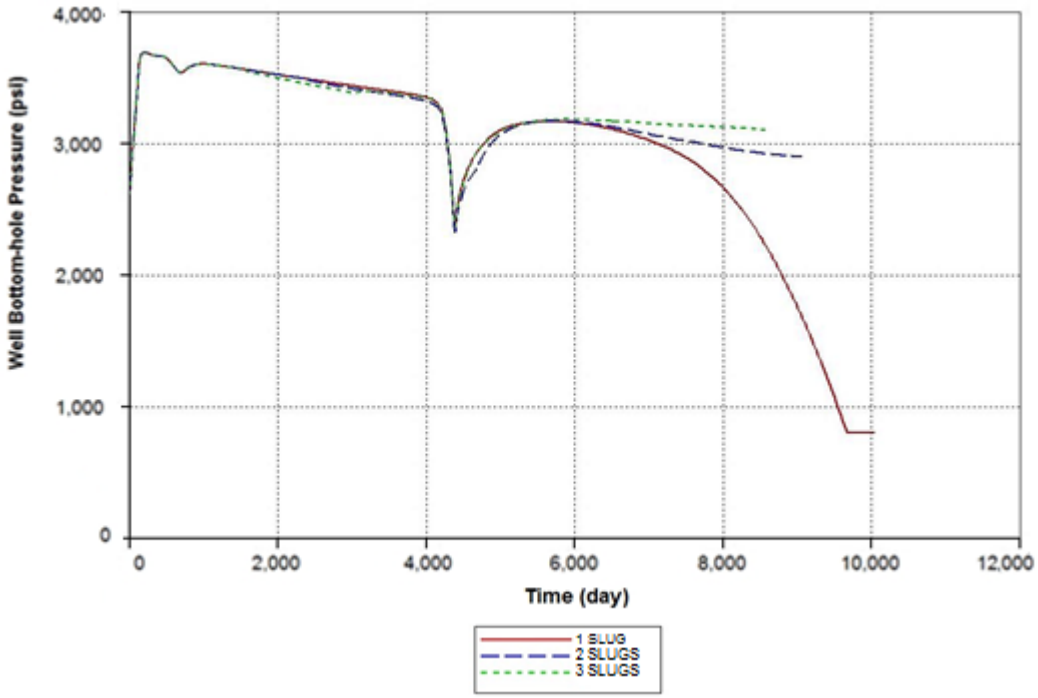

Figure 5.99 Bottomhole pressures at production well with variation of CO_2-foam slug as functions of time.

The lower pressure in the first stage of 2 and 3 slug cases result in the slightly slower water breakthrough and slower dropping of oil rate as shown in Figure 5.100. Pressure in latter stage is more important because high pressure leads to maintaining of produced water after water breakthrough. Therefore, production is terminated due to the water cut reaches the value of 95% for both double-slug and triple-slug cases. On the other hand, lower pressure of single-slug case causes drop of water production and hence, water cut does not reach the preset limit and oil can be produced until it approaches the economic limit of 100 STB/D. Oil production rates are shown in Figure 5.100. In summary, in order to obtain the best result from CO_2– foam flooding, single-slug mode is recommended.

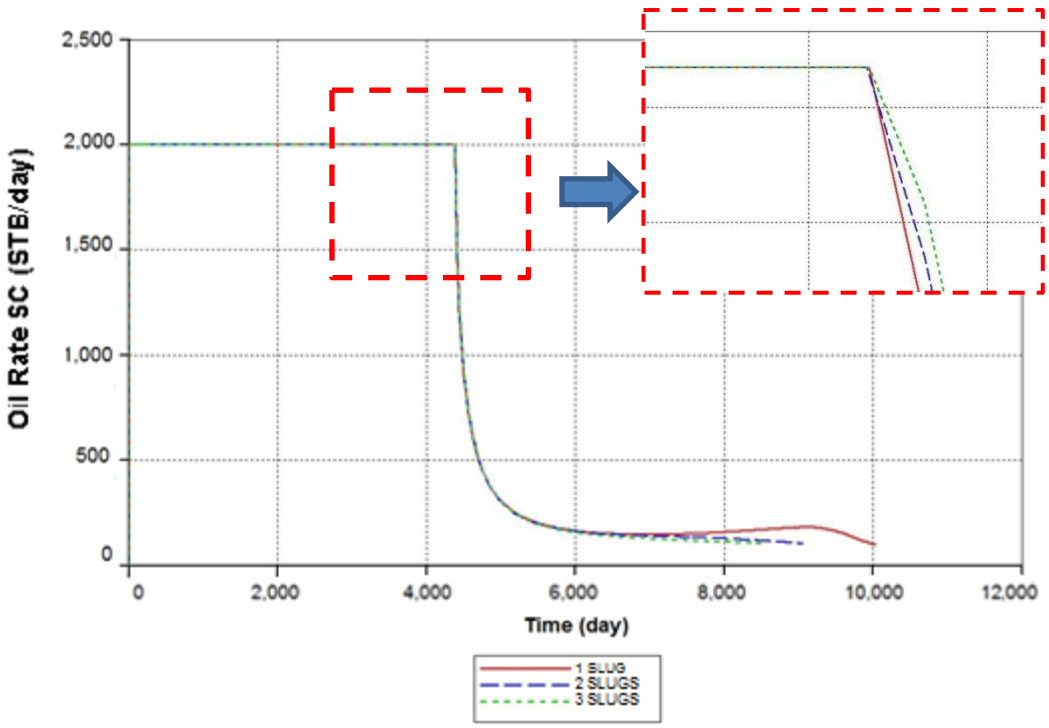

Figure 5.100 Oil production rate of CO_2–foam flooding with variation of CO_2-foam slug as functions of time.

CHAPTER VI

CONCLUSIONS AND RECOMMENDATIONS

Comparison between performances of CO_2-foam flooding and CO_2 flooding is summarized in this chapter. Influences of each parameter such as formation wettability, intermediate component of oil liquid hydrocarbon, and design of injection slug on flooding performance are concluded as well. The obtained conclusions from this study could be useful as screening criteria for future decision of CO_2-foam flooding implementation. Moreover, recommendations for further study are also mentioned in this section.

6.1 Conclusions

According to simulation results that are previously discussed in previous chapter, it is obvious most of CO_2-foam flooding cases have higher potential to enhance hydrocarbon recovery in comparison to solely CO_2 flooding. This is because foam reduces mobility of gaseous CO_2 and provides smoother flood front. However, CO_2-foam is a combination of aqueous and gas phases (surfactant solution and CO_2), therefore, the breakthrough of aqueous phase in case of foam flooding is much quicker than that of CO_2 flooding. This consecutively causes the reduction of oil production rate.

Variation of foam stability does not significantly impact on production performance of CO_2-foam flooding. Foam stability does not show any trend on performance of CO_2-foam flooding. It could be possible that this is a result from injecting continuously big slug of CO_2-foam and there are other parameters involve such as the ability of foam generation. Although the generation rates of foam in all cases are set to be equal, the 3D simulation results show that foam is not generated equally in all cases. From this reason, effects of foam stability cannot be clearly seen. Nevertheless, the difference of oil recovery factors by varying foam stability is smaller than 2%. Hence, foam stability seems to be insensitive to the production performance of CO_2-foam flooding in this study. However, foam stability might show more effect on CO_2-foam flooding when it is injected in small slug (foam injecting

period is less than foam stability) and reservoir shape is long enough for foam to degrade during traveling through porous media.

The influences of study parameters on effectiveness and performance of CO_2-foam flooding are summarized as follows:

1. Effect of wettability

1) In order to achieve a good performance of CO_2-foam flooding, the best suit formation wettability should be in the range of neutral-wet to strongly water-wet. When rock surface has preference to be attached by water, flowing water in reservoir arrives to production well slower since it is captured by rock surface and this phenomenon leads to retardation of water breakthrough
2) CO_2 flooding yields better performance compared to CO_2-foam flooding when implementation is performed in reservoir having rock wettability ranging from oil-wet or strongly oil-wet condition.

2. Effect of intermediate component in liquid hydrocarbon.

1) Implementation of CO_2-foam flooding with light oil containing high component of intermediate (C_2-C_6) results in high velocity of injected foam as well as aqueous phase in reservoir. This can be explained that oil saturation after vaporization remains in small saturation. This results in an increment of relative permeability to water which is a direct function of water saturation.
2) Intermediate compound tends to destabilize foam more than oil containing higher component of heavy compound (C_{7+}). The rupture of foam is caused by smaller molecules of intermediate that can access into the interface of CO_2 and surfactant and results in breaking of the film of lamella.
3) The advantage of CO_2-foam over CO_2 flooding is higher when hydrocarbon in reservoir contains low intermediate component.

3. Effect of slug injection

1) Dividing CO_2-foam slug into smaller slugs such as double-slug or triple-slug modes can maintain pressure after water breakthrough slightly better than injection a single-slug. Therefore, when water reaches the production well, oil production is terminated by the reason that water cut reaches its production limitation.
2) In this study, single-slug mode of CO_2-foam provides more satisfied outcomes compared to double-slug or triple-slug injection of CO_2-foam.
3) For solely CO_2 flooding, double-slug and triple-slug modes yield better production performance due to reduction of gas breakthrough. This method is similar to Water Alternating Gas (WAG) injection.

6.2 Recommendations

The following issues are suggestions for the further study of CO_2-foam flooding.

1. In order to perform foam flooding simulation, it requires many reactions such as foam regeneration in reservoir, foam degradation with no oil, trapped lamella, absorption of surfactant etc. For simplification, this study basically concerns only foam generation and foam degradation. More details should be included in the foam flooding model in order to simulate a more realistic case.
2. Foam flooding should be executed in heterogeneity reservoir in order to investigate the abilities of blokage of thief zone and flow diversion.
3. Foam quality should be thoroughly considered since it is also important parameter to determine foam performance. It should be also kept constant throughout foam injection period.
4. In reality, foam injection is performed by injecting surfactant and gas alternately as a sequence which may lead to a more pratical result.

5. Due to the limitation of educational license, CMG software can provide only 10,000 grid blocks constructed model which may cause in imprecise results. For more accuracy, current license should be upgraded.

REFERENCES

[1] Bond, D.C. and Holbrook, O.C. Gas Drive Oil Recovery Process, U.S. Patent No. 2 866 507, December 1958

[2] Wang, G.C. A Laboratory Study of CO_2 Foam Properties and Displacement Mechanism. Paper SPE/DOE 12645 presented at the SPE/DOE Fourth Symposium on Enhanced Oil Recovery, Tulsa, Oklahoma, USA, April 1984.

[3] Zhang, Y., Yue, X., Dong, J. and Yu, L. New and Effective Foam Flooding To Recover Oil in Heterogeneous Reservoir. Paper SPE 59367 presented at the 2000 SPE/DOE on Improved Oil Recovery Symposium, Tulsa, Oklahoma, USA, April 2000.

[4] Liu, Y., Grigg, R.B. and Svec, R.K. CO_2 Foam Behavior: Influence of Temperature, Pressure, and Concentration of Surfactant. Paper SPE 94307 presented at the 2005 SPE Production and Operations Symposium, Oklahoma City, Oklahoma, USA, April 2005

[5] Ashoori, E. and Rossen, W.R. Can Formation Relative Permeabilities Rule Out a Foam EOR Process?. Paper SPE 134906 presented at the SPE Annual Technical Conference and Exhibition, Florence, Italy, September 2010.

[6] Schramm, L.L. and Mannhardt, K. The Effect of Wettability on Foam Sensitivity to Crude Oil in Porous Media. Journal of Petroleum Science and Engineering 15, 101-113 Petroleum Recovery Institute 100, Calgary, Alta, Canada, 1996.

[7] Sanchez, J.M. and Hazletett, R.D. Foam Flow through an Oil-Wet Porous Medium: A Laboratory Study. Paper SPE 19687 presented at the 1990 SPE Annual Technical Conference and Exhibition, San Antonio, Texas, USA, October 1990.

[8] Suffridge, F.E., Raterman, K.T. and Russell, G.C. Foam Performance Under Reservoir Conditions. Paper SPE 19691 presented at the 64th Annual Technical Conference and Exhibition of Society of Petroleum Engineers, San Antonio, Texas, USA, October 1989.

[9] Schramm, L.L. and Novosad, J.J. The destabilization of foams for improved oil recovery by crude oil: Effect of nature of oil. Journal of Petroleum Science and Engineering 7, 77-90 Elsevier Science Publishers B.B., Amsterdam, September 1992

[10] Schramm, L.L. Foams: Fundamentals and Appliacations in the Petroleum Industry, American Chemical Society, Washington, DC, USA, 1994.

[11] Donaldson, E.C. Chilingarian, G.V. and Yen, T.F. Enhanced Oil Recovery, I: Fundamentals and Analysis. Elsevier Science Publishers B.V., Amsterdam, The Netherlands, 1985.

[12] Dholkawala, Z. F. Application of fractional flow theory to foams in porous media. Master's Thesis, The University of Adelide, Australia, 2006.

[13] Zhang,Z.F., Freedman, V.L. and Zhong, L. Foam Transport in Porous Media – A Review. Prepared for the U.S. Department of Energy, November 2009.

[14] Aveyard, R., Binks, B. P., Fletcher, P. D. I., Peck, T. G. and Garrett, P. R. Entry and spreading of alkane drops at the air/surfactant solution interface in relation to foam and soap film stability. Journal of the Chemical Society, Faraday Transactions,Issue 24, 1993

[15] Allawzi, M.A. and Patton, J.T. Thermal Stability of Foam Additive in Steamflood Core Tests. Paper SPE/DOE 27790 presented at the SPE/DOE Ninth Symposium on Improved Oil, Tulsa, Oklahoma, USA, April 1994.

[16] Green, D.W. and Willhite, G.P. Enhanced Oil Recovery. Society of Petroleum Engineers Inc, Second printing, USA, 2003.

[17] Zanganeh, M.N., Kam, S.I., LaForce, T.c., and Rossen, W.R. The Method of Characteristics Applied to Oil Displacement by Foam. Paper SPE 121580 presented SPE EUROPEC/EAGE Annual Conference and Exhibition, Amsterdam, Netherlands, June 2009.

[18] Rossen, W.R., Zeilinger, S.C., Shi, J., and Lim, M.T. Mechanistic Simulation of Foam Processes in Porous Media. Paper SPE 28940 presented at the SPE 69th Annual Technical Conference and Exhibition, New Orleans, LA, USA, September 1994

[19] Computer Modelling Group, User's Guide STARS : Advanced Process and Thermanl Reservoir Simulator Version 2009, Alberta, Canada, 2009

[20] Shen, C., EXPERIMENTAL AND SIMULATION STUDY OF FOAM IN POROUS MEDIA. Doctor's dissertation, Faculty of the Graduate School of The University of Texas at Austin, August 2006.

[21] Skoreyko, F., Pino, A.V., Prada, H.R., and Nguyen, Q.P., Development of a New Foam EOR Model Laboratofy and Field Data of the Naturally Fractured Canterell Field, Paper SPE 145718 presented at the SPE reservoir Characterisation and Simulation Conference and Exhibition, Abu Dhabi,UAE, October 2011.

APPENDIX

APPENDIX

RESERVOIR MODEL CONSTRUCTION

Builder Win 32 is an application for all CMG software products which are used to create, edit, and visualized for generating input data. STARS software is selected as simulation tool in this study.

Simulator Setting

Simulator STARS

Working Units Field

Porosity Single porosity

1. Reservoir Section

Grid Type Cartesian

K Direction Down

Number of Grid Blocks30×15×20 (I, J, K direction respectively)

Block widths I direction: 30*100

J direction: 15*100

1.2 General Property Specification

Parameter	Whole grid
Thickness (ft)	10
Porosity	0.25
Permeability I (mD)	220
Permeability J (mD)	Equals I(equal)
Permeability K (mD)	Equals I*0.1
Mole Fraction (C_2 to C_6)	0.3408
Mole Fraction (C_{7+})	0.3112

Mole Fraction (CH_4)	0.3383
Mole Fraction (CO_2)	0.0091
Mole Fraction (N_2)	0.006
Oil saturation	0.72
Water saturation	0.28
Water Mole Fraction	1

2. Component

Component properties are imported from Winprop-generated model. The required information is inputted are shown below.

2.1 Composition (Winprop)

The composition is enter in mole fraction. Normally, “primary” corresponds to the reservoir fluid and “Secondary” corresponds to the injection fluid.

Composition	**Primary**	**Secondary**
CO_2	0.0091	1.0
N_2	0.0006	0.0
C_1	0.3383	0.0
C_2	0.0904	0.0
C_3	0.0799	0.0
i-C_4	0.0197	0.0
n-C_4	0.0469	0.0
i-C_5	0.036	0.0
n-C_5	0.0178	0.0
C_6	0.0501	0.0
C_{7+}	0.3112	0.0
Molecular weight of C_{7+}	267	
S.G. of C_{7+}	0.8615	

2.2 Saturation Pressure (Winprop)

Calculation option : Bubble or Upper dew point

Tempurature (^{o}F) : 198

Saturation Pressure Estimate (psia) : 2,363

2.3 Two-phase Envelope (Winprop)

Envelope Type : X-Y Phase Envelope

Y-Axis min pressure (psia) : 0

Y-Axis max pressure (psia) : 14,695.95

X-Axis min temperature (^{o}F) : -148

X-Axis min temperature (^{o}F) : 1,292

2.4Multiple Contacts (Winprop)

Tempurature (^{o}F) : 198

Solvent increment ratio : 0.01 (default value)

Equilibrium gas/original oil mixing ratio : 0.1

MMP/MME calculation method selection : Cell to Cell Simulation

2.5 CMG STARS PVT Data (Winprop)

Reference pressure (psia) : 2,775

Reference temperature (^{o}F) : 198.0

2.6 Process Wizard (Builder)

Process : Alkaline, surfactant, foam, and/or polymer model

Model : Foam flood with liquid foam model (add 4 components)

Option : Use CO_2 gas to generate foam

Surfactant : 0.5 weight percent used to generate the foam

No. of rel perm : 2 sets

Adsorption for surfactant : Use

Rock type : Sandstone

Rock density, gm/cm^3 : 2.65

Add new component : Foam_Gas, Lamella, CO_2

Interfacial Tension values

Weight% Sufactant	Interfacial Tension, (dyne/cm)
0	18.2
0.05	0.5
0.1	0.028
0.2	0.028
0.4	0.0057
0.6	0.00121
0.8	0.00037
1	0.5

2.7 Reaction

1. *Water + Surfactant + CO_2 ➔ Lamella + CO_2* FREQFAC = 10,000
2. *Lamella + CO_2 ➔ Foam_Gas + Lamella* FREQFAC = 10,000
3. *Foam_Gas + C_2 to C_6 ➔ CO_2 + C_2 to C_6* Varied FREQFAC
4. *Foam_Gas + C_7 ➔ CO_2 + C_7* Varied FREQFAC

Foam stability (days)	FREQFAC
20	0.0346574
40	0.0173287
80	0.0086643
160	0.0043322
320	0.0021661

3. Rock-Fluid

3.1 Rock type properties

Rock Fluid Properties	
Rock Wettability	Water Wet
Method for Evaluating 3-phase KRO	Stone's Second Model
Interpolation Components (INTCOMP)	Interpolation enabled
Rock-fluid interpolation will depend on component	Foam_Gas
Phase for which component's composition will be taken	water (aqueous) mole fraction
Foam Interpolation Parameters	
Critical component mole fraction (FMSURF)	7.10E-05
Critical oil saturation value	0.3
Exponent for composition contribution (EPSURF)	1
Exponent for oil saturation contribution (EPOIL)	1

3.2 Relative Permeability Table

Generate table using correlation wizard

Keyword	Description	Value
SWCON	Endpoint Saturation: Connate Water	0.28
SWCRIT	Endpoint Saturation: Critical Water	0.28
SOIRW	Endpoint Saturation: Irreducible Oil for Water-Oil Table	0.24
SORW	Endpoint Saturation: Residual Oil for Water-Oil Table	0.24
SOIRG	Endpoint Saturation: Irreducible Oil for Gas-Liquid Table	0.05
SORG	Endpoint Saturation: Residual Oil for Gas-Liquid Table	0.10
SGCON	Endpoint Saturation: Connate Gas	0.00
SGCRIT	Endpoint Saturation: Critical Gas	0.15
KROCW	Kro at Connate Water	0.41
KRWIRO	Krw at Irreducible Oil	0.13
KRGCL	Krg at Connate Liquid	0.6

	Exponent for calculating Krw from KRWIRO	3
	Exponent for calculating Krow from KROCW	3
	Exponent for calculating Krog from KROGCG	3
	Exponent for calculating Krg from KRGCL	3

4. Initialization

Vertical Equilibrium Calculation Methods	Depth-Average Capillary-Gravity Method
Reference pressure (REFPRES)	2,775 psi
Reference depth (REFDEPTH)	6,000ft

5. Numerical

Keyword Description	**Dataset value**	**Unit**
Timestep Control Keywords		
Max Number of timesteps (MAXSTEPS)	50,000	
Max Time Step Size (DTMAX)	1.00E+20	day
Min Time Step Size (DTMIN)	5.00E-05	day
First time Step Size after Well Change (DTWELL)	1	day
Solution Method Keywords		
Isothermal Option (ISOTHERMAL)	ON	
MAX Newton Iterations (NEWTONCYC)	20	
Max Time Step Cuts (NCUTS)	20	

6. Wells and recurrent

6.1 Inj_gas (Gas injection well)

Well radius 0.28 ft

Constraint:

Constraint	Parameter	Limit/Mode	Value	Action
OPERATE	STG surface gas rate	MAX	8.78 MMSCF/day	CONT
OPERATE	BHP bottom hole pressure	MAX	4100 psi	CONT

Injected fluid: Gas

- Injection pressure 3,000 psi

Component	Mole Fraction
Water	0
Surfact	0
Foam_gas	0
Lamella	0
CO_2	0
N_2	0
CH_4	0
C_2 to C_6	0
C_{7+}	0
CO_2_i	1
Total	1

6.2 Injector (Water injection well)

Well radius 0.28 ft

Constraint:

Constraint	Parameter	Limit/Mode	Value	Action
OPERATE	STW surface water rate	MAX	500 STB/day	CONT
OPERATE	BHP bottom hole pressure	MAX	4100 psi	CONT

Injected fluid : Water

- Injection pressure 3,000 psi

Component	Mole Fraction
Water	0.999929002
Surfact	7.0998e-005
Foam_gas	0
Lamella	0
CO_2	0
N_2	0
CH_4	0
C_2 to C_6	0
C_{7+}	0
CO_2_i	0
Total	1

Mole fraction of water and surfactant are calculate as shown in the table

Concentration of surf.			weight fraction Wti	Mw	Wti/Mw	mole fraction Xi
-		Water	0.995	0.044	22.61363636	0.999287265
0.5	%wt	Surfactant	0.005	0.31	0.016129032	0.000712735
			0.005	8.794	22.6297654	1

Surfactant is used in this study is Chaser SD 1000 which the average molecular weight is shown in the table.

TABLE 1. - Properties of bulk surfactants

Surfactant	% Active	Avg. molecular weight, Daltons	% Inorganic
Chaser SD1000	40	310	1
Sellogen WL	32.5	326	5
Enordet AOS 1416	39	325	3
Hüls 6.5	90.9	586	9
MA-18	90	696	–
AOS / MA-18 mixture	–	513	–

The surface tension of Chaser SD 1000 is displayed below

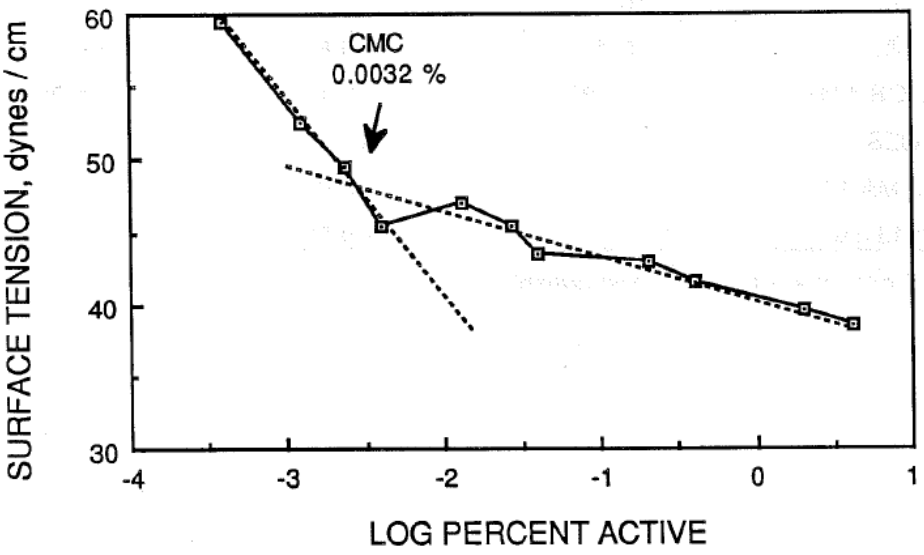

FIGURE 2. - Surface tension of Chaser SD1000 as a function of log concentration at 25° C.

6.3 Producer Well

Well radius 0.28 ft

Constraint:

Constraint	Parameter	Limit/Mode	Value	Action
OPERATE	BHP bottom hole pressure	MIN	800 psi	CONT
OPERATE	STO surface oil rate	MAX	2000 STB/day	CONT
OPERATE	STW surface water rate	MAX	2000 STB/day	CONT
OPERATE	STG surface gas rate	MAX	10 MMSCF/day	CONT
MONITOR	WCUT water-cut (fraction)		0.95	STOP
MONITOR	STO surface oil rate	MIN	100 STB/day	STOP

Vitae

Kunwadee Teerakijpaiboon was born on March 6th, 1988 in Bangkok, Thailand. She received her Bachelor degree in Mechanical Engineering from Faculty of Engineering, Chulalongkorn University in 2010. Afterwards, she joined Siam Kubota Corporation as a purchasing engineer for one year and seven months. After that, she continued her study in Master Degree of Petroleum Engineering at graduate school of the Department of Mining and Petroleum Engineering, Chulalongkorn University since 2011.